Liquid Chromatography Stationary Phases Made Using the Thiol-yne Reaction

by

Erin Peter Shields

BS Chemistry, Pennsylvania State University, 2001

Submitted to the Graduate Faculty of

The Kenneth P. Dietrich School of Arts and Sciences in partial fulfillment

of the requirements for the degree of

Doctor of Philosophy

University of Pittsburgh

2019

UNIVERSITY OF PITTSBURGH

DIETRICH SCHOOL OF ARTS AND SCIENCES

This dissertation was presented

by

Erin Peter Shields

It was defended on

August 19, 2019

and approved by

Adrian Michael, Professor, Department of Chemistry

Seth Horne, Associate Professor, Department of Chemistry

Luis Colón, Professor, Department of Chemistry, University at Buffalo

Dissertation Director: Stephen G. Weber, Professor, Department of Chemistry

Liquid Chromatography Stationary Phases Made Using the Thiol-yne Reaction

Erin Peter Shields, PhD

University of Pittsburgh, 2019

Stationary phases for HPLC that can withstand extremes of pH and temperature are needed to allow a single column to accommodate a wider set of solutes and separation criteria. This work investigates the use of the click chemistry thiol-yne reaction to create unique stationary phases that are stable at extreme pHs. Stationary phases were made by adding either 1,4-diethynylbenzene (DEB) or 1,7-octadiyne to propylthiol modified silica particles. The diynes were then crosslinked using 1,6-hexanedithiol. The main difference between the two types of phases was the presence of the benzene ring with the DEB modifier particles. Both phases show high stability in a 50:50 pH 0.5 5% TFA:acetonitrile mobile phase at 70 $^{\circ}$C. With the retention of triphenylene dropping 10% for the DEB based phase and 20% for the octadiyne phase. It was found that all the thiol-yne and thiol based stationary phases have a nitrobenzene to benzene selectivity factor greater than 1, indicating the phases possess electron donating charge-transfer characteristics due to the presence of the sulfur atom. The DEB phase's electron-donating characteristic is enhanced by a conjugated pi system between the sulfur and benzene ring. The DEB based phase also has an enhanced Tanaka test shape selectivity factor, between the flat triphenylene and bulky o-terphenyl molecules, of 4.91 ± 0.08, which is higher than almost all other reversed-phase stationary phases. The octadiyne phase's shape selectivity was 2.71 ± 0.03, still high, but much lower than with the DEB moiety in the phase. Cation-exchange characteristics were apparent in both phases, indicated by the Tanaka test. The DEB based phase had a benzylamine and phenol selectivity factor of around 22, while the octadiyne phase's was almost 4 at pH 2.7. With the methylene selectivities around 1.2 for all

the phases, in the range of a typical C18 column, it is apparent that the thiol-yne phases are mixed-mode stationary phases. The octadiyne phase was used to separate monoamine neurotransmitters showing the phase's hydrophobic and cation-exchange nature. These stable phases can provide a complementary phase to reversed-phase stationary phases and can be useful in many different fields.

Table of Contents

List of Tables

List of Figures

List of Equations

Preface

I wanted to first and foremost thank my family for their support and patience doing my graduate school career. I could not have completed this work without them.

Thank you to my advisor, Dr. Stephen Weber. Your help, guidance, and understanding were definitely essential to my completion of this program. I couldn't have done it without you. Thank you to Dr. Adrian Michael, possibly the first professor I talked to at Pitt. From the potential graduate student visit dinner until my defense, it was always fun to talk with you. Thank you, Dr. Seth Horne, for your help setting goals to work towards graduating. Your input was very helpful to discern what should be done to graduate. A special thank you to Dr. Luis Colón for agreeing to be my 4th committee member on a short notice. Your willingness to take the time to help me out is greatly appreciated.

1.0 Introduction

High performance liquid chromatography, HPLC, is a commonly used analytical technique used to separate and analyze mixtures of molecules in a solution. HPLC consists of a pump that moves a solution, the mobile phase, through a column to a detector. The column is filled with the stationary phase that the mobile phase passes over and/or through as it moves through the column. A detector at the end of the column records the signal versus time to create a chromatogram. To separate a mixture, a small aliquot of the sample is loaded at the beginning of the column and is moved through the column by the mobile phase. The moving sample interacts with the stationary phase and the mobile phase, and the solutes are separated based on how they partition between the phases. Solutes with a greater affinity for the stationary phase travel slower and are separated from solutes with a greater affinity for the mobile phase.

The chemical characteristics of the stationary phase and the mobile phase can be manipulated to provide the desired selectivity to separate a mixture. The most common forms of chromatography consist of mobile and stationary phases that have different, often opposite, characteristics. Reversed-phase HPLC (RP-LC), the most commonly used form, has a polar mobile phase and a nonpolar stationary phase. While normal phase has a polar stationary phase and a nonpolar mobile phase. Ion exchange chromatography utilizes opposite charges between the stationary phase and the charged solutes, causing retention due to the electrostatic force. Cation exchange consists of a negatively charged stationary phase, while anion exchange columns have a positively charged stationary phase. Counterions in the mobile phase compete with the solute for the ion exchange sites, helping to elute the ionic solutes.

1

RP-LC is the most the most used kind of HPLC because it is more reproducible and can be used with more molecules than normal phase or ion exchange. The RP-LC stationary phase is non-polar and interacts with the solutes mainly with hydrophobic interactions and the intermolecular dispersion forces [1, 2]. The more polar mobile phase usually contains water and a less polar miscible organic solvent, such as methanol or acetonitrile. The water is usually buffered at a pH that keeps ionizable analytes either neutral or in one given charge state to allow for a more consistent separation. By varying the mobile phase makeup, a large percentage of molecules can be separated using the common octadecylsilane, C18, modified RP-LC stationary phase.

Ionizable analytes make up an important segment of molecules that are commonly separated by HPLC. Most drugs and biological compounds can be ionized at neutral pH. Altering the pH to allow for neutral molecules to be separated often requires low pH, pH < 3, for acids or high pH, pH > 9, for most amines [3, 4]. To operate in acidic or basic conditions the stationary phase must be rugged and able to withstand harsh conditions.

Temperature is a critical component of modern chromatography, used to create ultra-fast separations [5, 6] and improve peak shape and separation [7]. As the temperature increases, the viscosity of the mobile decreases [8]. This reduces the backpressure, allowing for high mobile phase velocities and faster separations [6]. Increasing temperature generally decreases the retention time by reducing free energy of partitioning. This increases the speed of the solute partitioning between the mobile phase and stationary phase, increasing the efficiency and decreasing the retention. The stationary phase is often impacted by temperature as well [9]. Changing the conformation and selectivity of long chain alkyl chain ligands and other temperature sensitive polymers, like poly(N-isopropylacrylamide) [10]. The manipulation of column

temperature and high temperatures require robust stationary phases that are able to withstand the extreme conditions.

The ideal stationary phase support for HPLC has several key characteristics [11]. The material needs to be uniform in shape and size, allowing for efficient packing of the column. High surface areas, 100+ m^2/g, to provide adequate space for the solutes to interact with the stationary phase. This high surface area needs to be provided by uniform shaped pores, or flow pathways, that limit the multiple unique paths a solute may take [12]. High mechanical strength is needed to allow for high pressures and flow rates. The support should not have characteristics that can interact with a solute, creating unwanted and uncontrolled retention of the solute [13].

1.1 Silica supports

Silica, SiO_2, and silicates not only make up the majority of the earth's crust, but also accounts for over 90% of HPLC columns' stationary phase supports [14]. Silica particles have many advantages to other types of stationary phase supports. They are rigid and able to withstand high pressures and flow rates, can be synthesized with a variety of diameters, pore sizes, and pore volumes, have high efficiencies due to its porosity and consistent pore structure, and can be covalently modified to give a variety of potential column chemistries [11, 13-15]. However, silica does possess some drawbacks. The siloxane bond, Si-O-Si, can be hydrolyzed. Increased temperature increases the hydrolysis rate [16, 17], so silica based stationary phases degrade faster at higher temperatures. The hydrolysis is also increased in acidic or basic environments, limiting the pH range of early stationary phases to pH 4-7 at temperatures less than 60 °C [11, 13, 14, 16]. The silanols, pKa between 4-5, are mostly deprotonated at these pHs, so a pH below 3 is needed

3

to help reduce poor separation of basic components caused by the electrostatic interactions between the negatively charged silanols and positively charged amines. This creates the need for more pH resistant robust silica supports to allow separations of bases with silica based stationary phases [13, 14].

The benefits of RP-LC and silica supports outweigh the drawbacks and research into creating stable silica based RP-LC stationary phases has been a major focus in chromatography for over 40 years, led by Unger [18, 19], Kirkland [2, 16, 20-24], Carr [25-27], and many others. There are three main approaches to creating stable silica stationary phases, slowing the hydrolysis by sterically limiting access to the ligand's siloxane bond, shielding the silica surface with polymers, and increasing the silica's resistance to hydrolysis.

1.1.1 Sterically protected stationary phases

Sterically protected stationary phases are the most popular stable stationary phases and are the standard for stable phases. Steric hindrance can slow reactions by restricting access to the reactive site. This idea has been used to make stationary phases more resistant to hydrolysis since the late 1980s. Kirkland and others at DuPont developed a sterically protected phase that consisted of diisopropylalkylsilane or a diisobutylalkylsilane that showed little degradation over time at pH < 3 [16]. The large bulky groups attached to the silicon atom in the silane shielded the siloxane bond from the acidic mobile phase. These phases provide high stability from pH 2 – 8 and are still sold and used today.

Bidentate ligand stationary phases were first developed with Glajch, Farlee, and Kirkland's sterically hindered phases in the late 1980s [16], but were not pursued further until the late 1990s [21]. Steric hindrance and increased ligand densities, compared to the sterically hindered phases,

can be achieved by using bidentate silanes, consisting of two silicon atoms joined by an ethyl or propyl linker chain [21]. These stationary phases exhibited reasonable stability at pH < 2 and high stability at pH 11. This allows the silica based stationary phase to be used from pH 2 to 11, allowing for the analysis of many types of molecules, including free neutral amines [24]. By their nature, sterically hindered phases have a reduced ligand density compared to other alkylsilane phases and endcapping is required if separations are to be carried out at high pH.

1.1.2 Polymer modified silica

For over 50 years silica particles have been modified with a polymeric layer to create chromatographic stationary phases. This type of stationary phase is still explored and developed today. A polymer coating on silica particles helps prevent hydrolysis at the silica surface, increasing the stability. The layer shields the surface from acidic and basic mobile phases extending the operable pH range of the silica particle. The particle can have the layer adsorbed onto the surface or the layer can be covalently attached to the surface. Both types of modification have the option of the polymerization happening on the surface or a preformed polymer can either be physically or chemically attached to the surface [28, 29].

Horvath first polymerically modified the surface of silica particles by polymerizing divinylbenzene and styrene on the surface of the particles. This resulted in a thick polymer layer that filled pores and decreased the chromatographic performance [30]. Besides solution based polymerization, more recent techniques involve adsorbing the monomers and radical initiator to the surface and polymerizing the dried mixture [31]. This reduces some of the negative aspects, but still results in decreased performance. The poor performance of these techniques has shifted the research focus to other methods of polymer modification [28].

The adsorption of preformed polymers to silica's surface can help reduce the problems of polymer thickness and clogged pores that plague the surface polymerization techniques. The preformed polymer stationary phases are usually made by mixing the polymers with the silica particles, and adsorbing them by evaporating the solvent. Often these polymers are then crosslinked to create a more stable surface [29]. The main polymers used for this technique include polybutadiene [19, 32], divinylbenzene-polystyrene [33], and polymethacrylate [34, 35]. The adsorption of polymers generally creates a patchwork covering of the silica particle. This can result in poor performance by the solutes interaction with the silica surface [32], and this limits their effectiveness in creating a highly stable silica stationary phase. The technique is still in use and is especially important for coating other metal oxide particles that will be discussed later.

Covalently attached polymer coatings are another method to help increase silica's stability. In the mid-1970s, Wheals used vinylsilane modified silica to covalently build various acrylate based polymeric layers from the surface. He noted reduced silanol activity, increased stability with multiple mobile phases, and that the polymer adhered to the particle longer than an adsorbed polymer [36]. Others have built polymeric coatings from the surface [34], but without controlled reactions the pores can clog and thick polymer layers can form reducing the performance of the stationary phases [28].

Most chemically bonded polymer coated stationary phases graft the preformed polymer to the surface of the silica. This technique gives reproducible polymer layers that provide an abundance of column chemistries and increase the silica supports stability [11, 28, 29]. In 1983, Kurganov first reported a chirally active polystyrene copolymerized with vinyltriethoxysilane being covalently attached to a silica particle [37]. The vinylsilane anchor is common for the many alkene based polymers used, like styrene or methacrylate based polymers [38, 39]. Other anchors

are used, including chlorophenylsilanes used in Carr's hypercrosslinked stationary phases [25, 40-42]. These phases show how post-polymerization modifications can create customizable stationary phases with a variety of column chemistries. Either by post-polymerization modification or grafting a variety of polymers to the surface of the silica particle, a large variety of column chemistries can be synthesized. Polymers made with peptides, polysaccharides, ethers, sulfonate or amine groups, along with styrene, butadiene, and divinylbenzene have all been used to create unique and stable stationary phases [43].

Cross-linking the polymers is not always needed, Ihara has created polymer chains of poly(4-vinylpyridine) [44] and poly(2-N-carbazolylethyl acrylate) [45] that are covalently attached to the silica without crosslinking. They adhere to the silica surface with hydrogen bonding and greatly reduce the mobile phase's and solutes' interaction with the silica. This helps increase the silica's stability.

Inorganic polymers based on poly(alkylsiloxanes) are also used to coat the silica particles and enhance their stability. An early commercial phase used poly(dimethylsiloxane) coated particles. The dimethyl substituents on the silica eliminated the hydroxyls reducing the silanol activity and the rate of hydrolysis [39]. The use of longer chain alkyl groups, like methyloctyl [46] and methyloctadecyl [47], helped to create stationary phases with similar chromatographic behavior to traditional RP-LC columns. Besides using polysiloxanes, silanes can be polymerized by using either trichloro or trialkoxy silanes when synthesizing stationary phases. In the presences of a small amount of water the silanes will form polymeric chains that bond to the silica in a vertical chain or horizontally across the surface. This results in a high surface coverage over 4 $\mu mol/m^2$ and can increase the stability of the RP-LC stationary phase [11, 48].

1.1.3 Robust silica particles

Over 50 years ago, Stöber introduced a process to synthesize monodisperse nonporous silica particles with diameters from 50 nm to 2.0 μm [49]. Shortly thereafter, methods were found to create monodisperse 2.0 to 10 μm diameter porous particles by coalescing the small 10 to 300 nm sols, small particles made by the Stöber process, into larger porous particles [50, 51]. The methods and chemicals used improved [52], giving the highly pure silica supports used today.

The surface area and porosity of the silica particle impacts the stability of the stationary phase. Silica particles that have a high surface area (over 300 m^2/g) and high porosity are less hydrolytically stable than those with lower surface areas and porosities. Particles made to have a very high surface area are usually made by coalescing soluble or fumed silicates. This results in thin pore walls that can be dissolved faster. While the lower surface area and lower porosity silicas are made using larger more insoluble sols and have thicker more uniform pore walls, creating a support that is more resistant to dissolution [22, 23].

Reactions with silica are slowed by the addition of carbon substituents to a silicon atom. The silicon atom has more electron density when bonded to carbon versus a silicon atom bonded to oxygen. The increased electron density reduces electrophilicity of the silicon atom, slowing hydrolysis and other reactions. The carbon substituents also sterically hinder a nucleophile's attack on the silicon atom. This is evident in the evolution of chemically bonded reversed-phase stationary phases, with alkylsilanes, Si-C, being more stable than the silicic esters, Si-O-R, originally used for stationary phases [53, 54]. In the mid-1970s, Unger helped develop organosilica hybrid particles that were synthesized using the standard tetraethoxysilane and an organotriethoxysilane, with benzyl or 1,2-dial-3-propoxypropyl organic groups [18]. It took nearly

25 years for an organosilica based stationary phase to make it to market, when Waters released their methyltrialkoxysilane hybrid phase that shows high stability up to pH 11.5 [55]. A few years later, Waters released an ethylene-bridged particle that showed even higher base stability and reduced silanol activity [56]. Continued research into organosilica particles has developed a stable high flow through phase [57], and particles with alkyl ligands, C18 and others, mixed into the particle [58].

1.2 Other stationary phase supports

Organic polymer particles are often used as an alternative to silica. They can be hydrophilic or hydrophobic, and can be functionalized covalently with stable carbon – carbon bonds. This gives polymeric phases their main advantage of a very broad pH range, generally from pH 1-13, enabling their use for many applications. Hydrophobic polymers, like divinylbenzene, poly(styrene-divinylbenzene), and poly(alkylmethacrylate), are used as reversed-phases or functionalized to have a hydrophilic nature for use with water for ion exchange and other applications. Hydrophilic polymers, such as poly(vinylalcohol) or poly(hydroxyalkylmethacrylate) [11], or hydrophobic polymers functionalized with hydrophilic ligands [59, 60] may be used for ion exchange or size exclusion chromatography. The hydrophilic surface eliminates any secondary retention characteristics that may interfere with the techniques.

Recent research into polymer stationary phases has produced interesting results. Molecularly imprinted polymers have been made to separate specific drugs [61], chiral molecules [62], biological molecules [63, 64], and other molecules [65]. These offer unique selectivity for the target molecule. The polymer particle itself has been "imprinted" on a porous silica particle

9

template, leaving the porous structure behind after dissolution of the silica particle [66]. A more efficient polymer column was made by mixing 2 μm nonporous and 4 μm porous polystyrene-divinylbenzene particles creating a better packed column that could withstand up to 10000 psi, high pressure for a polymer support [67].

Polymer based stationary phases provide excellent pH stability, but have many disadvantages that keep them from wide spread use. Polymer particles have low mechanical strength and deform at high pressures, limiting porous polymers to at most 6000 psi. This limits their use with many modern high pressure methods. Polymers have the tendency to swell or shrink in various solvents. Hydrophobic polymers swell in nonpolar solvents and shrink in more polar solvents and vice versa with hydrophilic polymers. This can cause problems because of the associated change in permeability and in retention characteristics with varying mobile phase composition. The polymer's pore structure decreases their efficiency with some molecules as well. The particles have larger pores with smaller pores inside. It is known that the resistance to mass transfer increases with small and flat rigid molecules due to their interaction with the small pores, decreasing the efficiency of the column [11, 68].

Metal oxides, other than silica, have been used in chromatography for a long time. Alumina, Al_2O_3, zirconia, ZrO_2, and titania, TiO_2, are the most common metal oxides that are in use. The primary benefits of these metal oxides are their high mechanical strength with excellent temperature and pH stability. They can be used regularly at 200 °C and from pH 1-13, much more extreme conditions than silica [68, 69]. Alumina, has been used in normal phase TLC and chromatography for decades, but has not been adequately developed for RP-LC [68, 69]. Titania phases are the least used support mainly due to the lack of availability of particles that permit their use in HPLC columns [69]. Zirconia supports have been studied and modified more than the others,

and can be found with a variety of particle sizes and pore diameters [26, 69]. The surface chemistries for the metal oxide particles are complex with hydroxyls, Lewis acid, and Lewis basic sites [69]. The approaches used for both using and blocking these active sites are similar for all the metal oxides, so zirconia will be the focus below.

Unlike silica, zirconia and the other metal oxides cannot undergo simple covalent modification. There have been few positive results silanizing the hydroxyl groups [70, 71], but little has come from them. Indicating the difficulty with the weak Zi-O-Si bond. One way to counter this is to polymerize tetraalkoxyzirconium onto the surface of a silica particle creating a zirconized silica particle. Then poly(alkylsiloxane) is polymerized on the surface to give a reversed phase highly pH resistant stationary phase [72-74]. The polymer coatings increase the binding strength between the zirconium and silicon esters, but these phases still can have strong Lewis acid sites and silanols exposed, reducing the efficiency and stability.

The most common way to modify metal oxide surfaces is to adsorb polymers on the surface [68], much like the adsorption of polymers on silica. Polybutadiene modified zirconia is the most common type recorded [68, 75]. The polymer is adsorbed to the surface by evaporation of the solvent and then crosslinked to add to the stability [75]. This gives the particles a hydrophobic reversed-phase characteristic, but the patchy coverage leaves Lewis acid sites that are detrimental to the chromatography of bases and ionizable analytes. For better separations of ions, several ion exchange phases have been synthesized using a zirconia support. Anion exchange phases can be made using a polyethyleneimine coating, allowing the controlled separation of anions [76]. Likewise, cation exchange phases have been made by adsorbing a poly(acrylic acid) anhydride or reacting the polyethyleneimine phase with succinic anhydride [77]. The versatility of the polymeric coverings and improved coverages allow zirconia to be a highly stable and useful

alternative to silica. However, the Lewis acid sites, lack of stable covalent bonds, and few particle size and porosity options readily available keep zirconia and metal oxide phases from dominating the market.

Carbon based supports offer high pH resistance and unique retention mechanisms. The most common form is a porous graphitic carbon support developed and evaluated by Knox in the early 1980s [78]. For over 30 years, there have been several commercially available porous graphitic support stationary phases based on this work [79]. The graphitic particles are made by pyrolyzing an organic phenol polymer in a highly porous silica particle. The silica was then dissolved and the porous carbon is them graphitized in a furnace. This gives a very hydrophobic surface that has strong pi-pi interactions and stereoselectivity caused by the flat sections of the graphitic surface [78, 79]. Coupled with the resistance to a broad pH range and these particles are often a useful stationary phase. However, they have a pressure limit of about 8000 psi, can easily be fouled by large molecules, and require high organic content mobile phases [11], limiting their usefulness.

Stationary phases have been developed recently that utilize diamonds and nanodiamonds to help improve the stability of the supports and offer unique selectivities. Polystyrene-divinylbenzene particles were synthesized with oxidized nanodiamonds creating a hybrid particle structure. The hybrid particles could withstand higher pressures than the pure polymer, and was used as a reversed-phase and modified to act as an anion exchange phase [80]. Core-shell particles have been produced by coating a diamond core with alternating layers of polyallylamine and nanodiamonds. The final amine rich layer is functionalized with epoxyoctadecane to create a C18 like stationary phase that is stable at high pressure and across a wide pH range [81]. Another application of this process used a carbon core to produce a very stable and efficient stationary

phase [82]. Nanodiamonds have also been used to coat silica particles to increase their stability and various column chemistries [83]. Both oxidized and hydrogenated nanodiamonds can be bonded to silica using a radical reaction. The oxidized nanodiamonds produce a hydrophilic stationary phase, while the hydrogenated ones act like a reversed-phase stationary phase [83].

Despite the recent achievements in developing alternatives to silica stationary phase supports, silica is still the most popular and most researched support. It's dominance in industry for decades has made it difficult to replace. Despite the futility, new phases are still being researched. As newer chromatographic techniques are developed that require extreme temperatures and pHs, new commercially viable supports may start to become more popular.

1.3 Thiol-ene and thiol-yne "click" chemistry stationary phases

The focus of this work is to develop a robust and simple way to produce higher stability silica based stationary phases. A group of simple, robust, and efficient reactions has been collected over the last twenty years using the term "click-chemistry" reactions. Sharpless coined the term in the early 2000s [84], as a class of reactions that have high yields, are insensitive to oxygen and water, have products that are easily purified, the reaction conditions are mild, the reactions are orthogonal to other click reactions, they can use a variety of starting materials, and they have stereospecificity and regiospecificity [84-86]. The use of these reactions to produce stationary phases opens the door for the simple production of a large variety of custom designed phases with unique selectivities and features.

The thiol-ene and thiol-yne click reactions are two related reactions that produce stable alkylsulfides. The thiol-ene reaction involves a radical reaction between a thiol and an alkene to

give the anti-Markonikov addition of the sulfide. The thiol-yne is the same, but two thiols react with the alkyne to give a 1,2-diakylsulfide. These reactions fit the click-chemistry criteria and can be performed under a variety of conditions and with many different thiols and alkenes or alkynes [85, 86]. Both reactions can be used to create polymers when dithiols and dienes/diynes are used, and are used in a wide array of materials.

The thiol-ene reaction has been used to synthesize HPLC stationary phases for over 25 years [87, 88]. Generally, it is used to link unique ligands onto thiol or vinyl functionalized silica to produce chiral stationary phases [87, 89, 90], ion exchange phases [88, 91-93], embedded polar phases [94], and more typical reversed-phase phases [95, 96]. Thiol-ene polymers are occasionally used, but mainly to synthesize polymeric monoliths [97, 98].

The thiol-yne reaction is seldom used to modify silica particles, with only a brush ligand phase [99] as the only other paper published besides the chapters in this work. The highly crosslinked polymers that can be synthesized with the thiol-yne reaction allow it to be used to create polymeric monoliths [100-103]. This work looks to expand the use of the thiol-yne polymer as a stationary phase on silica particles.

1.4 Scope of work

In this work the development of stationary phases synthesized by using the thiol-yne reaction to create a crosslinked surface on silica particles is discussed. The second chapter looks at the synthesis of a stationary phase made with thiol functionalized silica modified with diethynylbenzene and crosslinked with 1,6-hexanedithiol. The stability of the phase in a broad pH range is studied and the chromatographic properties are reported. The third chapter discusses the

unique shape selectivity of the stationary phase described in chapter two. It was found that the phase possesses electron donating charge-transfer characteristics that enhance its shape selectivity. The fourth chapter discusses another crosslinked thiol-yne phase made with 1,7-octadiyne instead of diethynylbenzene. The chromatographic characteristics and the stability of the stationary phase are discussed.

2.0 A pH-stable, Crosslinked Stationary Phase Based on the Thiol-yne Reaction

2.1 Introduction

Extremes of pH and temperature can be used to improve chromatographic separations of complex mixtures when the stationary phases are stable to the extreme conditions [4, 104-111]. Silica-based stationary phases have limited stability in such conditions without some form of protection from hydrolysis or dissolution [2, 22, 112]. More robust silica-based stationary phases have been made using sterically protected silanes [2, 16, 21] and occasionally polymer coated silica particles [113, 114]. Carr developed a hyper-cross-linked stationary phase that is highly stable at low pH and high temperatures [25, 40-42, 115, 116]. These phases, which are prepared using the Friedel-Crafts reaction, can have a variety of functional groups to change the column chemistry. This gives very robust and customizable stationary phases. However, the Friedel-Crafts reaction has some drawbacks. The adsorption of the metal catalyst can harm chromatographic performance, and the reaction requires very dry and carefully maintained conditions for a successful synthesis.

The thiol-yne reaction is a "click-chemistry" reaction that can produce a highly crosslinked polymer [85, 86, 117, 118]. This radical reaction meets the requirements of a "click-chemistry"

reaction: it has a high yield, is insensitive to oxygen and water, products are easily purified, the reaction conditions are mild, the reaction is orthogonal to other click reactions, it can use a variety of starting materials, and it has stereospecificity and regiospecificity [84, 85, 118]. A crosslinked polymer can be synthesized using a variety of alkynes and thiol-containing molecules, as shown in Figure 2.1. This reaction can be used to modify surfaces [86, 117-119] and has been used a small extent in the synthesis of HPLC stationary phases. It has primarily been used to create thiol-yne polymeric monoliths for electrochromatography and liquid chromatography [100-103]. As far as we are aware, only Zou's group has created a particulate stationary phase with the thiol-yne reaction, a multi-branched C18 brush like stationary phase [99]. This preparation did not include crosslinking or assessment of the stability of the phase. Here, we introduce the thiol-yne reaction as a means to make a crosslinked stationary phase that can increase the pH stability of silica supports.
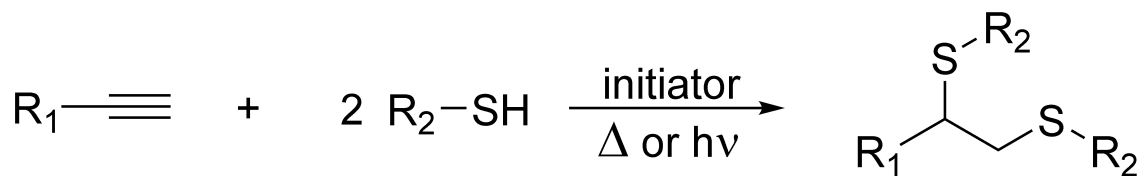
Figure 2.1: The thiol-yne reaction.

2.2 Experimental

2.2.1 Chemicals

Synthesis Reagents: All reagents were ACS grade or better and used without further purification. Extra dry toluene over molecular sieves and 1,4-diethynylbenzene (DEB) were

17

purchased from Acros Organics (Geel, Belgium). The 3-mercaptopropyltrimethoxysilane (MPTMS), benzene, hexanes, acetonitrile (ACN), and acetone were from Fisher Chemical (Fairlawn, NJ). Triethylamine, 2,2′-azobis(2-methylpropionitrile) (AIBN), and 1,6-hexanedithiol were purchased from Sigma-Aldrich (St. Louis, MO). The water used was prepared using a Millipore Milli-Q Synthesis A10 (Billerica, MA). The Zorbax RX-Sil 1.8 μm silica support (180 m^2/g, 8 nm pore size) and the Zorbax SB-C18 (1.8 μm, 180 m^2/g, 8 nm pore size) was gifted to us by Agilent Technologies (Palo Alto, CA).

HPLC reagents: Unless mentioned the reagents were ACS grade or higher rated. The LC-MS grade methanol and acetonitrile, phosphoric acid (80%), ammonium hydroxide (30%), glacial acetic acid, and sodium hydroxide were purchased from Fisher Chemical (Fair Lawn, NJ). Potassium phosphate dibasic and potassium phosphate monobasic were from E. Merck (Darmstadt, Germany). The trifluoroacetic acid was purchased from Acros Organics (Geel, Belgium). The water was prepared with the Milli-Q system above. Mobile phases were prepared with the indicated volume percentages.

HPLC solutes: All solutes were purchased as ACS grade of better and used without further purification. Butylbenzene and pentylbenzene were purchased from Alfa Aesar (Ward Hill, MA). The *o*-terphenyl, ethyl 4-hydroxybenzoate (ethylparaben), caffeine, heptanophenone, octanophenone and uracil were purchased from Sigma Aldrich (St. Louis, MO). Triphenylene and benzylamine were from Acros Organics (Geel, Belgium). The methyl, propyl, and butyl 4-hydroxybenzoate (parabens), and phenol were from Fluka (Buchs, Switzerland). For the hydrophobic subtraction model characterization, the amitriptyline, *n*-butylbenzoic acid, *N,N*-diethylacetamide, 5,5-diphenylhydantoin, nortriptyline, *p*-nitrophenol, *trans*-chalcone, and berberine were provided by Dr. Dwight Stoll at Gustavus Adolphus College (St. Peter, MN). The

5-phenyl-1-pentanol, ethylbenzene, toluene, *N*,*N*-dimethylacetamide, acetophenone, anisole, and benzonitrile were purchased from Sigma Aldrich (St. Louis, MO). The mefenamic acid was purchased from TCI America (Portland, OR). The thiourea was from Fisher Chemical (Fairlawn, NJ).

Column packing reagents: The HPLC grade methanol and ethyl acetate were purchased from Sigma-Aldrich (St. Louis, MO). HPLC grade isopropanol was from Fisher Chemical (Fair Lawn, NJ). The formamide was from Acros Organics (Geel, Belgium). Kasil 1 was given to us by PQ Corporation (Valley Forge, PA). GF/C glass fiber filters were obtained from Whatman (Buckinghamshire, UK).

2.2.2 Synthesis of the crosslinked stationary phase

2.2.2.1 Synthesis of thiol silica

About 16 mL of extra dry toluene, stored over molecular sieves, were added to 2.002 g of 1.8 μm Zorbax RX-Sil silica particles that had been dried overnight in a 100 °C vacuum oven. Triethylamine (400 μL) was added and the solution was stirred for five minutes, sonicated for one minute, and stirred for three more minutes before adding 1.61 mL of MPTMS. The mixture was stirred and refluxed under nitrogen dried by passage through calcium sulfate for about 44 h. The solution was vacuum filtered using a Millipore 0.45 nm nylon membrane (Burlington, MA). The flask was rinsed with 15 mL of toluene and poured over the particles on the membrane. The particles were rinsed two times with 15 mL of each of the following solvents in order: benzene, hexanes, ACN, water, and one more ACN rinse. The thiol-functionalized silica was dried at 95 °C in a vacuum oven overnight.

2.2.2.2 Synthesis of DEB silica

Around 10 mL of extra dry toluene was added to 1.120 g of the thiol silica, 32.8 mg AIBN, and 252 mg of DEB in a round bottom flask. The mixture was sonicated for one minute and stirred for two minutes before refluxing for 28 h. The suspension was transferred to centrifuge tubes, the flask was rinsed and the rinse solution was added to the centrifuge tubes. These were centrifuged and the liquid decanted. The particles were rinsed one time using 15 mL of toluene, resuspended in 15 mL of toluene, and vacuum filtered using a Millipore 0.45 nm nylon membrane. The particles were rinsed two times with 15 mL of each of the following solvents: hexanes, ACN, water, and acetone and then were dried overnight in a 100 °C vacuum oven.

2.2.2.3 Synthesis of the crosslinked stationary phase

About 5 mL of extra dry toluene was added to 298 mg of DEB silica and 19.9 mg AIBN, and stirred for three min. 1,6-hexanedithiol, 100 μL, was added to the suspension and refluxing was begun for 24 h. 2 mL of toluene was added to the suspension, and the mixture was refluxed 22 h. The suspension plus 10 mL of toluene rinse was centrifuged and the liquid decanted. The particles were rinsed twice with toluene, ACN, 20 mM phosphoric acid (pH 2.08), water, and one time with acetone by adding in each case 10 mL of the liquid, suspending the particles, centrifuging, and decanting the liquid. The particles were transferred to a Petri dish with 5 mL of acetone to dry in a 100 °C oven until the acetone was evaporated. The particles were dried overnight in a 100 °C vacuum oven.

2.2.3 Elemental analysis

A small sample of the product of each step was sent to Atlantic Microlabs, Inc. (Norcross, GA) for analysis of %C, %H, and %S. The surface coverage of the thiol, DEB, and crosslinking moieties were calculated using equation 1, adapted from Carr [116]. Where *%X* is the elemental percent of sulfur or carbon added during the synthesis step, M_X is the atomic mass of sulfur or carbon, N_X is the number of sulfur or carbon atoms in the added molecule or ligand, S_A is the surface area of the silica, and *%C*, *%H*, and *%S* are the mass percents of the respective elements after the synthesis.

$$\mu mol/m^2 = \frac{\%X \times 10^6}{M_X \times N_X \times S_A \times (100 - \%C - \%H - \%S)}$$

(1)

2.2.4 Column packing

Column blanks: Approximately 15 cm pieces of 150 μm ID, 360 μm OD fused-silica capillary from Polymicro Technologies (Pheonix, AZ) were used for columns. A glass fiber sol-gel frit was made at one end of the capillary piece using the method developed by Maiolica et al. [120]. Briefly, 100 μL 25% formamide was added to 100 μL Kasil 1 and dropped onto a GF/C filter. The capillary end was pushed into the wet filter three times and heated at 85 ºC overnight.

Packed columns: Capillary columns were packed using the downward slurry method with a Model DSHF-302 pneumatic amplification pump from Haskel (Burbank, CA). A 65 mg/mL slurry of the crosslinked stationary phase was made in ethyl acetate, and the 1.8 μm Zorbax SB-C18 (a gift from Agilent, Palo Alto, CA) was suspended in isopropanol. An aliquot of the slurry,

45 µL, was added to the system and, using methanol, brought to 20000 psi for 30 min. The columns were trimmed to length, installed on the HPLC system, and flushed with mobile phase.

2.2.5 HPLC instrumentation

The HPLC system was a Thermo Fisher Ultimate 3000 RSLC Nano System (Germering, Germany). The NCS-3500RS pump and column oven was equipped with the capillary flow selector. Samples were loaded using the WPS-3000SL autosampler. The VWD-3400RS Variable Wavelength Detector had a 45 nL capillary flow cell installed. The system was controlled with Chromeleon 7 software run on a PC. The mobile phase was degassed using a model G1379B Agilent 1260 µ-Degasser (Palo Alto, CA).

2.2.6 Tanaka test

The Tanaka test [121] was run under the conditions set by Euerby et al. [122]. The temperature was 40 $^{\circ}$C with an adjusted flow rate of 1.06 µL/min, a timed 148 nL injection volume, and the UV detector was set at 254 nm for all the samples except butylbenzene and pentylbenzene where 205 nm was used. The aqueous and organic portions of the mobile phases were mixed by the Thermo HPLC pump after passing through the degasser. Analyte stock solutions were made in methanol or water at 25 mM, and diluted to 62.5 µM, 31 µM for *o*-terphenyl and triphenylene, in mobile phase with 62.5 µM uracil added as the void marker. Butylbenzene, pentylbenzene, *o*-terphenyl, and triphenylene were run in 80:20 methanol:water. Caffeine and phenol were run in 30:70 methanol:water. Benzylamine and phenol were run in 30:70 methanol:phosphate buffer, 20

mM at pH 2.62 and pH 7.56. The samples were run five times to determine the 95% confidence intervals.

2.2.7 Hydrophobic subtraction model characterization

The CTY stationary phase was evaluated using the hydrophobic subtraction model (HSM) [1, 123, 124]. The procedure was the same as that of Snyder and Dolan [123, 124], except the solutes were prepared at 5.0 µg/mL. A 60 mM potassium phosphate pH 2.80 buffer was made and mixed online with acetonitrile, 50:50. The mixing was tested by manually preparing a 50:50 buffer/acetonitrile sample, injecting it, and ensuring that there were no changes in the baseline following injection. The column was flushed with the mobile phase and then left to sit without flow to equilibrate for 12-16 h, followed by 20 min of flow before injecting the samples. The flow rate for the 150 µm ID X 10 cm column was set at 2.12 µL/min, 12 cm/min, with a column temperature of 35 °C, and the UV detector set at 205 nm. Samples of the solutes listed above were prepared in the 50:50 buffer/acetonitrile mobile phase, and 70 nL samples were injected onto the column using a timed injection. Each injection was performed in triplicate. Each solute was run by itself to identify the components of the mixtures by their retention times. Thiourea was retained, so a 62.5 µM sample of uracil in the mobile phase was used to determine the void time. The *cis*-chalcone sample was prepared by letting a 1 mg/mL solution of *trans*-chalcone in acetonitrile sit in front of a window for a day to isomerize. A 60 mM potassium phosphate pH 7.00 buffer was made to run the berberine sample in the 50:50 pH 7.00 buffer/acetonitrile mobile phase. The berberine peak was not seen at pH 7.00 despite increasing the injection volume.

The retention factors were calculated using t_0 from uracil's retention. The selectivity, α, was determined for each solute versus ethylbenzene. The HSM ($\mathbf{H}$, $\mathbf{S^*}$, . . .) parameters were calculated by multiple linear regression of equation 2 using the solute parameters (η', σ', β', α', and κ') given by Dolan and Snyder [123, 124].

$$\log \alpha = \log\left(\frac{k}{k_{EB}}\right) = \eta'\boldsymbol{H} - \sigma'\boldsymbol{S^*} + \beta'\boldsymbol{A} + \alpha'\boldsymbol{B} + \kappa'\boldsymbol{C} \qquad (2)$$

2.2.8 Stability in acid eluents

2.2.8.1 Low pH with 85:15 aqueous acid:acetonitrile mobile phase

A 62.5 µM sample of methyl, ethyl, propyl, and butylparaben with uracil as the void marker was made in 85:15 water:acetonitrile. The mobile phase was 85:15 5% TFA (pH 0.53):ACN with a flow rate of 6 µL/min. Note that the pH electrode was calibrated at a pH about 1.5 units higher than the value measured for the TFA solution. This measurement, and the one referred to in section 2.8.2 below, should be viewed at being approximate. The oven temperature was set at 70 °C, and the detector wavelength was set at 254 nm. Approximately every 11 minutes a 148 nL sample was injected onto a 6 cm long crosslinked phase column or a 6 cm long SB-C18 column for 114 h. The column degradation was measured using the retention factor of butylparaben.

2.2.8.2 Low pH with 50:50 aqueous acid:acetonitrile mobile phase

A mobile phase with a 50:50 5% TFA (pH 0.56):acetonitrile composition was used to evaluate the stationary phases' stability at low pH using newly packed 10 cm long columns. The mobile phase was mixed online. The flow was 4.0 µL/min, the UV detector was set at 254 nm, and the column oven set at 70 °C. For the SB-C18 column, 148 nL of a 62.5 µM mixture of uracil,

heptanophenone, and octanophenone was injected about every 31 min. The CTY column did not retain octanophenone well at the 50:50 mobile phase composition, so an alternative solute was used. The CTY phase had 148 nL of a 62.5 μM uracil, 50 μM *o*-terphenyl, and 50 μM triphenylene sample injected about every 31 min. All samples were made in the mobile phase. The column degradation was monitored using the percent change of octanophenone and triphenylene's retention factor.

2.2.9 Stability in basic eluent

To evaluate the CTY and SB-C18 stationary phases' stabilities at high pH, the columns had a basic mobile phase flow through them for an hour, then were rinsed and tested with an unbuffered mobile phase. The process was repeated two more times for three hours of exposure, as described in the following. A pH 12.6 20 mM NaOH solution was premixed with acetonitrile to make a 50:50 (v/v) 20 mM NaOH:acetonitrile mobile phase. The pH 12.6 mobile phase was pumped through the column, but not through the detector, at 1.5 μL/min for 1 h at 70 °C. The mobile phase was switched to 80:20 water:acetonitrile and the column was flushed at 4.0 μL/min at 50 °C for an hour and then connected to the UV detector. Flow was continued until equilibrated, usually 2-6 h until an injection of parabens had a consistent retention factor. After equilibration, the column was tested by injecting 148 nL of a 62.5 μM sample of uracil, methyl, ethyl, propyl, and butylparaben made in 80:20 water:acetonitrile. For testing the flow rate was 4.0 μL/min, with the oven at 50 °C, and the UV detector at 254 nm. The percent change in the retention factor of butylparaben was used to evaluate the columns. The tests started with new 10 cm long columns.

The plate counts were determined using the Foley-Dorsey method [125] and converted to plates per meter.

2.3 Results and discussion

2.3.1 Elemental analysis

The crosslinked thiol-yne (CTY) stationary phase was made in a stepwise procedure to control the thickness of the polymer, shown in Figure 2.2. Adding the monomers at the same time could create a thick polymer that could clog the pores of the silica particles. A propylthiol ligand was added to silica using MPTMS. The elemental analysis data, shown in Table 2.1, can be used to assess the success of the reaction. The surface coverage of the thiol ligands from the first step is based on the percent sulfur, since there is only one sulfur per ligand. The propylthiol coverage based on 2.88 wt% sulfur is 5.40 μmol/m^2, implying that about 67% of the the silanols reacted. This is high enough to indicate that polymerization of the MPTMS occurred [126, 127]. The addition of DEB should not change the sulfur content. With that assumption, the added carbon is 1.63 times the initial carbon from the mercaptopropyl group alone. This calculation assumes that all of the increase in the particle's weight is due to the carbon in the DEB. It accounts for the added carbon, but not the added (or lost) hydrogens. It also assumes that there is no loss of carbon from hydrolysis of methoxy groups from the silane. This increase is less than expected for the addition of one DEB to each thiol. If all of the thiol ligands were functionalized the %C should have increased by more than 10 %C. However, it only increased about 6 %C from the thiol amount, from about 4 %C to almost 10 %C. There are two things that could have happened: some thiols

did not react with the DEB, or one DEB added to two thiols creating a bridged ligand, shown in

Figure 2.3A. A surface coverage of close to five µmol/m^2 leads to the expectation that there are

three thiols/nm^2, so a single DEB molecule can have easy access to multiple thiols.

A.
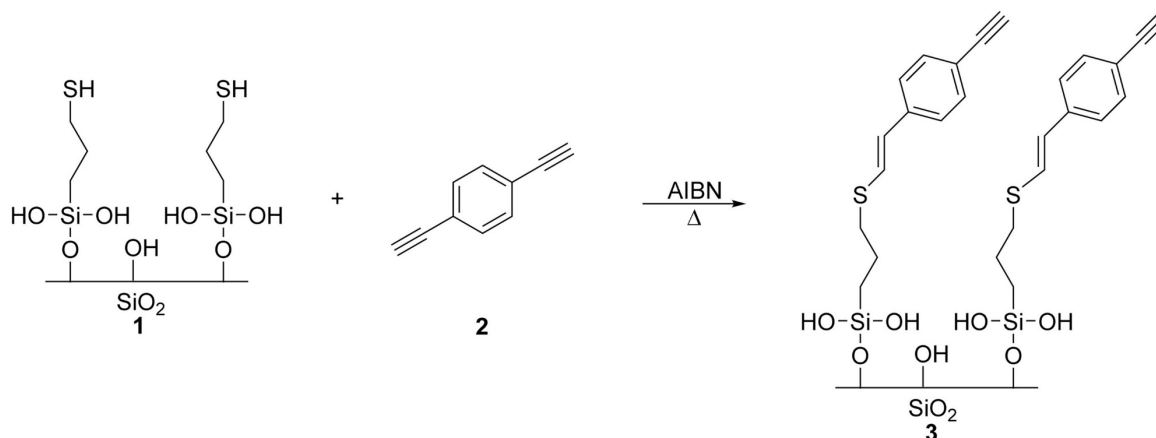
B.
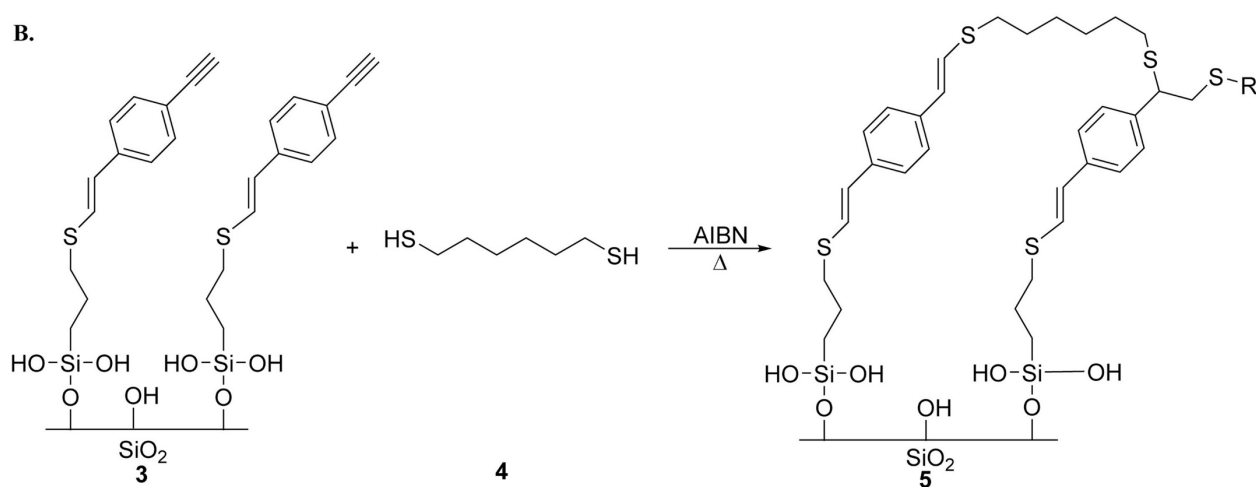
Figure 2.2: Crosslinked stationary phase synthesis. A. Thiol functionalized silica, 1, is reacted with diethynylbenzene (DEB), 2, to produce DEB functionalized silica particles, 3. B. Crosslinking is performed using 1,6-hexanedithiol, 4, to give the crosslinked polymer, 5. Reactions were performed in refluxing toluene using azobisisobutyronitrile (AIBN) to catalyze the thiol-yne reactions.

Table 2.1 : Elemental analysis at each step of the synthesis

Added Molecule	% C	% H	% S	Coverage (μmol/m^2)
Thiol	4.04	0.75	2.88	5.40
DEB	9.97	1.00	2.66	3.18
Crosslinker	12.49	1.41	5.01	2.27

The addition of the dithiol crosslinker doubles the amount of sulfur per square meter. This indicates that about one 1,6-hexanedithiol molecule was added per DEB ligand. The %C is consistent with the addition of one dithiol per DEB. In the typical thiol-yne reaction shown Figure 2.1, two thiols should react with one alkyne. The crosslinking step should add three additional sulfur atoms to the DEB ligand, but this does not happen here. There are a couple of reasons that are consistent with a less than complete reaction. It has been reported that benzylalkynes have slower reactions with thiols than alkylalkynes, and often benzylalkynes only add one thiol group [118, 128]. This helps explain the limited addition of the crosslinker. Also, to the degree that DEB creates a bridged ligand with two close propylthiol ligands, as described above, there are fewer alkynes available to react with the crosslinker. From these data, a plausible idea of the structure of the crosslinked stationary phase can be proposed and is shown in Figure 2.3.
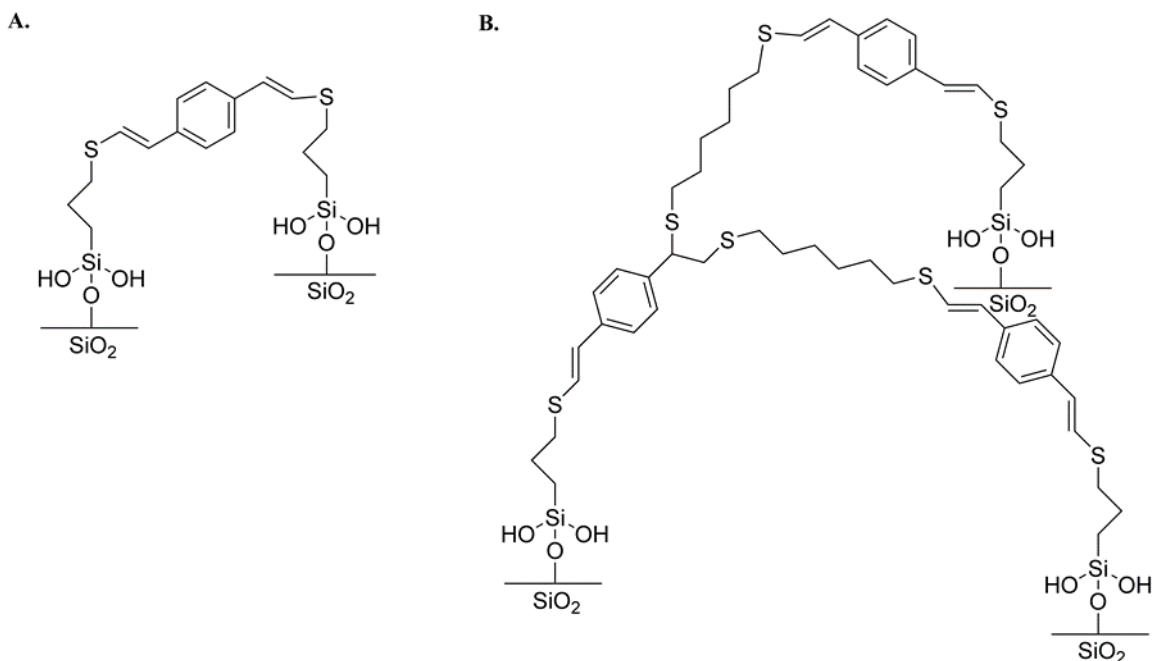
Figure 2.3: Possible structure of crosslinked stationary phase. A. The bidentate DEB ligand that is likely found on the silica. B. Example of the dithiol crosslinker with the majority of the DEB only substituted one time. The surface is likely a mixture of A and B.

2.3.2   The Tanaka test

To understand the crosslinked stationary phase's potential utility the Tanaka test was performed [121, 122]. This characterization method uses seven solutes and four mobile phase compositions to determine the ligand coverage, hydrophobicity or methylene selectivity, shape selectivity, hydrogen bond capacity, and the ion exchange characteristics. The results for the CTY phase are shown in Table 2.2. The values for the Zorbax SB-C18 stationary phase and the typical ranges for reverse phased columns were taken from Euerby et al. [122, 129, 130].

Table 2.2: Tanaka test data for the crosslinked polymer

Parameter	Measurement	Property	CTY	SB-C18 [122]	Typical Range [122]
k'_{pb}	k' pentylbenzene	Ligand coverage	0.42 ± 0.02	6.00	~6.0
α_{CH2}	$\dfrac{\text{k' pentylbenzene}}{\text{k' butylbenzene}}$	Hydrophobicity	1.21 ± 0.05	1.49	1.3 – 1.6
$\alpha_{T/O}$	$\dfrac{\text{k' triphenylene}}{\text{k' } o\text{-terphenyl}}$	Shape selectivity	4.91 ± 0.08	1.20	1.1 - 1.5
$\alpha_{C/P}$	$\dfrac{\text{k' caffeine}}{\text{k' phenol}}$	Hydrogen bonding capacity	0.61 ± 0.01	0.65	0.3 - 0.6

The ion exchange characteristics are not shown because the benzylamine peak was not seen at pH 2.62 or pH 7.56. The very long retention at pH 2.62 shows that the benzylamine was retained with intermolecular forces other than the cation's interaction with deprotonated silanols. The silica support also has a high coverage of the conjugated sulfur-benzene moieties (up to 3.2 μmol/m^2) that can participate as electron donors in charge transfer complexes with solutes [131]. Dougherty has shown that cation-pi interactions in aqueous matrices usually have binding energies from 8-21 kJ/mol [132]. An interaction between the charged amine and the pi systems along the surface of the stationary phase in this energy range would help account for the high retention of benzylamine even at low pH. There are also free thiols on the surface that over time could oxidize to sulfonates, adding to the cation exchange characteristics of the CTY phase.

The CTY phase showed some similarities with typical reverse phase columns. The hydrophobicity value of 1.21 ± 0.05 is close to typical columns. The hydrogen bonding capacity is very close to the SB-C18 phase and within the range of typical reversed-phase columns. There are some big differences as well. The k' of pentylbenzene is very low, 0.42 ± 0.02, indicating low

ligand coverage. This is to be expected with a stationary phase that goes along the surface of the silica without any brush type ligands. This low value supports the structures shown in Figure 2.3, that the ligands are attached to the surface at both ends in a crosslinked structure.

The value that makes the CTY phase very unusual is the shape selectivity. The $\alpha_{T/O}$ = 4.91 ± 0.08 value is the highest found under standard Tanaka conditions, with a value almost twice as high as the highest reported value for commercially available reversed phases - close to 2.5. The flat triphenylene molecule was retained significantly more than *o*-terphenyl with its similar composition but bulkier shape. Sander and Wise presented the "slot" model for shape selectivity [9, 133, 134]. Briefly, holes or slots in the stationary phase accommodate flat molecules but not bulkier molecules. The ability to fit into the slots in the stationary phase gives the flat molecule more retention. Phases that have high ligand density have more shape selectivity. The CTY phase has a fairly high surface coverage and with the crosslinking may have holes or slots that may give rise to shape selectivity. Another option for the shape selectivity may be the π–π interactions of the aromatic solutes and the DEB based stationary phase. Charge transfer interactions are known to give shape selectivity as well [135]. Some charge transfer phases developed by Ihara have shown very high $\alpha_{T/O}$ values near 15 under reverse phase conditions that are similar to but different from those used here [44, 45, 136]. Lucy recently showed that a 3-(2,4-dinitroanilino)propyl (DNAP) charge transfer phase has an $\alpha_{T/O}$ over 22 when used with normal phase conditions. A deeper exploration of the CTY phase's mechanism of shape selectivity has been reported in another paper [131].

2.3.3 Hydrophobic subtraction model characteristics

The hydrophobic subtraction model is a common method to characterize reversed-phase LC columns [1, 123, 124, 137]. The column's hydrophobicity, H, the steric resistance to insertion, S^*, column hydrogen-bond acidity, A, the column hydrogen-bond basicity, B, and the column cation-exchange activity, C, can be derived from the linear regression of equation 2. The values used for the regression, the solute parameters from Snyder and Dolan [123], the experimental retention data, and the regression data are given in Table A.1, Table A.2, and Table A.3 in Appendix A, respectively. The calculated column parameters for the CTY phase, with the 95% confidence intervals, are given in Table 2.3.

Table 2.3: Derived HSM parameters for the CTY phase

Coefficient	CTY	95% Confidence	SB-C18 [38]
H	0.640	$\pm$ 0.156	0.995
S^*	0.352	$\pm$ 0.208	-0.029
A	-0.612	$\pm$ 0.427	0.262
B	0.081	$\pm$ 0.162	-0.003
C	3.003	$\pm$ 0.316	0.136

The CTY phase possesses unique HSM coefficient values. The hydrophobicity is low compared to C18 columns, but is in the range of some C4, pentafluoro, and cyano phases. The steric selectivity is very different to that of typical reverse phase stationary phases. Generally, S^* is small and may be positive or negative, but the CTY phase has a large positive value. Higher surface coverages can increase S^*, but an increase from about 2.0 $\mu mol/m^2$ to 5.0 $\mu mol/m^2$ only increases S^* by 0.08 [6]. The positive S^* provides evidence that the thiol-yne crosslinking was successful and there are no brush-like ligands or cavities for the solute to enter that would add to

the retention. If the crosslinking did not occur, the ligands would be brush-like and would allow solute insertion to occur, creating a more negative value of S^*. The large negative value for A indicates that the silanols on the silica surface do not act as H-bond donors. This implies that the crosslinked polymer was formed on the surface of the silica restricting the access to the silanols. Large positive S^* and large negative A values are found on very few commercial columns. The column with the closest S^* and A values is another polymer coated silica based stationary phase, the Purospher RP-18 from Merck, with values of 0.254 for S^* and -0.560 for A [1]. The value for B is in the range of most other stationary phases, with a small positive value indicating there are basic H-bonding sites on the surface that can increase the retention. This is expected due to the embedded sulfur atoms, probable sulfonates from oxidized unreacted thiols, and the electron donating charge transfer moieties [131]. These features also contribute to the very large C values. The only commercial column with a close C term is the Primesep A mixed mode strong cation exchange column from SIELC, that has $C = 2.732$.

The CTY's unique charge transfer column chemistry may contribute to the large 95% confidence intervals in the HSM values derived from the regression. Carr et al., noted that the presence of $\pi-\pi$ interactions would benefit from a sixth term in the HSM equation that accounts for these interactions [6]. In the case of the CTY phase, the $\pi-\pi$ interactions are the charge transfer interactions. The absence of this extra term may be responsible for the modest correlation that the CTY phase's retention behavior has with the HSM solute characteristics. Overall though, the HSM characterization, as well as the Tanaka characterization, show that the CTY phase possesses a very unique column chemistry.

2.3.4 Low pH stability

2.3.4.1 85% pH 0.5 aqueous mobile phase

The stabilities of the CTY and Zorbax SB-C18 phases at low pH were determined using 85:15 pH 0.53 5% TFA:acetonitrile at 70 °C. These conditions were similar to the testing that Carr's group performed on their hyper-crosslinked phase, but they were able to increase the temperature to 150 °C to accelerate the aging [25, 40, 41, 115]. To determine the stability, the k' of butylparaben was monitored for 114 h or almost 41000 column volumes, shown in Figure 2.4A. The CTY phase showed no significant change over the course of the study with the k' at 114 h only 0.6% less than the k' during the first hour. The chromatograms at hour one and hour 114 are shown in Figure 2.4B. Both chromatograms look almost identical, with the main difference resulting from the concentrations of the solutes. There is an interesting improvement in the plate count and the asymmetry that may be due to monomeric and non-crosslinked ligands being removed from the stationary phase and improving the efficiency.
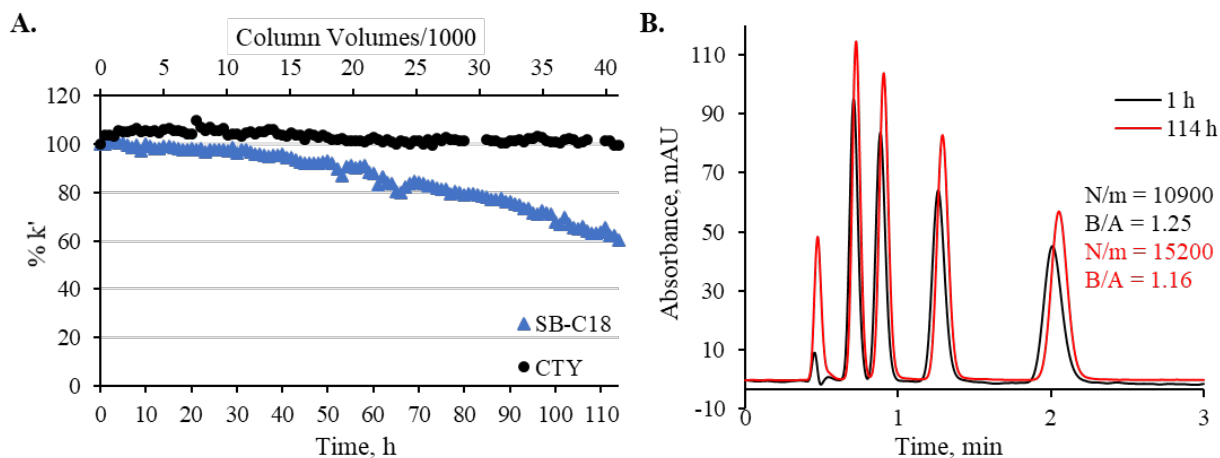
Figure 2.4: Low pH, 15% ACN, degradation study. A. Percent of original retention factor, k', for butylparaben versus hours/column volumes exposed to 5% TFA mobile phase, pH 0.53. Conditions were the same for the CTY phase, •, and the Zorbax SB-C18 phase, ▲, 85:15, 5% TFA:Acetonitrile, 70 °C, 6 μL/min. B. Chromatograms at 1 h, black, and 114 h, red, of uracil, methylparaben, ethylparaben, propylparaben, and butylparaben. Concentrations at 1 h were 50 μM and at 114 h were 62.5 μM. The N/m, as calculated with the Foley-Dorsey equation, and the asymmetry factors, B/A, are listed by the butylparaben peak. The conditions were the same as in A.

2.3.4.2 50% pH 0.5 aqueous mobile phase

To ensure any hydrolyzed ligand would be eluted from the column, the low pH degradation study was performed with 50% organic modifier in the mobile phase. Figure 2.5A shows octanophenone's retention factor on the SB-C18 phase and triphenylene's retention factor on the CTY phase. (The retention factor for octanophenone on the CTY phase was below 1.0 and the data were less reproducible than with a more highly retained solute, triphenylene. The octanophenone data for the CTY phase can be found in Appendix A, Fig. A 2.) Solute retention on the SB-C18 dropped to about 73% after about the same number of column volumes as described above (85% aqueous mobile phase) - almost 35000 column volumes. With the lower flow rate this took 144 h,

and the testing was stopped there. The CTY phase's retentivity was still about 89% of the k' at 35000 column volumes and was tested until it went below 75%. It took the CTY phase well over 50000 column volumes and four more days for the retention factor to get below 75%. As the SB-C18 phase degraded, the plate count dropped from 111000 N/m to 90900 N/m, a loss of almost 20%. The chromatograms for the CTY phase at 240 column volumes, 1 h, and 34600 column volumes, 144 h, are shown in Figure 2.5B. It is apparent that the retention declines slightly in that time and that the plate count increases while the asymmetry remains about the same. CTY's plate count improved during the first 35000 column volumes, going from 7430 N/m to 9900 N/m, improving about 30%. After 10 days and over 55000 column volumes the plate count had increased 59%, to about 11800 N/m. The increase in efficiency shows that the stationary phase's surface coverage was not optimized, and as the DEB ligands are hydrolyzed and removed the column becomes more efficient. This idea is supported by our observation that a low surface coverage DEB based stationary phase has increased efficiency compared to the high-coverage CTY phase [131].
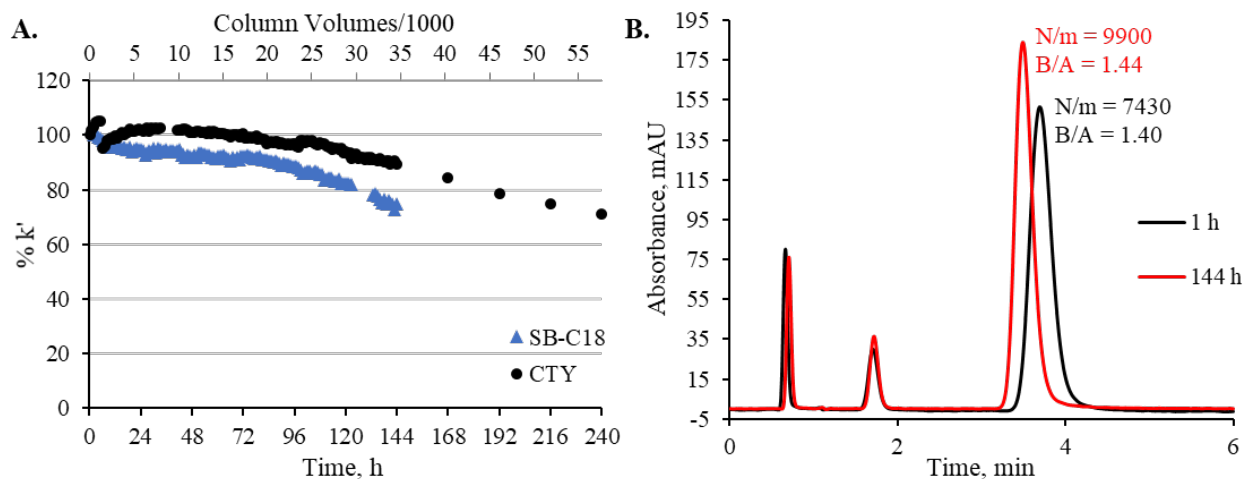
Figure 2.5: Low pH, 50% ACN, degradation study. A. Percent of original retention factor, k', for octanophenone for SB-C18 and triphenylene for CTY versus hours/column volumes exposed to 5% TFA mobile phase, pH 0.56. Conditions were the same for the CTY phase, •, and the Zorbax SB-C18 phase, ▲, 50:50, 5% TFA:Acetonitrile, 70 ºC, 4 μL/min. B. Chromatograms at 1 h, black, and 144 h, red, of 62.5 μM uracil, 50 μM *o*-terphenyl and 50 μM triphenylene. The N/m, as calculated with the Foley-Dorsey equation, and the asymmetry factors, B/A, are listed by the triphenylene peak. The conditions were the same as in A.

2.3.5 Stability at high pH

The CTY stationary phase's stability at intermediate pH and high pH was determined. The phase showed good stability at pH 9.0, see Appendix A sections A2 and A3. A separate CTY column was also aged using a 50:50 20 mM NaOH (pH12.6):acetonitrile mobile phase. After one hour of exposure to the high pH mobile phase at 70 ºC, the column's retentivity was measured using a paraben sample with an 80:20 water:acetonitrile mobile phase at 50 ºC. The CTY's performance was compared to the SB-C18 stationary phase, shown in Figure 2.6A. The SB-C18 column clogged towards the end of the second hour of exposure to the pH 12.6 mobile phase, and there was about a 4-5 mm void at the head of the column. Prior to continuing the testing, one cm

was cut from the head of the SB-C18 capillary column. At the end of the third hour of base exposure the SB-C18 column clogged again. The void was now about 3-4 mm, so a length of 0.5 cm of the column was removed to allow flow through the column again. The plate count per meter, used to account for the changing column length, continued to drop down to less than 40% of the N/m before the exposure to base. The CTY column went through all three hours of exposure to the base without a significant pressure change going from 469 bar at the beginning to 473 bar after three hours of exposure to the basic eluent. The % change in k' for butyl paraben stayed relatively constant, increasing about 15%. The plates per meter increased over 60% the first two hours, with the asymmetry factor improving from 1.34 to 1.16, before dropping down to about a 25% increase overall at three hours, as shown in Figure 2.6A. Figure 2.6B shows the chromatograms for the CTY phase before and after three hours of base exposure. The increased retention and plate count along with improved asymmetry are apparent. This could be due to some noncrosslinked ligands being removed, increasing the efficiency as discussed in section 3.4.2. It is possible that as the particles start to hydrolyze, they may settle into a less heterogeneous packing, which has been shown to improve efficiency by decreasing eddy dispersion [138].
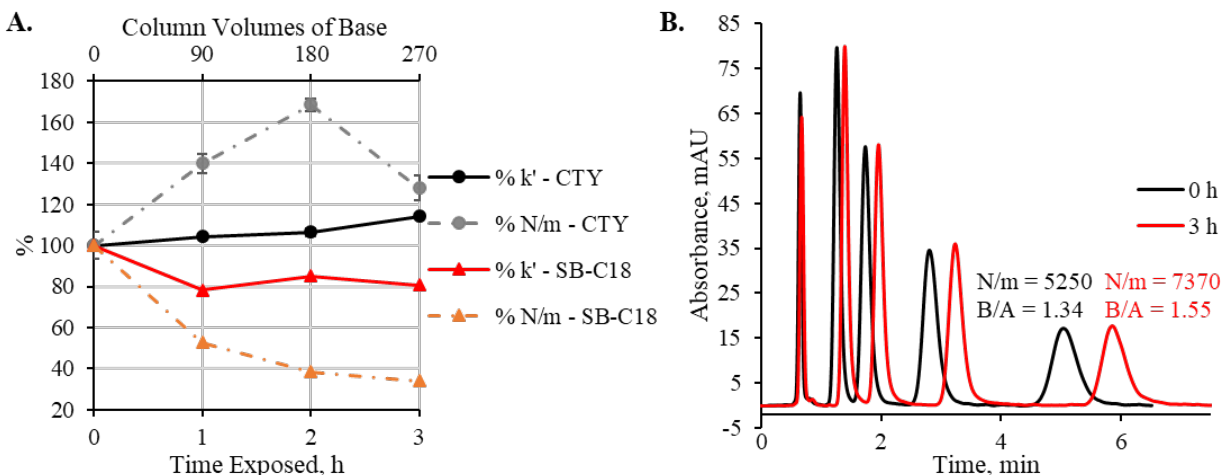
Figure 2.6: CTY phase's performance after exposure to high pH mobile phase. The columns were exposed to a 50:50 pH 12.6 20 mM NaOH:acetonitrile mobile phase at 70 ºC, 1.5 µL/min for hour increments, and then tested at each hour with a 62.5 µM uracil and paraben sample with 80:20 water:acetonitrile mobile phase, at 4 µL/min, and 50 ºC. A. Shows the % k' and N/m vs. the time exposed and column volumes/1000 of basic mobile phase. The CTY phase, ●, and the SB-C18 phase, ▲, both have the % k' denoted with the solid line and the % N/m with the dashed line. B. Chromatograms from the CTY phase of methyl, ethyl, propyl, and butylparaben before exposure to the basic mobile phase, black line, and after three hours of exposure, the red line. The N/m, Foley-Dorsey, and asymmetry factors, B/A, are shown for the butylparaben peak in the appropriate color.

2.4 Conclusion

The thiol-yne reaction easily produced a crosslinked stationary phase that is stable in low and high pH. The elemental analysis implies that the click-chemistry reactions work well without complex procedures to limit water exposure or the use of chromatographically harmful catalysts. The CTY phase shows excellent resistance to pH 0.5 mobile phase with both low and high amounts of organic modifier. The phase showed good stability at intermediate pH and at pH greater than 12.0. The CTY phase shows a low phase ratio and about average hydrophobicity that

could help with faster separations and larger molecules. The very high shape selectivity is an interesting feature, and adds a different selectivity than C18 phases, too. The HSM study shows that the CTY phase's column chemistry is very different from a traditional C18 phase and supports the presence of a crosslinked polymer surface. The unique properties of the CTY phase, and the unusual properties of a stationary phase having only the DEB modification [131], show the remarkable diversity that can be obtained with thiol-yne based stationary phases. These results show the promise of using the thiol-yne reaction to create robust and diverse stationary phases. This reaction is currently underutilized in the synthesis of chromatographic stationary phases. There are countless possibilities for new phases by adding copolymers and using different monomers. The reaction uses chromatographically safe catalysts to synthesize the polymer on the surface of the particle. Very thin layers can be formed, limiting pore clogging. The simplicity of the thiol-yne reaction opens the door to a diverse array of reagents to provide a wide range of possible column chemistries. Even more control can be gained by incorporating other orthogonal reactions to enhance the selectivity and stability of the phase [119, 139, 140].

3.0 A Liquid Chromatographic Charge Transfer Stationary Phase Based on the Thiol-yne

Reaction

The contents of this chapter were previously published in: Shields, E. P. and Weber, S. G. Journal of Chromatography A, **2019**, 1598, 132-140.

Reproduced with permission from Elsevier.

3.1 Introduction

The thiol-yne reaction is classified as a click chemistry reaction [84, 85, 118]. It can produce highly crosslinked polymers from *bis*-alkynes and *bis*-thiols. Crosslinks are created because both the alkyne and alkene functional groups react with thiols. Thus, two thiols can react with an alkyne forming a branch point, see Figure 3.1. The reaction, which has been used to modify surfaces [86, 117-119], looks very promising for the development of stationary phases. The related thiol-ene reaction has been used in stationary phases for many years [87, 88, 141], however, the thiol-yne reaction has been used sparingly in chromatography. Monoliths have been made for capillary electrochromatography and liquid chromatography [98, 100, 101, 103]. As far as we are aware, there is only one report, which is from Zou's lab, of particulate stationary phases using this reaction. It reports on a branched C18 phase on silica [142].
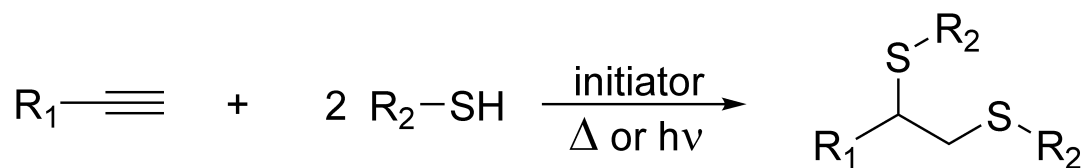
Figure 3.1: The thiol-yne reaction.

We started out to use the thiol-yne reaction to create a highly crosslinked stationary phase that would be stable over a broad pH and temperature range. The reaction is simpler to perform than the Friedel-Crafts based procedure used by Carr's group to create hypercrosslinked, stable phases on silica [25, 40-42, 115, 116]. The thiol-yne reaction can in principle create a very thin crosslinked layer on a suitable surface which is advantageous because it should increase the stability of the phase without clogging the pores of the particles. Here, we describe a new charge transfer ligand for liquid chromatography stationary phases that we discovered serendipitously while using the thiol-yne reaction with the intention to create a pH stable crosslinked stationary phase.

3.2 Experimental

3.2.1 Chemicals

All reagents were ACS grade or better and used without further purification. Extra dry toluene over molecular sieves, 1,4-diethynylbenzene (DEB), and triphenylene were purchased from Acros Organics (Geel, Belgium). The 3-mercaptopropyltriethoxysilane (MPTES), 3-mercaptopropyltrimethoxysilane (MPTMS), benzene, hexanes, tetrahydrofuran (THF), acetonitrile (ACN), ethanol, LC-MS grade methanol, and acetone were from Fisher Chemical

(Fairlawn, NJ). Triethylamine, 2,2′-azobis(2-methylpropionitrile) (AIBN), 1,6-hexanedithiol, *o*-terphenyl, 2-mercaptoethanol, and nitrobenzene were purchased from Sigma-Aldrich (St. Louis, MO). The hexamethyldisilazane (HMDS) was purchased from Alfa Aesar (Haverhill, MA). The water used was prepared using a Millipore Milli-Q Synthesis A10 (Billerica, MA). The Kasil 1 was given to us by PQ Corporation (Valley Forge, PA). The Zorbax RX-Sil silica particles (1.8 μm, 180 m^2/g, 8 nm pore size) and the Zorbax SB-C18 stationary phase (1.8 μm, 180 m^2/g, 8 nm pore size) were gifted to us by Agilent Technologies (Palo Alto, CA).

3.2.2 Stationary phase synthesis

The Zorbax RX-Sil was first functionalized by refluxing 4.00 g silica, 750 μL triethylamine, and 2.85 mL MPTES in 20 mL of extra dry toluene under nitrogen for 23 h. The mercaptopropyl-functionalized particles were rinsed two times with 20 mL of each of the following solvents: toluene, THF, ethanol, and acetone. The particles were then dried at 80 °C in a vacuum oven overnight. A thiol-functionalized silica with a higher density of ligands (HD-thiol) was synthesized the same way, but MPTMS was used and the reaction was refluxed for 44 h. The silica was not pretreated. Previous experiments showed that, in our lab, the reaction time and alkoxysilane type were the driving factors for increasing coverage.

The DEB functionalized silica, ESS stationary phase for the (4-ethynylstyryl)(propyl)sulfide ligand the DEB and mercaptopropyl reaction creates, was synthesized by adding 1.21 g of the thiol-functionalized silica, 24.3 mg AIBN, and 187 mg of DEB to 10 mL of extra dry toluene and refluxing for 40 h. The reaction time was not optimized, and was likely longer than necessary to ensure a complete reaction. The product was rinsed two times with 15 mL of each of the following solvents in this order: toluene, ACN, and ethanol. The

43

particles were dried overnight in a vacuum oven at 80 ºC. A higher density ESS phase (HD-ESS) was made in the same way using the HD-thiol-functionalized silica.

The crosslinked stationary phase was made by refluxing 298 mg HD-ESS with 100 μL 1,6-hexanedithiol and 19.9 mg AIBN in 5 mL of extra dry toluene. Two mL of extra dry toluene were added after 24 h and allowed to reflux another 22 h. The particles were rinsed two times with 10 mL toluene, ACN, 20 mM phosphoric acid (pH 2.08 to test for a pH dependent color change), water, and one time with acetone. The crosslinked particles were dried overnight at 100 ºC under vacuum.

3.2.3 Homogeneous thiol-yne synthesis of the proposed stationary phase ligand

The homogenous ligand synthsis was carried out by adding an excess of 2-mercaptoethanol, 10.0 mmol, to 2.0 mmol DEB and 1.0 mmol AIBN in 20.0 mL of extra dry toluene. The mixture was refluxed for 40 h to match the stationary phase synthesis time. The solution was filtered with a 0.20 μm membrane to collect the brown precipitate, which was rinsed with water, and dissolved in THF. The THF was evaporated and the oily brown substance was dried at 80 ºC in a vacuum oven overnight to dry and remove excess mercaptoethanol.

To prepare a sample of the product for GC/MS analysis, 3.0 mg were dissolved in 100 μL of THF and 45 μL of HMDS was added to form the trimethylsilyl ethers of products. The solution was shaken for 30 s, sonicated for 1 min, let sit for 5 min at room temperature, and heated at 50 ºC for 5 min. After sitting for 5 min longer, the solvent was evaporated using a stream of nitrogen. The silylated product was dissolved in enough dichloromethane to make a faintly colored solution, between 2-3 mL, and analyzed by the University of Pittsburgh Mass Spectrometry Center

(Pittsburgh, PA) using a Shimadzu (Kyoto, Japan) GCMS-QP2010S GC/MS with a Shimadzu SH-Rxi-5MS column, 30 m X 0.25 mm with a 0.25 μm film thickness. The injector was 200 ºC with the oven ramping from 100 to 320 ºC at 10 ºC/min. The He carrier gas flowed at 0.57 mL/min. The chromatogram and mass spectra of the major peaks are shown in Appendix B, Figures B 4 and B 5.

High resolution mass spectrometry was performed on the product by the University of Pittsburgh Mass Spectrometry Center using a Thermo Q-Exactive Orbitrap Mass Spectrometer (Waltham, MA). Less than 1 mg of the sample was dissolved 1 mL of methanol and infused into the ESI source on the mass spectrometer in positive ion mode. The spectra and corresponding chemical formulas are shown in Appendix B, Figures B 6, B 7, and B 8.

3.2.4 Characterization of the modified particles

A small sample of the product of each step in modifying the silica particle surfaces was sent to Atlantic Microlabs, Inc. (Norcross, GA) for analysis of %C, %H, and %S. The surface coverages were calculated using equation 3 used by Carr [116] where % X is the percentage of carbon or sulfur after the addition of the molecule minus the percentage carbon or sulfur before the addition, AM is the atomic mass of the X (carbon or sulfur), N_X is the number of atoms of carbon or sulfur in the added molecule, S_A is the specific surface area of the silica, and % C, % H, and % S are mass % of those elements after the addition of the molecule.

$$\mu mol/m^2 = \frac{\%X \times 10^6}{M_X \times N_X \times S_A \times (100 - \%C - \%H - \%S)} \qquad (3)$$

The reflectance spectroscopy was performed on a CRAIC QDI 2010 Microspectrophotometer, CRAIC Technologies, Inc. (San Dimas, CA) in reflectance mode. The sample was spread on a piece of 0.20 μm pore nylon membrane from Millipore (Burlington, MA) and wetted with hexanes or toluene. The reflectance was measured from 200 to 800 nm after allowing the excess solvent to evaporate for about 15-20 sec. Bare Zorbax RX-Sil particles were wetted with hexane or toluene in a similar matter for the reference spectrum.

3.2.5 Column packing

Approximately 15-cm long pieces of 150 μm ID, 360 μm OD fused-silica capillary from Polymicro Technologies (Pheonix, AZ) were used for column blanks. A glass fiber/sol-gel frit was made at one end of the capillary piece using the method developed by Maiolica et al. [120]. Briefly, 100 μL 25% formamide was added to 100 μL Kasil 1 and dropped onto a GF/C filter from Whatman (Buckinghamshire, UK). The capillary end was pushed into the wet filter three times and heated at 85 °C overnight.

Capillary columns were packed using the downward slurry method with a Model DSHF-302 pneumatic amplification pump from Haskel (Burbank, CA). Slurries (65 mg/mL) of the DEB silica and of crosslinked stationary phase were made in ethyl acetate, and the 1.8 μm Zorbax SB-C18 was suspended in isopropanol. An aliquot of slurry, 45 μL, was added to the system and, using methanol, brought to 20000 psi for 30 min. The columns were trimmed to 10 cm, installed on the HPLC system, and flushed with mobile phase.

3.2.6 HPLC instrumentation

The HPLC system was a Thermo Fisher Ultimate 3000 RSLC Nano System (Germering, Germany). The NCS-3500RS pump and column oven were equipped with the capillary flow selector. Samples were loaded using the WPS-3000SL autosampler. The VWD-3400RS Variable Wavelength Detector had a 45 nL capillary flow cell installed. Chromeleon 7 software from Thermo, run on a PC, was used to control the system and analyze the chromatograms. The mobile phase was degassed using a model G1379B Agilent 1260 μ-Degasser (Palo Alto, CA).

3.2.7 Chromatographic characterization

The shape selectivity from the Tanaka test [121] was determined by the selectivity factor of triphenylene and o-terphenyl, $\alpha_{T/OT} = k'_T/k'_{OT}$. The chromatographic conditions were 80:20 methanol:water, 40 $^{\circ}$C, 1.06 μL/min, with absorbance detection at 254 nm. Samples were 31 μM in mobile phase containing 62.5 μM uracil as the void marker. Each injection was 148 nL. Measurements were made five times each. Plate counts were calculated using the Foley-Dorsey equation [125]. Enthalpy determinations were made with the same conditions and samples, but with the temperature at 30, 40, 50, 60, and 70 $^{\circ}$C. Each sample was run three times at each temperature. Using van't Hoff plots, ln k' vs. 1/T, the apparent enthalpy of adsorption and the difference of the entropy changes between the solutes were determined. The error for all values was calculated as the 95% confidence interval and propagated accordingly.

The selectivity of the columns for nitrobenzene over benzene was determined with 148 nL injections of 62.5 μM nitrobenzene and benzene samples that had uracil as the void marker. The

HPLC was set up at 50 ℃, with a flow rate of 4.0 μL/min, the mobile phase was 70:30 water:methanol, and the detector was set at 254 nm. The samples were run with four replicates.

3.3 Results and discussion

3.3.1 Apparent solvatochromism of an intermediate product in the preparation of the crosslinked phase

Following the addition of DEB to the mercaptopropylsilane-functionalized silica, an intermediate in the preparation of the crosslinked phase, we observed that the color of the modified silica changed from dark reddish-brown to light tan when the rinsing solvent was switched from toluene to acetonitrile. The color switched back to reddish brown with the addition of any benzene-based aromatic solvent and then back to light tan with nonaromatic solvents like acetonitrile, ethanol, and hexanes. Figure 3.2 shows a photo of this stationary phase on a filter membrane after being rinsed with hexanes and benzene. When the DEB-modified silica was crosslinked with 1,6-hexanedithiol the color change was still apparent. This color change was interesting, but was not explored further for some time.

A.   **B.**
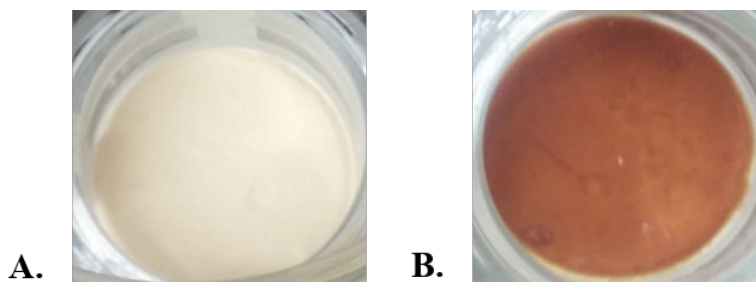
Figure 3.2: Photograph of ESS stationary phase wetted with (A) hexanes and (B) benzene.

3.3.2 High shape selectivity of the crosslinked phase

In assessing the crosslinked phase with the Tanaka test [121] we found that it has low efficiency, 590 theoretical plates for *o*-terphenyl and 280 theoretical plates for triphenylene. For a crosslinked phase this poor efficiency is not unusual, as Carr's unmodified hypercrosslinked phase shows lower efficiency as well [41]. On the other hand, the phase has a very high shape selectivity based on the selectivity factor of triphenylene and *o*-terphenyl, $\alpha_{T/OT}$. The crosslinked phase's $\alpha_{T/OT}$ is a remarkable 4.91 ± 0.08 with Tanaka conditions (a chromatogram is shown in Appendix B, Figure B.1). According to Sander and Wise's slot model for shape selectivity [133], the higher the surface coverage, the greater the shape selectivity. The mercaptosilane-modified silica that forms the basis for the crosslinked phase has a ligand surface coverage of $5.4 \ \mu mol/m^2$. This degree of surface coverage, which is in the middle of the polymeric range described by Sander and Wise, is known to enhance shape selectivity [48, 133]. As a result of the crosslinked phase having high coverage as well as having crosslinks from the 1,6-hexanedithiol, we suggest that this phase may provide a favorable environment for shape selectivity according to the slot model. Quantitatively, to put the $\alpha_{T/OT}$ in perspective, we note that most published commercial reversed phase $\alpha_{T/OT}$ values are between 1 and 1.5 [122, 129, 130]. Higher values of $\alpha_{T/OT}$ are found with amide, sulfonamide, and pentafluorophenyl phases ($\sim 2.5 - 2.8$). Amine-, pyridyl-, and carbazole-based phases can have very high $\alpha_{T/OT}$ up to about 15, although these are not taken at Tanaka conditions [44, 45, 135, 136]. Under normal phase conditions a value of 22 was found for a dinitroanilino propyl (DNAP) based phase [143]. Thus, for a phase with no significant H-bond donor or acceptor strength, the crosslinked phase described here has a very high value of $\alpha_{T/OT}$.

We created van't Hoff plots to determine the observed enthalpy of adsorption and the difference in the observed retention enthalpies of *o*-terphenyl and triphenylene on a C18 phase commercially made on the same silica particles, the Zorbax SB-C18 phase, and on the crosslinked phase, see Table 3.1 for the values calculated at 298K. The ln k' vs. 1/T plots showed good linearity over the 30-70 °C temperature range, raw regression data shown in Appendix B Table B.2. Note that the retention of both *o*-terphenyl and triphenylene are exothermic, with the latter being modestly greater in magnitude on the SB-C18 phase. The pattern of retention enthalpies is similar on the crosslinked phase, but the individual enthalpies are greater in magnitude than on the C18 phase and the difference in enthalpies is larger as well.

Table 3.1: Thermodynamic data at 298 K, with 95% confidence intervals

	SB-C18 Phase		Crosslinked Phase	
	ΔH^o (kJ/mol)	$T(\Delta S^o + R ln\phi)$ (kJ/mol)	ΔH^o (kJ/mol)	$T(\Delta S^o + R ln\phi)$ (kJ/mol)
Triphenylene	-21.6 ± 0.3	-18.0 ± 0.3	-28.6 ± 0.6	-20.5 ± 0.5
o-Terphenyl	-19.6 ± 0.3	-16.6 ± 0.3	-24.3 ± 0.7	-20.4 ± 0.7
Triphenylene - *o*-Terphenyl	-2.0 ± 0.4	-1.4 ± 0.3	-4.3 ± 0.9	-0.1 ± 0.9

The differences in values of $T\Delta S^o$, $\Delta T\Delta S^o$, between the triphenylene and *o*-terphenyl could help verify whether the shape selectivity is consistent with the slot model. Sander and Wise found that shape selectivity increases with increasing ligand bonding density [48, 133]. With increasing bonding density, the insertion of any solute into the stationary phase becomes less entropically favorable due to the need for more neighboring ligands to become ordered to make room for the solute [144]. Dorsey observed that the retention of planar molecules is less entropically favorable compared to their non-planar analogs [145]. So, if the slot model is the cause of the crosslinked stationary phase's shape selectivity, the $\Delta T\Delta S^o$ should have a value less than zero. With the SB-

C18 phase the $\Delta T \Delta S^o$ was -1.4 $\pm$ 0.4 kJ/mol, while the crosslinked phase had a value of -0.1 $\pm$ 0.9 kJ/mol. While the SB-C18 phase fits the expected model, the crosslinked phase's $\Delta T \Delta S^o$ is essentially zero and contradicts what is expected with the slot model.

It turns out that Sander had described an alternative shape selectivity mechanism based on charge transfer [135]. Lucy has attributed at least some of the high selectivity seen with a dinitroaniline-based phase in a normal phase determination of $\alpha_{T/OT}$ to charge transfer: the stationary phase is an electron acceptor [143]. Looking back on the color changing property of the DEB based phases, we began to wonder if a charge transfer interaction in the polymer may be responsible for the observed high shape selectivity of our crosslinked stationary phase.

3.3.3 Solvatochromic properties

Changes in a solute's color when it is dissolved in different solvents have been observed for over 100 years. Benisi and Hildebrand showed that differences in electron donor-acceptor interactions in different solvents can shift the absorbance spectrum of a solute [146]. So, the color change observed when first reacting DEB with the mercaptopropyl silane-modified silica was likely caused by a charge transfer interaction. To verify what we saw, we used spectroscopy. The nearly 2 μm diameter particles make absorbance hard to measure, so the reflectance spectrum was recorded. Figure 3.3 shows the reflectance spectrum for this reaction product wetted with hexanes and toluene. Toluene shifts the spectrum towards the red wavelengths compared to the spectrum in hexanes. This solvatochromism is very good evidence that this reaction product is capable of charge transfer interactions [146, 147].
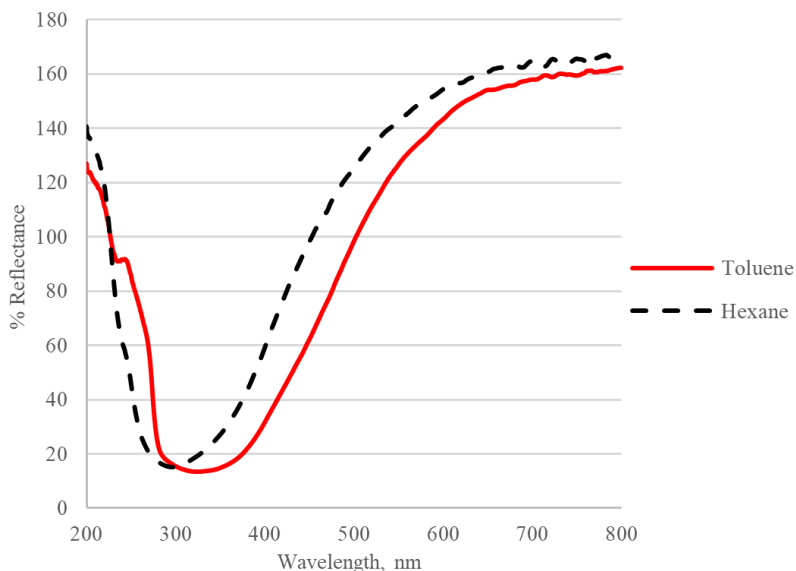
Figure 3.3: Reflectance spectrum for ESS stationary phase wetted with benzene and hexanes.

3.3.4 Shape selectivity of a low coverage silica with the 4-ethynyl styrylsulfide moiety

In order to minimize the contribution of the crosslinked phase's high surface coverage and crosslinking to the observed high value of $\alpha_{T/OT}$, we prepared a phase from silica with a propylthiol coverage of only 1.7 µmol/m^2. Subsequent reaction with DEB yielded a phase with 2.3 µmol/m^2 DEB ligands. Based on the commercial lab's published uncertainty of ± 0.3 wt%, the sulfur to DEB ratio is close to 1:1. We hypothesized that the DEB ligand has a structure as shown in Figure 3.4, with a 4-ethynyl styrylsulfide (ESS) moiety which is an electron rich aromatic system. The low coverage and absence of crosslinking should greatly reduce the contribution of "slots" to the shape selectivity. The ESS phase has $\alpha_{T/OT} = 3.23 \pm 0.01$, still very high (a chromatogram is shown in Appendix B Figure B.2). Also, the efficiency improved notably in comparison to the crosslinked phase to $N_{sys} = 1040$ for *o*-terphenyl, and 760 for triphenylene on the 10 cm column. From the van't Hoff plots (data shown in Appendix B Table B.2), the adsorption enthalpies for triphenylene

and *o*-terphenyl are -23.3 $\pm$ 0.3 kJ/mol and -21.5 $\pm$ 0.3 kJ/mol, respectively. Their enthalpy values fall between the SB-C18 and crosslinked phases, and still show the same pattern of exothermic retention with triphenylene having the greater ΔH^o. The $\Delta T \Delta S^o$ term for the ESS phase is 1.2 $\pm$ 0.4 kJ/mol at 298K. This indicates that the planar triphenylene molecule's retention is more entropically favored than the bulkier *o*-terphenyl, in contradiction with the slot model [145].
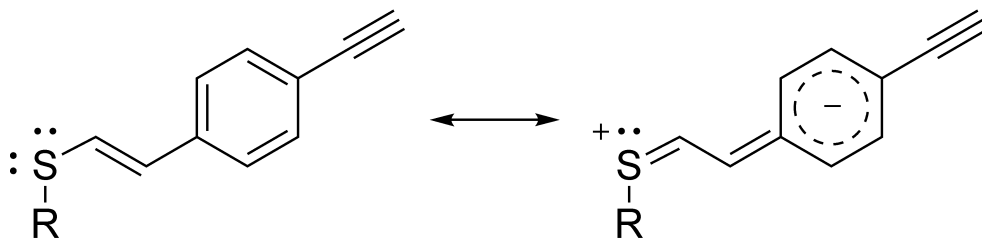
Figure 3.4: The ESS structure with electron donating resonance structures.

Shape selectivity is often desired for polycyclic aromatic hydrocarbons. Since most polycyclic aromatic hydrocarbons, like triphenylene, are electron rich, most current charge transfer stationary phases have an electron poor aromatic system to create an electron acceptor stationary phase [135, 143, 148-150]. Some electron donor phases have been tested and show the opposite selectivity for electron-poor aromatics [135, 148, 151]. Notably, charge transfer processes can occur between two electron donors or two acceptors if their relative charge transfer characteristics differ [152]. Davankov's hyper-crosslinked polystryrene phase shows retention and interesting selectivity for the electron rich PAHs [152], and Kimata has shown that electron acceptor phases can retain and resolve electron acceptor solutes [148]. The conjugated system in the ESS stationary phase ligands may be electron rich enough to contribute to the ESS stationary phase's shape selectivity.

3.3.5 Homogeneous preparation of DEB-thiol adducts

Because both the ESS ligand and the crosslinked phase have novel ligands for chromatography, we decided to carry out a reaction of DEB with an excess of 2-mercaptoethanol to determine the composition of the reaction product(s) that might occur. The reaction was carried out with the same solvent, temperature, and time as the reactions leading to the stationary phases, except that the thiol is in excess in the homogeneous reaction. Recall that DEB is in excess in the preparation of the ESS phase, but a thiol, 1,6-dithiohexane, is in excess during the preparation of the crosslinked phase from the ESS material. For GC/MS analysis, we carried out a further reaction on samples of the product of the DEB/mercaptoethanol reaction to form the trimethylsilyl ethers using hexamethyldisilazane (HMDS). The GS/MS of the product shows two peaks with the molecular ion of 426 m/z and similar retention times. The chromatogram is shown in Figure B.3 and mass spectra are in Figure B.4. These peaks correspond to DEB plus two thiols, likely the trans/trans and cis/trans isomers of the product. We also analyzed the product by infusing the sample into the ESI source on a Thermo Q-Exactive mass spectrometer. The $[M-H]^+$ peak at 281.06734, shown in Figure B.5, was the most abundant peak in the spectrum by an order of magnitude more than the peak at 357.06609 m/z, shown in Figure B.6. The former corresponds to DEB reacting with two thiols while the latter $[M-H]^+$ peak corresponds DEB reacting with three thiols. There are peaks two orders of magnitude smaller than the former peak near 438 m/z, shown in Figure B.7, that correspond to the $[M-H]^+$, and $[M-3H]^+$ peaks for the addition of four thiols to DEB. We conclude that reaction of an ESS phase with 1,6-hexanedithiol is likely to be crosslinked, justifying our description of it above. When low coverage, thiol-bearing silica reacts with excess DEB, the stoichiometry is near 1:1 as shown by the elemental analysis and crosslinks are unlikely.

3.3.6 Charge transfer nature of the ESS phase

To verify that the ESS stationary phase is an electron donor, we investigated the selectivity of the ESS phase for nitrobenzene vs. benzene, $\alpha_{NB/B}$, and compared it to that on a Zorbax SB-C18 column. On the SB-C18 column $\alpha_{NB/B}$ was 0.64 ± 0.01. Nitrobenzene is more polar than benzene so $\alpha_{NB/B}$ is consistent with the expectation that it is less than unity. The $\alpha_{NB/B}$ for the ESS phase is 1.83 ± 0.10, significantly different from that of the C18 phase. Chromatograms are shown in Appendix B Figure B.8. We conclude that the ESS phase's selectivity is due in a large part to its electron donor property in charge transfer interactions.

3.4 Conclusion

The addition of DEB to thiol-functionalized silica creates an electron rich conjugated system that can participate in charge transfer interactions as an electron donor. This property, while it may not be the only factor, certainly helps the ESS phase exhibit high shape selectivity. The ESS phase has about one DEB molecule to every thiol, so it will mainly have the structure as in Figure 3.4. The crosslinked phase, with a higher thiol:DEB ratio will likely have two vinylene sulfides per aromatic ring. The increase in electron donating groups and presence of some crosslinking may explain the crosslinked phase's increased adsorption enthalpies and higher shape selectivity compared to the ESS stationary phase. The discovery of this charge transfer characteristic adds even more diversity to the column chemistry that can be created using the thiol-yne reaction.

4.0 A Crosslinked, Low pH-stable, Mixed-mode Cation-exchange Stationary Phase Made Using the Thiol-yne Reaction

4.1 Introduction

Mixed-mode stationary phases possess both hydrophobic properties and electrostatic moieties for cation or anion exchange. The mixed-mode column separates solutes according to their charge and their hydrophobic nature. This characteristic makes mixed-mode stationary phases useful in many areas of research, such as peptides, carbohydrates, neurotransmitters, and many other types of charged biomolecules [153-156]. The different retention mechanism compared to reversed-phase stationary phases also makes mixed-mode phases useful as a complementary stationary phase for two dimensional HPLC [42, 157, 158]. These important applications have fueled the growth of mixed-mode stationary phase research over the last decade [156].

Increasing the stability of mixed-mode stationary phases can provide more useful applications. The ideal mixed-mode stationary phase would need to withstand extreme pHs to ensure complete ionization of weak acids or bases, and extreme temperatures and pressures to provide the adequate speed and resolution desired for many applications. Mixed-mode phases are often made on polymeric supports, but these possess poor mechanical strength, have slow re-equilibration times when using gradients, and generally have poor efficiency due to the slow mass transfer through the polymers [42, 158]. Silica supports have been modified with mixed-mode ligands and can provide higher efficiencies and mechanical strength. There are some commercial silica based phases, and Lindner's group has used the thiol-ene reaction to produce a number of mixed-mode phases on silica [159]. The versatility of these phases is limited due to the extreme

56

pH often needed to ensure complete ionization of some weak acids and bases. At low pH the siloxane bonds are readily hydrolyzed, cleaving the ligands [42, 158], and at high pH the silica can easily dissolve [22], limiting the pH range for most silica supports. There are a few examples of mixed-mode stationary phases made with polymer modified silica, providing increased stability. Bäuer et al. recently introduced a thiol-ene- and siloxane polymer-coated mixed-mode anion-exchange phase that shows good stability at pH 5 and 60 $^{\circ}$C [92], and Carr's group developed hypercrosslinked mixed-mode cation-exchange stationary phases that are very stable down to pH 0.5 and up to 150 $^{\circ}$C [25, 41, 116]. The Carr group's silica-based, hypercrosslinked phase uses a polystyrene block copolymer and the Friedel-Crafts reaction to create the crosslinked surface. Post-polymerization Friedel-Crafts reactions can add a variety of ligands onto the polymer surface, such as alkyl chains or carboxylic acids to create a mixed-mode phase [42, 115, 158]. This highly stable mixed-mode phase could be very useful, but is not commercially available, is very difficult to synthesize, and the metal catalysts can harm the chromatographic performance.

We recently reported creating a stable crosslinked thiol-yne stationary phase using 1,4-diethynylbenzene (DEB) crosslinked with 1,6-hexanedithiol using the thiol-yne click reaction (the CTY phase) [131, 160]. This stationary phase showed high stability in low and high pH mobile phases [160]. The combination of the benzene ring and the sulfur atoms created a strong electron-donating charge-transfer phase [131] that also had cation exchange characteristics [160]. When used with cationic solutes the DEB based phase retained solutes too well and provided very poor separations, but the simple synthesis and the stability of the phase were promising.

In this study, we report another thiol-yne based crosslinked phase made without the DEB monomer to attempt to simplify the column chemistry. We used 1,7-octadiyne crosslinked with 1,6-hexanedithiol to create a crosslinked octadiyne thiol-yne based stationary phase (COTY)

across the silica surface without any benzene rings. The COTY phase was stable at low pH, had similar methylene selectivity to a reversed phase, showed charge-transfer characteristics, and had cation exchange characteristics that allowed the separation of monoamine neurotransmitters without ion-pairing agents.

4.2 Experimental

4.2.1 Chemicals

The 3-mercaptopropyltriethoxysilane (MPTES) was purchased from Alfa Aesar (Haverhill, MA). The 1,7-octadiyne was obtained from TCI America (Portland, OR). Food grade 99% 1,6-hexanedithiol, 98% 2,2′-azobis(2-methylpropionitrile) (AIBN), and triethylamine were purchased from Sigma-Aldrich (St. Louis, MO). The 99.9% extra dry toluene over molecular sieves and 99.5% formamide were obtained from Acros Organics (Geel, Belgium). The HPLC grade chloroform, hexanes, tetrahydrofuran, dichloromethane, LC-MS grade methanol, LC-MS grade acetonitrile, HPLC grade isopropanol, HPLC grade ethyl acetate, HPLC grade trifluoroacetic acid (TFA), HPLC grade phosphoric acid (80%), ethanol, pentane, sodium hydroxide pellets, sodium chloride, magnesium chloride, calcium chloride, potassium chloride, and concentrated hydrochloric acid were purchased from Fisher Chemical (Fairlawn, NJ). The potassium phosphate monobasic and potassium phosphate dibasic were purchased from EM Science (Gibbstown, NJ). The water used was prepared using a Millipore Milli-Q Synthesis A10 water purification system (Billerica, MA). Kasil 1 was given to us by PQ Corporation (Valley

Forge, PA). The Zorbax RX-Sil silica particles (1.8 μm diameter, 180 m^2/g surface area, and 8 nm pore size) were a gift from Agilent Technologies, Inc. (Santa Clara, CA).

All solutes were purchased as ACS grade or better and used without further purification. *n*-Butylbenzene, *n*-pentylbenzene, dopamine hydrochloride, and serotonin hydrochloride were purchased from Alfa Aesar (Ward Hill, MA). The *o*-terphenyl, caffeine, heptanophenone, octanophenone, uracil, 5-phenyl-1-pentanol, ethylbenzene, toluene, *N,N*-dimethylacetamide, acetophenone, anisole, benzonitrile, L-ascorbic acid, and DL-norepinephrine were purchased from Sigma Aldrich (St. Louis, MO). Triphenylene and benzylamine were from Acros Organics (Geel, Belgium). The phenol was from Fluka (Buchs, Switzerland). The mefenamic acid was purchased from TCI America (Portland, OR). The amitriptyline, *n*-butylbenzoic acid, *N,N*-diethylacetamide, 5,5-diphenylhydantoin, nortriptyline, *p*-nitrophenol, *trans*-chalcone, and berberine were provided by Dr. Dwight Stoll at Gustavus Adolphus College (St. Peter, MN). The *cis*-chalcone was made by letting a 25 mM solution of *trans*-chalcone sit in the sunlight in a glass vial for around 4 h. The artificial cerebrospinal fluid (aCSF) was made by making a pH 7.40 solution of 142 mM NaCl, 1.2 mM $CaCl_2$, 2.7 mM KCl, 1.0 mM $MgCl_2$, 2.0 mM NaH_2PO_4 in the Milli-Q purified DI water.

4.2.2 HPLC instrumentation

A Thermo Fisher Ultimate 3000 RSLC Nano System (Germering, Germany) controlled with Chromeleon 7 was used for the chromatographic experiments. The system was equipped with an NCS-3500RS pump with the 0.5 – 10.0 μL/minute capillary flow selector, a WPS-3000SL autosampler, and a VWD-3400RS Variable Wavelength Detector with a 45 nL capillary flow cell installed. The mobile phase was degassed using a model G1379B Agilent 1260 μ-Degasser (Palo

Alto, CA). The pHs of the aqueous portion of the mobile phases were measured using a Thermo Fisher Orion Star A211 benchtop pH meter (Waltham, MA).

4.2.3 Column packing

The method used for column packing was described previously [160]. Briefly, a glass fiber frit was made in a 15 cm X 150 µm ID fused silica capillary, from Polymicro (Phoenix, AZ), using the method developed by Maiolica et al. [120] using a 50:50 25% formamide in water:Kasil 1 solution and a GF/C filter (Whatman (Buckinghamshire, UK)). After curing in an 85 ºC oven overnight, the column blank was packed with a 65 mg/mL slurry of the stationary phase in isopropanol using the downward slurry method. The columns were brought to 20000 psi for 30 minutes using a Model DSHF-302 pneumatic amplification pump from Haskel (Burbank, CA) and allowed to depressurize. The columns were cut to 10 cm, installed on the HPLC, and flushed with mobile phase.

4.2.4 Thiol silica synthesis

The Zorbax RX-sil and glassware were dried in an approximately 110 ºC vacuum oven overnight. To 4.00 g of the dried Zorbax silica 25 mL of extra dry toluene stored over molecular sieves was added and the mixture was sonicated for 1 minute and stirred for 1 minute. To the slurry, 836 µL triethylamine was added and the mixture sonicated for 1 minute and stirred for 10 minutes under nitrogen before adding 3.00 mL MPTES. The suspension was stirred for 10 minutes and brought to a boil. The solution was refluxed for 32 h under nitrogen and allowed to cool to room temperature. The suspension was vacuum filtered (0.45 µm nylon membrane from Millipore

(Billerica, MA)) and rinsed two times each with 20 mL toluene, 25 mL hexanes, and 25 mL tetrahydrofuran and dried overnight in a 100 ºC vacuum oven.

4.2.5 Octadiyne silica synthesis

To 300.20 mg of the thiol silica and 3.28 mg AIBN, 4 mL of chloroform was added and the mixture was sonicated 1 minute and stirred 1 minute. While stirring 200 µL of 1,7-octadiyne was added and allowed to stir 10 minutes. The suspension was refluxed for 30 h and cooled. The modified silica was rinsed on a vacuum filter two times each with 20 mL chloroform, 20 mL pentane, 20 mL methanol, and one time with 20 mL chloroform. The particles were dried overnight in a 100 ºC vacuum oven.

4.2.6 Crosslinked octadiyne silica synthesis

Octadiyne silica (OTY, 251.0 mg), 10.42 mg AIBN, 4.00 mL chloroform, and 103.5 µL 1,6-hexandithiol were added to a flask, sonicated for 1 min, and stirred for 5 minutes to suspend the particles. The suspension was refluxed for 25 h and poured into a vacuum filter to rinse 3 times each with 10 mL chloroform, 15 mL hot ethanol, and two times with 10 mL hexanes. The particles were dried in a vacuum oven at 100 ºC overnight. The particles were further rinsed by suspending them in 10 mL chloroform and pouring onto a vacuum filter then rinsed with 10 mL chloroform, two times with 20 mL ethyl acetate, and 10 mL of chloroform. The particles were dried for 3 h in a 100 ºC vacuum oven. A 2.1 mm ID X 5 cm stainless steel blank column was dry packed with the particles and flushed with methanol at 0.1 mL/minute for 25 h on an Isco Model 100DM Syringe Pump (Lincoln, NE). The particles were dried overnight in a 100 ºC vacuum oven.

4.2.7 Elemental analysis

Approximately 10 mg of the stationary phase samples were analyzed by Atlantic Microlab, Inc. (Norcross, GA) for percent carbon, hydrogen, and sulfur. The surface coverage of the thiol, DEB, and crosslinking moieties were calculated using equation 4, adapted from Carr [116]. Where *%X* is the elemental percent of sulfur or carbon added during the synthesis step, M_X is the atomic mass of sulfur or carbon, N_X is the number of sulfur or carbon atoms in the added molecule or ligand, S_A is the surface area of the silica, and *%C, %H*, and *%S* are the mass percents of the respective elements after the synthesis.

$$\mu mol/m^2 = \frac{\%X \times 10^6}{M_X \times N_X \times S_A \times (100 - \%C - \%H - \%S)} \qquad (4)$$

4.2.8 Low pH degradation experiment

The stability of the COTY phase at low pH was tested in the same manner reported previously [160]. Briefly, a 50:50 5% TFA (pH = 0.50):acetonitrile mobile phase was mixed by the pump online and passed through the COTY column at 70 °C. Every 30 min, 148 nL of a 50 μM filtered (13 mm GD/X 0.45 μm PTFE syringe filters, Whatman (Buckinghamshire, UK)) sample of o-terphenyl and triphenylene, with uracil as the void marker, was injected onto the column. The flow rate was 4.0 μL/min and the UV detector was set at 254 nm. The performance was monitored for 144 h, or six days. The retention factors, *k*, were calculated using the first moments of the peaks. The plate counts were calculated using the Foley-Dorsey equation [125].

4.2.9 Chromatographic characterization

The stationary phases were chromatographically characterized using the Tanaka test [121] and the hydrophobic subtraction model (HSM) [1]. These tests were described previously [160], and are described briefly below. For both tests the mobile phase was mixed online by the HPLC, and composition verified by the baseline upon injection of a manually mixed mobile phase sample. The Tanaka test was run to be equivalent to the data from Euerby et al. [122], with the temperature at 40 °C and the flow rate at 1.06 μL/min to achieve the same average velocity with the capillary column as Euerby et al.'s 1.0 mL/min with a 4.6 mm I.D. column. The samples were 100 μM, made in the appropriate mobile phase, and 148 nL was injected. The HSM study had a scaled flow rate of 2.12 μL/min flow rate, 10 μg/mL sample concentration in mobile phase, 148 nL injections, and was run at 35 °C. The samples were run individually to identify the peaks in the sample mixes. The data was used to perform a linear regression of the HSM equation [1], shown in equation 5.

$$\log \alpha = \log\left(\frac{k}{k_{EB}}\right) = \eta' \boldsymbol{H} - \sigma' \boldsymbol{S}^* + \beta' \boldsymbol{A} + \alpha' \boldsymbol{B} + \kappa' \boldsymbol{C} \qquad \textbf{(5)}$$

The electron donating charge transfer capabilities of the stationary phases were assessed as before [131]. Briefly, 100 μM samples of benzene and nitrobenzene with uracil, in 70:30 water:methanol were injected onto the columns. The flow rate of the 70:30 water:methanol mobile phase was 4.00 μL/min, with the oven at 50 °C and UV detector at 205 nm. The retention factors, *k*, were calculated using the first moments of the peaks. The plate counts were calculated using the Foley-Dorsey equation [125].

4.2.10 Monoamine neurotransmitter separations

Samples, either 74 or 148 nL, containing 50 μM each of ascorbic acid, norepinephrine, dopamine, and serotonin were made in aCSF or the mobile phase being tested. The ascorbic acid was used as the void marker, since its retention time was the same as uracil. Chromatography took place at various flow rates and temperatures (as noted in the text), with UV detection at 275 nm.

4.3 Results and discussion

4.3.1 Elemental analysis

The COTY stationary phase was synthesized in a stepwise procedure, as shown Figure 4.1. The weight percent values of carbon, hydrogen, and sulfur were determined for each step, and are displayed along with surface coverage values in Table 4.1. The addition of the MPTES gave particle with 2.01 μmol/m^2 of the propyl thiol, calculated from the %S. Reacting the 1,7-octadiyne with the thiol silica, to give the octadiyne thiol-yne modified silica (OTY), yielded 0.38 μmol/m^2 of octadiyne molecule coverage, calculated by the added %C. This is only an addition of about one octadiyne per five thiols on the silica. This could be due to steric interactions and the creation of some bidentate octadiyne ligand, with one octadiyne being shared by two neighboring propylthiol ligands, see Figure 4.2A. The coverage was enough to create interfering fluorescence, likely from the vinyl sulfides, when Raman spectroscopy of the sample was attempted. The crosslinking step with 1,6-hexanedithiol resulted in a 0.55 μmol/m^2 dithiol coverage, calculated from the added sulfur. One alkyne moiety must be used in the previous reaction converting it to

an alkene, so the dithiol coverage of 0.55 μmol/m^2 means that each octadiyne bound to the surface

bonds to almost three sulfur atoms on average during the crosslinking step. Thus, the structure

could be a combination of the structures shown in Figure 4.2B and 4.2C. Because of the low

coverage of octadiyne, it is possible that some octadiyne ligands are spaced too far apart for the

1,6-hexanedithiol to crosslink adjacent, π-bond-containing, surface-bound species. Therefore,

these thiols may have made a disulfide bond with nearby propylthiol ligands, reacted with itself,

or remained unreacted.
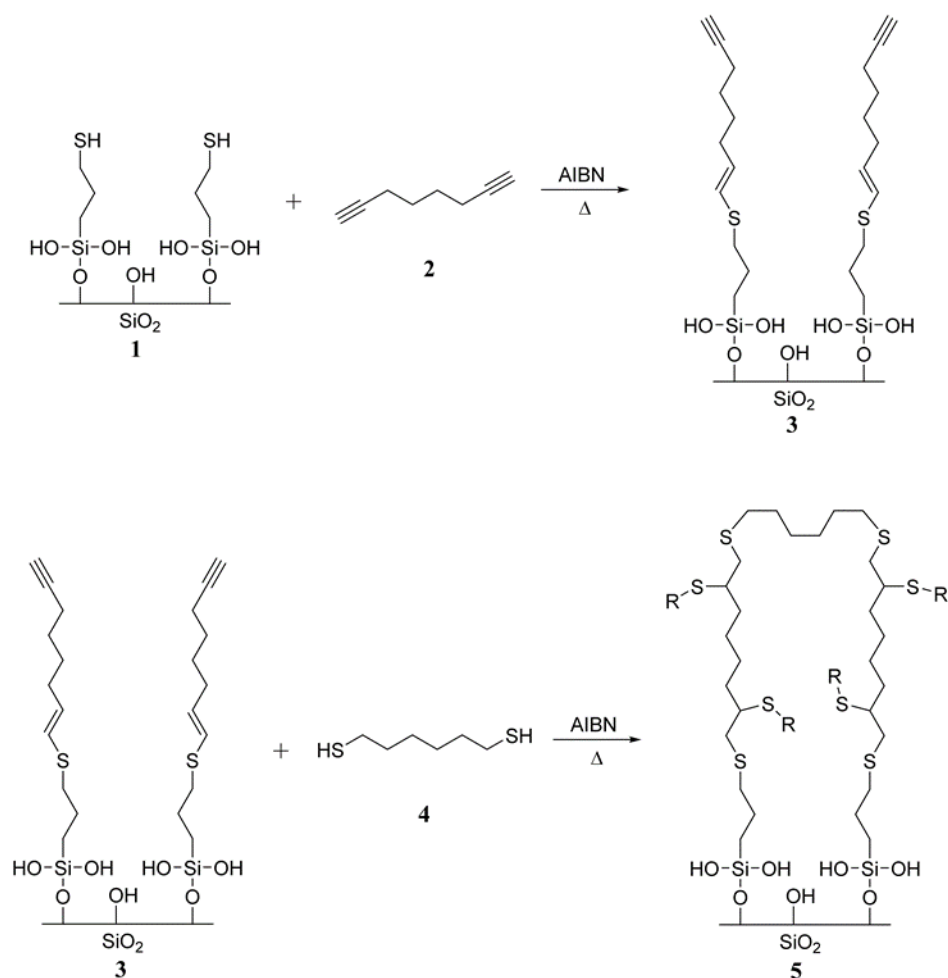
Figure 4.1: COTY synthesis. Thiol silica, 1, and 1,7-octadiyne, 2, are reacted at 61 °C using AIBN as the catalyst. The OTY product, 3, is crosslinked using 1,6-hexanedithiol, 4, and AIBN at 61 °C to give the COTY stationary phase, 5.

Table 4.1: Elemental results and surface coverages for the COTY synthesis

	% C	% H	% S	$\mu mol/m^2$ S	$\mu mol/m^2$ Octadiyne	$\mu mol/m^2$ Dithiol
Thiol	2.44	0.49	1.11	2.01	-	-
OTY	3.06	0.53	1.04	1.89	0.38	-
COTY	3.71	0.68	1.64	3.03	-	0.55
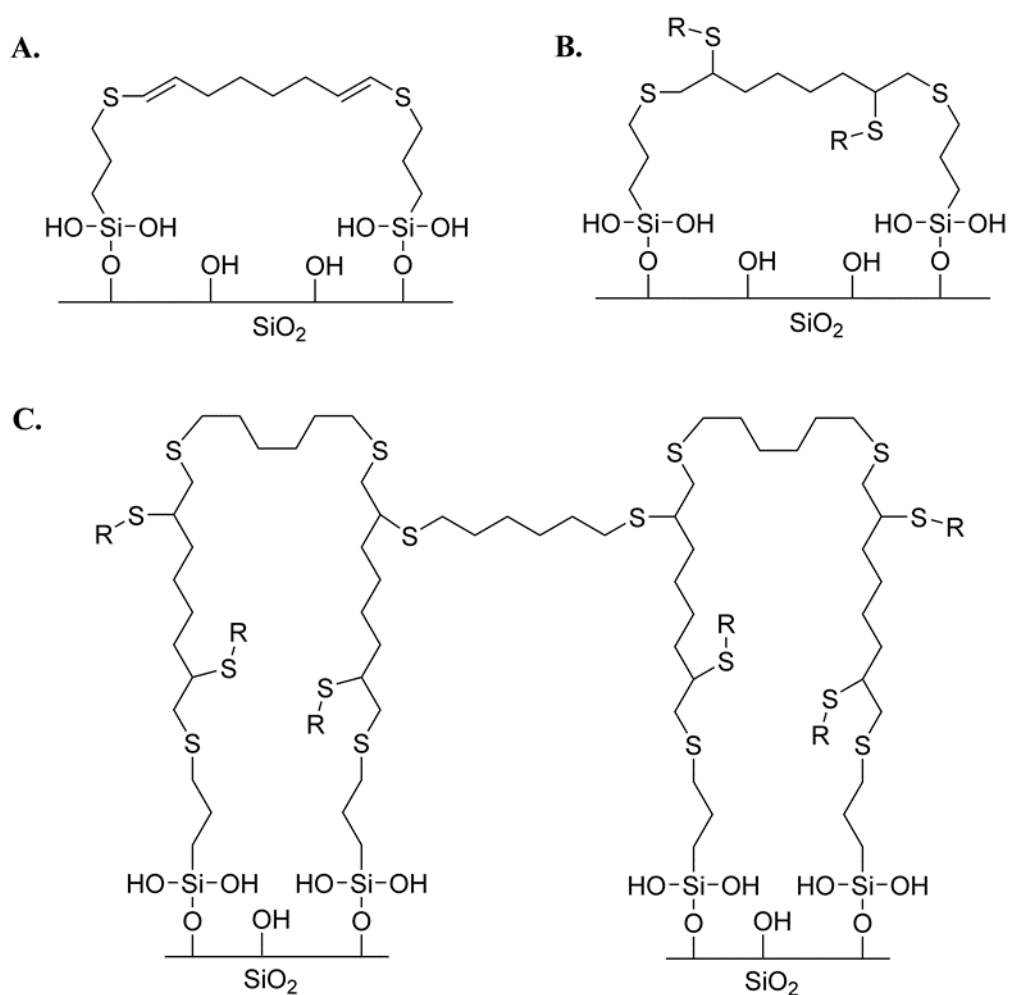
Figure 4.2: Possible structures of the COTY stationary phase. The bidentate octadiyne structure (A), the crosslinked bidentate structure (B), and the hexanedithiol crosslinked structure (C).

4.3.2 The Tanaka test

The Tanaka test [121, 122, 129] calculates column characteristics using experimental values, so the error in the values is not dependent on the fit of the model like the HSM characterization. A series of molecular probes helps discern the characteristics of the stationary phase. The COTY phase and its precursors were tested and the results with their 95% confidence intervals are displayed in Table 4.2. All the stationary phases exhibit a small k for pentylbenzene, k_{pb}, indicating a low phase ratio and ligand density, as expected with 4 %C. The methylene selectivity, from the selectivity factor of pentylbenzene and butylbenzene, increases as the synthesis goes from the thiol silica to the OTY intermediate and to the COTY phase. Interestingly, methylene selectivity for the COTY phase is about the same as the CTY phase and standard C18 phases despite the low %C. Although none of the phases have the DEB moiety, they still have high shape selectivity based on the selectivity between triphenylene and o-terphenyl. This is due to the presence of the sulfur atoms. Horak and Lindner reported that the sulfur in thiol-ene based stationary phases contributes to higher shape selectivities due to the sulfur-aromatic interactions [95]. This interaction is well studied in other areas of chemistry and is known to involve a charge transfer interaction between the sulfur atom and the aromatic rings [161-164]. It is apparent in the data shown here that as more sulfur is added to the surface the stationary phase gains more shape selectivity. The surface coverage of the octadiyne is low enough that it should not provide much additional shape selectivity as envisioned in the slot model, but it may impact the selectivity by adding π systems to the sulfur atoms that can enhance their preference for flat aromatic molecules.

Table 4.2: Tanaka test values, with 95% confidence intervals, for the stationary phases

	Thiol	OTY	COTY	CTY [160]	SB-C18 [122]
k_{pb}	0.09 ± 0.01	0.11 ± 0.01	0.18 ± 0.01	0.42	6.00
α_{CH_2}	1.07 ± 0.14	1.13 ± 0.09	1.20 ± 0.04	1.21	1.49
$\alpha_{T/O}$	1.58 ± 0.01	2.21 ± 0.01	2.71 ± 0.03	4.91	1.20
$\alpha_{C/P}$	1.34 ± 0.02	1.11 ± 0.04	1.21 ± 0.01	0.61	0.65
$\alpha_{B/P}$ (pH 2.7)	0.32 ± 0.02	3.76 ± 0.02	3.98 ± 0.05	22.32	0.13
$\alpha_{B/P}$ (pH 7.6)	--	16.59 ± 1.56	11.73 ± 0.18	--	1.46

The other value of note is the cation-exchange term, shown by the selectivity factor between benzylamine and phenol, $\alpha_{B/P}$. The values are much less than the CTY phase, but are still much higher than a standard C18 phase. The greater cation-exchange value at pH 7.6, 11.73, vs 3.98 at pH 2.7, shows that at the elevated pH deprotonated silanols play a large role in the cation-exchange properties, and that at pH 2.7 the silanols play a small role in the cation-exchange. The thiol silica has about the same $\alpha_{B/P}$ value as the SB-C18 phase at pH 2.7. Indicating the cation-exchange characteristic is not due to the thiols, but introduced during the radical thiol-yne reactions. The radical reaction may oxidize some of the thiols to sulfonates creating cation-exchange sites. The OTY phase's $\alpha_{B/P}$ value is about the same as the COTY phase's, so most of the oxidation would occur during the addition of octadiyne. The vinylsulfides may also contribute to the cation exchange for the OTY phase as well, since they would be formed by the addition of one thiol to octadiyne. This contribution is likely minimal, as lone pair-cation and cation-π interactions have been studied, but should not be very substantial with a vinylsulfide in the mobile phase [165]. The cation-exchange characteristic and normal methylene selectivity show that the COTY phase is a mixed-mode cation-exchange stationary phase.

4.3.3 The HSM characterization

The COTY stationary phase was characterized using the HSM [1, 123]. This standard characterization method uses experimental values to perform a linear regression of the HSM equation, equation 5, to understand contributions of particular selectivity-generating properties of (typically) reversed-phases. As with the DEB based stationary phase (CTY) [160], the HSM regression yielded very large uncertainties in the coefficients, see Tables C.1, C.2, and C.3 in Appendix C. Since the experimental uncertainty was small, shown in Table C.3, the presence of the large uncertainties in the regression indicates the presence of an interaction not accounted for by the HSM [123]. This interaction is likely a charge-transfer interaction due to the presence of sulfur atoms, and is detailed further below.

4.3.4 Electron donating charge transfer test

To verify the electron-donating characteristics of a stationary phase, we have developed a test that involves running samples of benzene and nitrobenzene in a water:methanol mobile phase [131]. Nitrobenzene is more polar than benzene. Thus, on a standard reversed-phase column nitrobenzene elutes before benzene, and the selectivity factor measured for nitrobenzene/benzene, $\alpha_{NB/B}$, is less than one. When the stationary phase is electron donating, stronger interactions with the electron deficient nitrobenzene occur giving an $\alpha_{NB/B}$ greater than one. The $\alpha_{NB/B}$ for the SB-C18 column is 0.64 ± 0.01 [131]. While the COTY phase has a $\alpha_{NB/B}$ value of 1.41 ± 0.01, indicating it has electron donating characteristics. Overlayed chromatograms of benzene and nitrobenzene from the COTY phase are shown in Appendix C, Figure C.1. The COTY phase's precursors, OTY and the thiol silica were tested in this manner, their proposed structures are shown

in Figure 4.3. All three stationary phases had $\alpha_{NB/B}$ values greater than one, see Table 4.3. The electron donating charge-transfer characteristics and sulfur-π interactions are well documented [95, 161-163, 166, 167], so this result is not surprising. These values are much higher than with a C18 phase, but are significantly lower than the ESS phase reported previously [131], a DEB modified phase, see the structure in Figure 4.3, with about the same thiol surface coverage, about 2.0 μmol/m^2, without any crosslinking. The ESS phase features the conjugated benzene ring that enhances the charge-transfer interactions.
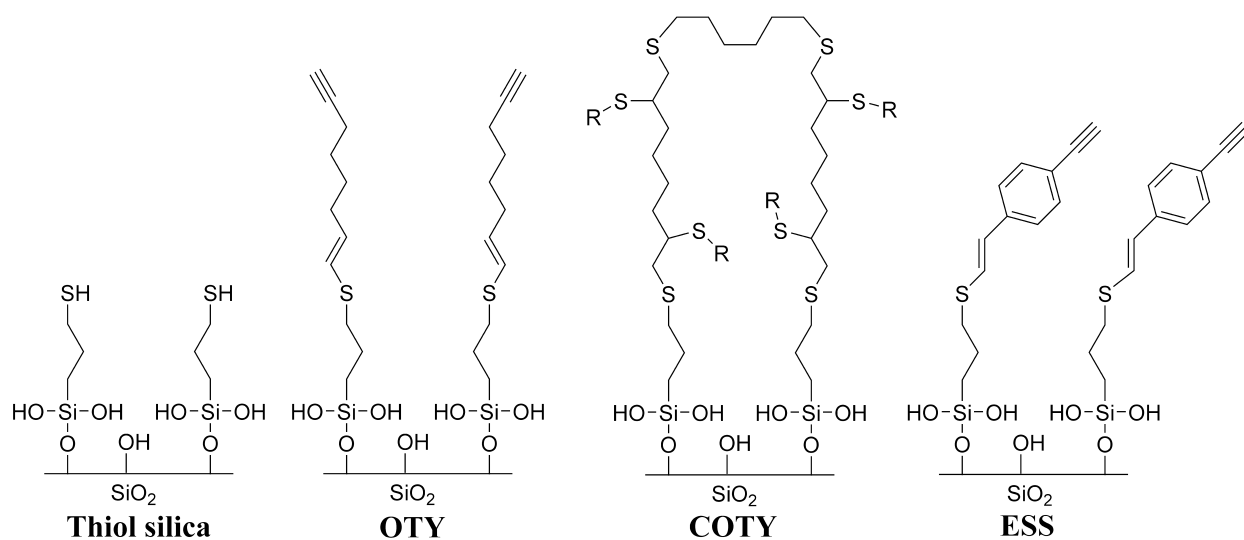
Figure 4.3: Proposed structures for tested stationary phases, other structures and functional groups may be present. From left to right: thiol silica, OTY, COTY, and the ESS phases.

Table 4.3: The selectivity between nitrobenzene and benzene

Stationary Phase	$\alpha_{NB/B}$	95% Confidence
COTY	1.41	± 0.01
OTY	1.34	± 0.10
Thiol	1.30	± 0.04
ESS [131]	1.83	± 0.10
SB-C18 [131]	0.64	± 0.01

4.3.5 Separation of monoamine neurotransmitters

The usefulness of the mixed-mode characteristics of the COTY phase were studied using a mixture of monoamine neurotransmitters prepared in aCSF to mimic a sample from a microdialysis probe. The sample contained ascorbic acid, norepinephrine, dopamine, and serotonin. Initially, the mixture was run under the same conditions as the pH 2.7 Tanaka test. With just a 20 mM potassium phosphate buffer, the 70:30 buffer:methanol mobile phase provided a separation with baseline resolution with the sample made in aCSF, an approximately 150 mM salt solution. Increasing the temperature to 50 °C and the flow rate to 2.0 μL/min improved serotonin's asymmetry factor, B/A, from 1.93 to 1.25, and improved the resolution between norepinephrine and dopamine from 1.01 to 1.55. At these conditions the hydrophobic retention characteristics were investigated by changing the amount of methanol in the mobile phase from 30%, to 20%, and to 10% methanol. The retention increased for the dopamine, from k = 0.69, 0.77, to 0.87, and serotonin, from k = 1.51, 1.86, to 2.47, as the methanol decreased from 30%, to 20%, and to 10%, respectively. The resolution between norepinephrine and dopamine improved as the methanol

decreased, increasing from 1.55, to 1.78, to 2.27 at 10% methanol. The changes are apparent in the chromatograms in Figure 4.4. Of note, norepinephrine's retention stayed almost the same in each chromatogram, only changing from $k = 0.45$ to 0.49 at 10% methanol.
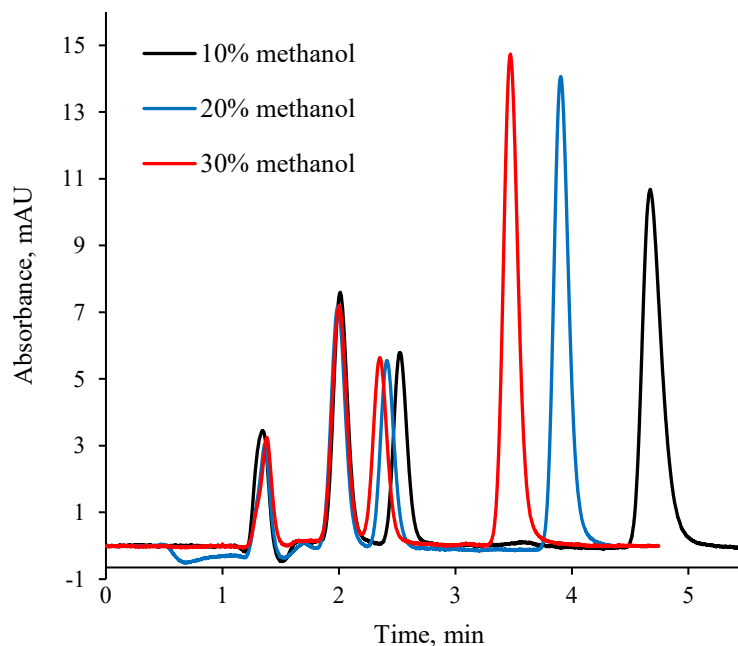
Figure 4.4: Chromatograms of a 50 μM sample of ascorbic acid, norepinephrine, dopamine, and serotonin made in aCSF, listed in order of retention. The pH 2.7 20 mM potassium phosphate buffer remained the same, but the percent of methanol was different in each run 10% (black), 20% (blue), and 30% (red). The other parameters were constant: 74 nL injection, 2.0 μL/min flow rate, 50 ºC oven temperature, and the UV detector at 275 nm.

The cation exchange characteristic of the mixed-mode phase was examined by changing the concentration of the potassium phosphate buffer while keeping everything else the same. Cation exchange phases have less retention as the concentration of the counterion in the mobile phase increases. As the concentration of K^+ increased from 20 mM to 60 mM the retention of the monoamines decreased, as shown in Figure 4.5. The k for each monoamine dropped over 50% going from 20 mM to 60 mM. The least hydrophobic monoamine, norepinephrine, had its k drop from 0.36 to 0.13. This and the lack of effect of organic modifier content stated above support the

hypothesis that norepinephrine is retained predominately by cation-exchange interactions, as tripling the concentration of K^+ reduces the k to $1/3^{rd}$ the initial value. Dopamine goes from a k of 0.54 to 0.20, a little greater than $1/3^{rd}$ the original value, indicating it is retained predominately by cation-exchange interactions with some hydrophobic interaction. The larger, more hydrophobic serotonin's k changed from 1.11 to 0.47, indicating its relatively greater hydrophobic nature affecting its retention. The mixed-mode nature of the COTY phase is highlighted by the varying degrees of the retention change caused by the changes to the mobile phase.
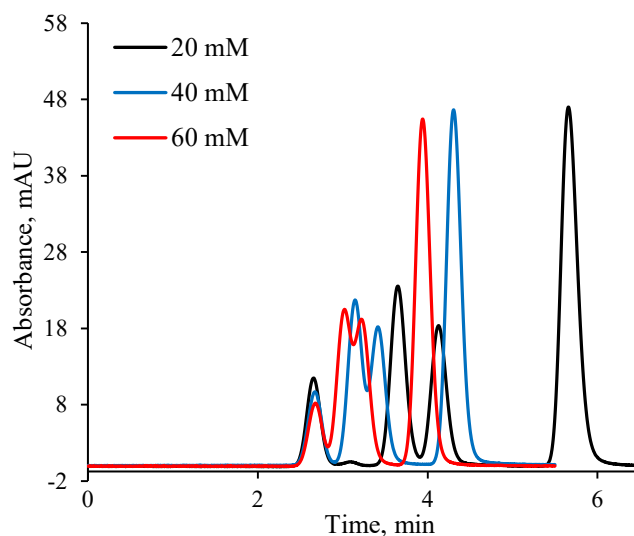
Figure 4.5: Chromatograms of a 50 μM sample of ascorbic acid, norepinephrine, dopamine, and serotonin made in aCSF, solutes are listed in order of elution. The concentration of K^+ was varied in each run, with 20 mM (black), 40 mM (blue), and 60 mM (red). Besides the K^+, everything stayed the same, 70:30 pH 2.7 potassium phosphate buffer:methanol, 1.0 μL/min flow rate, 40 ºC oven temperature, 148 nL injection, and the UV detector at 275 nm.

4.3.6 Low pH degradation study

The stability of the COTY phase was investigated using the same conditions used to test the CTY and SB-C18 phases previously [160]. The results of the COTY phase are compared to

the other stationary phases in Figure 4.6. During the testing of the COTY phase the union to the detector leaked causing the gap in retention data for the COTY. The acidic mobile phase continued to flow through the column, so the analysis was continued. Over the course of six days or almost 35000 column volumes, the COTY phase's retention of triphenylene dropped to about 80% of the k at 1 h, from $k = 0.85$ to 0.68. It is apparent that, under these conditions, the COTY phase is more stable than the SB-C18 with its decrease in k of 27%, and less stable than the CTY, for which k only decreased 11%. This is an interesting result given the low coverage of the octadiyne and crosslinked ligands. The COTY phase's plate count declined about 18% at the same rate as the k, unlike the CTY phase's increasing plate count with decreasing k.
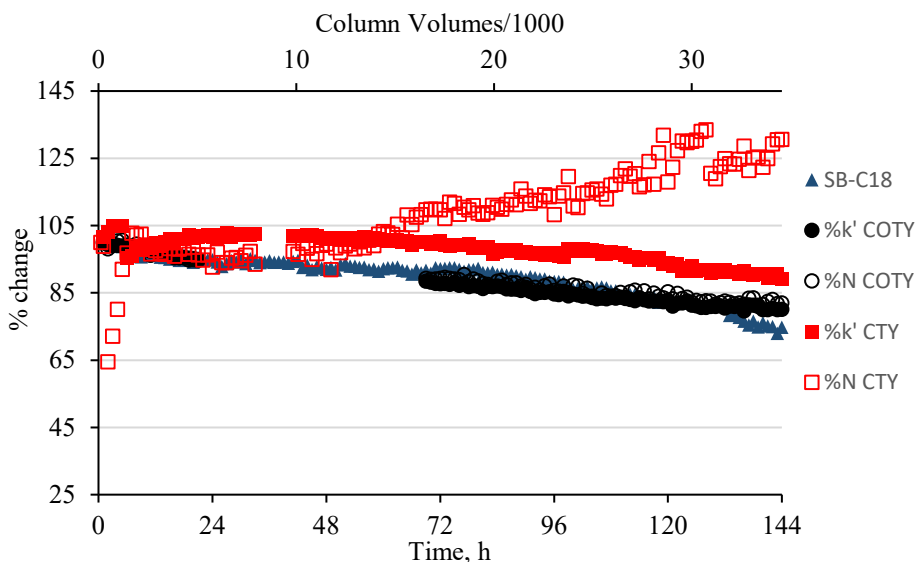
Figure 4.6: Acid degradation study using 50:50 pH 0.5 5% TFA:ACN at 70 ⁰C. The chart shows the percent change, for both k and N, vs. the time or column volumes divided by 1000 for the COTY phase (%k, ●, %N, ○), CTY phase (%k, ■ and %N, □), and the SB-C18 phase (%k, ▲). Gaps in the COTY data set are from the union to the detector leaking, flow continued through the column.

4.3.7 Post degradation characteristics

The COTY phase was also characterized again after the TFA degradation. The Tanaka test results are shown in Table 4.4. The k_{pb} for the phase decreased as expected due to the loss of some stationary phase ligands. The cation-exchange characteristics at pH 2.7 decreased, while at pH 7.6 the $\alpha_{B/P}$ increased presumably due to more surface of the silica being exposed as ligands are hydrolyzed. The increase in exposed silica is also shown by the selectivity between caffeine and phenol in the water:methanol mobile phase. The $\alpha_{C/P}$ value increased from 1.34 ± 0.02 to 2.17 ± 0.07, indicating an increased silanol activity.

Table 4.4: The post-TFA degradation Tanaka test values with 95% confidence intervals for the COTY phase

	TFA COTY	COTY
k'_{pb}	0.10 ± 0.01	0.18 ± 0.01
α_{CH_2}	1.27 ± 0.18	1.20 ± 0.04
$\alpha_{T/O}$	3.15 ± 0.02	2.71 ± 0.03
$\alpha_{C/P}$	2.17 ± 0.07	1.21 ± 0.01
$\alpha_{B/P}$ (pH 2.7)	2.34 ± 0.02	3.98 ± 0.05
$\alpha_{B/P}$ (pH 7.6)	16.07 ± 0.58	11.73 ± 0.18

A van Deemter curve for triphenylene was made for the reduced velocities 1.3 to 8.4 for the initial COTY column, and from 1.2 to 7.0 for the column after degradation, see Figure C.2 in Appendix C. The instrument was not setup for lower velocities for a complete van Deemter, but the resistance to mass transfer term could be determined from the higher velocities. The initial C term was approximately 3.1, and it increased to about 6.3 after the exposure to the TFA solution. The values are very high compared to most reversed-phase silica based phases, but are closer to some polymeric supports and other phases that have slow intraparticle mass transport. It appears

that the reduced plate height minimum at about $\nu = 1.9$ before the degradation was about 8.0, implying poor packing, which was not optimized for this stationary phase. The reduced plate height increases substantially after degradation to nearly 20, at $\nu = 1.9$. The van Deemter studies do show that the column undergoes changes that are detrimental to its efficiency during the exposure to the 5% TFA mobile phase.

The monoamine neurotransmitters are still retained, and have good resolution between dopamine and serotonin. The resolution between dopamine and norepinephrine decreased, with the peaks co-eluting after the TFA degradation, see the chromatogram in Figure 4.7. The k of the neurotransmitters fell from 0.37 to 0.19, 0.56 to 0.24, and from 1.14 to 0.54 for norepinephrine, dopamine and serotonin, respectively. Even with the very extreme conditions for six days, the COTY phase could still be useful in studies where serotonin is being studied.
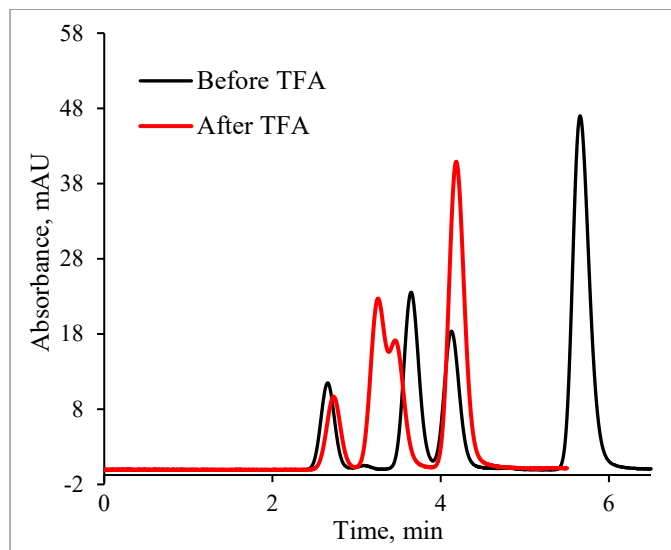
Figure 4.7: Chromatograms before exposure to TFA (black) and after exposure (red) of a 50 μM solution of ascorbic acid, norepinephrine, dopamine, and serotonin, listed in elution order. The conditions were the same for both chromatograms: 148 nL injection, 70:30 pH 2.7 20 mM potassium phosphate:methanol, 1.0 μL/min flow rate, 40 ºC oven temperature, and the UV detector set at 275 nm.

4.4 Conclusion

The COTY phase high shape selectivity and electron-donating charge-transfer characteristics much like the other thiol-yne phases we have previously made [131, 160]. This is mainly due to the electron donating nature of the sulfur atom. As the surface density of sulfur increases, the shape selectivity increases as well. Stationary phases made using the thiol-yne reaction in general should possess greater shape selectivity and charge-transfer characteristics due to the higher amount of sulfur in the stationary phase compared to other synthesis techniques.

The reaction byproducts and other functional groups formed on the surface of the COTY phase were not investigated fully. The small quantities of ligands, 1.8 μm particles, and fluorescence that occurs with the vinyl sulfide containing phases create challenges to adequate analysis. The Tanaka test cation exchange capacities shown by Lindner [95] and in our studies [131, 160], show that oxidation of thiols occurs during the thiol-ene and thiol-yne reactions. The extent of this oxidation has not been studied, and Lindner study [95] is the only such characterization of the thiol-ene or thiol-yne based phases that could be found. Thioethers can be readily oxidized by hydrogen peroxide [168] and other oxidizers [169], but can also react in air. Determining the extent of the oxidation in a stationary phase is difficult, as shown recently by Lui et al. [94]. They created an embedded sulfone stationary phase by oxidizing a thioether stationary phase with *m*-chloroperoxybenzoic acid. The FTIR analysis had poor signal and interference from the silica bonds, so it was compared chromatographically with the thioether phase to characterize the stationary phase. Improved methods to identify structures and functional groups on the silica particles would be beneficial to fully understanding the stationary phases and to improve their performance.

The COTY phase is a fairly stable stationary phase. The phase has about average methylene selectivity, and its selectivity factor benzylamine/phenol is high, indicating mixed-mode cation-exchange characteristics. The cation exchange capacity is apparently lower than our previous DEB based phase from which charged amines often did not elute without salt concentrations over 200 mM. The COTY phase allows the cationic species to elute from the column without high salt concentrations or gradients. A common, 20 mM potassium phosphate buffer is strong enough to elute the amines, as shown with benzylamine and the monoamine neurotransmitters. The ability for a cation-exchange/hydrophobic stationary phase to operate isocratically with low ionic strength, could be useful for two dimensional HPLC. These characteristics could help alleviate the solvent mismatch problem that is often faced in two dimensional HPLC [170-172], and provide orthogonal retention mechanisms and selectivity compared to reversed-phase columns.

The COTY phase can provide good separations of several monoamine neurotransmitters in aCSF. The ability of the phase to retain and separate amines in a high salt sample solution could be beneficial for online microdialysis experiments. An advantage of the separation of the monoamines without the use of an ion-pairing agent is to minimze system peak interference and other detector baseline disturbances that occur during the ion-pairing agent re-equilibration following injection. Here, the three neurotransmitters were separated in about 3.5 min. With a higher pressure HPLC pump and optimization of the mobile phase, it is likely dopamine and serotonin could be separated in under one minute, enabling the high temporal resolution that our group currently obtains [173-176].

The COTY phase is another example of using the thiol-yne reaction to create a stationary phase that is stable in low pHs. The good stability of the phase in extreme conditions, shows that

it can withstand the low pHs needed to ensure even weak bases can be fully protonated to enhance

their separation. Helping improve the phase's usefulness as a mixed-mode stationary phase.

Appendix A Supplemental Information for Chapter 2

A.1 Supplemental tables and figures

Table A.1: HSM solute parameters[a]

Solute	η'	σ'	β'	α'	κ'
amitriptyline	-1.094	0.163	-0.041	0.3	0.817
n-butylbenzioc acid	-0.266	-0.223	0.013	0.838	0.045
N, N-diethylacetamide	-1.39	0.214	0.369	-0.215	0.047
5-phenylpentanol	-0.495	0.136	0.03	0.61	0.013
ethylbenzene	0	0	0	0	0
N, N-dimethylacetamide	-1.903	0.001	0.994	-0.012	0.001
5,5-diphenylhydantoin	-0.94	0.026	0.003	0.568	0.007
toluene	-0.205	-0.095	0.011	-0.214	0.005
nortriptyline	-1.163	-0.018	-0.024	0.289	0.845
acetophenone	-0.744	0.133	0.059	-0.152	-0.009
mefenamic acid	0.049	0.333	-0.049	1.123	-0.008
4-nitrophenol	-0.968	0.04	0.009	0.098	-0.021
anisole	-0.467	0.062	0.006	-0.156	-0.009
benzonitrile	-0.703	0.317	0.003	0.08	-0.03
cis-chalcone	-0.048	0.821	-0.03	0.466	-0.045
trans-chalcone	0.029	0.918	-0.021	-0.292	-0.017

a: Parameter values are from reference [123].

Table A.2: HSM retention data and calculated log α

	k'	α (x/eb)	log α	calculated log α
amitriptyline	44.798	68.803	1.838	1.860
n-butylbenzioc acid	0.496	0.762	-0.118	-0.054
N, N-diethylacetamide	0.044	0.068	-1.169	-0.916
5-phenylpentanol	0.296	0.455	-0.342	-0.199
ethylbenzene	0.651	1.000	0.000	0.000
N, N-dimethylacetamide	0.012	0.019	-1.723	-1.823
5,5-diphenylhydantoin	0.188	0.289	-0.539	-0.527
toluene	0.496	0.761	-0.119	-0.174
nortriptyline	48.464	74.434	1.872	1.825
acetophenone	0.223	0.342	-0.466	-0.505
mefenamic acid	1.460	2.243	0.351	0.245
4-nitrophenol	0.231	0.355	-0.449	-0.666
anisole	0.338	0.519	-0.284	-0.320
benzonitrile	0.224	0.344	-0.464	-0.424
cis-chalcone	0.934	1.435	0.157	0.179
trans-chalcone	1.399	2.149	0.332	0.280
berberine	54.748	84.085	1.925	-

Table A.3: Linear regression data from Excel for the HSM analysis

Regression Statistics	
Multiple R	0.9932
R Square	0.9865
Adjusted R Square	0.8907
Standard Error	0.1244
Observations	16.0000

ANOVA

	df	SS	MS	F	Significance F
Regression	5.0000	12.4548	2.4910	160.9117	0.0000
Residual	11.0000	0.1703	0.0155		
Total	16.0000	12.6251			

	Coefficients	Standard Error	t Stat	P-value	Lower 95%	Upper 95%	Lower 95.0%	Upper 95.0%
Intercept	0.0000	#N/A	#N/A	#N/A	#N/A	#N/A	#N/A	#N/A
H	0.6398	0.0706	9.0573	0.0000	0.4843	0.7953	0.4843	0.7953
S*	0.3516	0.0945	3.7208	0.0034	0.1436	0.5595	0.1436	0.5595
A	-0.6117	0.1943	-3.1487	0.0093	-1.0393	-0.1841	-1.0393	-0.1841
B	0.0806	0.0739	1.0906	0.2988	-0.0821	0.2434	-0.0821	0.2434
C	3.0030	0.1435	20.9337	0.0000	2.6872	3.3187	2.6872	3.3187
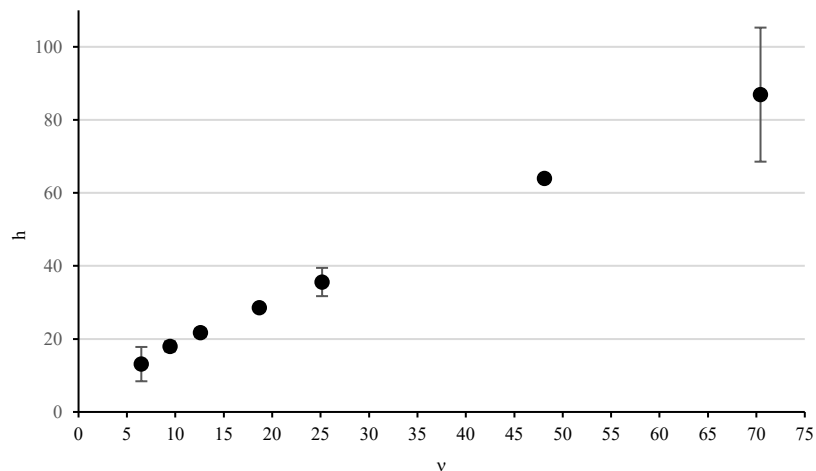
Figure A.1: The reduced van Deemter curve for the CTY column using butylparaben. The mobile phase was 80/20 water/acetonitrile at flow rates from 0.5 to 6.0 μL/min. The temperature was 50 ºC, and 148 nL of the 62.5 μM sample of uracil, for t_0, and butyl paraben was injected onto the 150 μm ID x 10 cm column. The plate counts were calculated using the Foley-Dorsey equation.
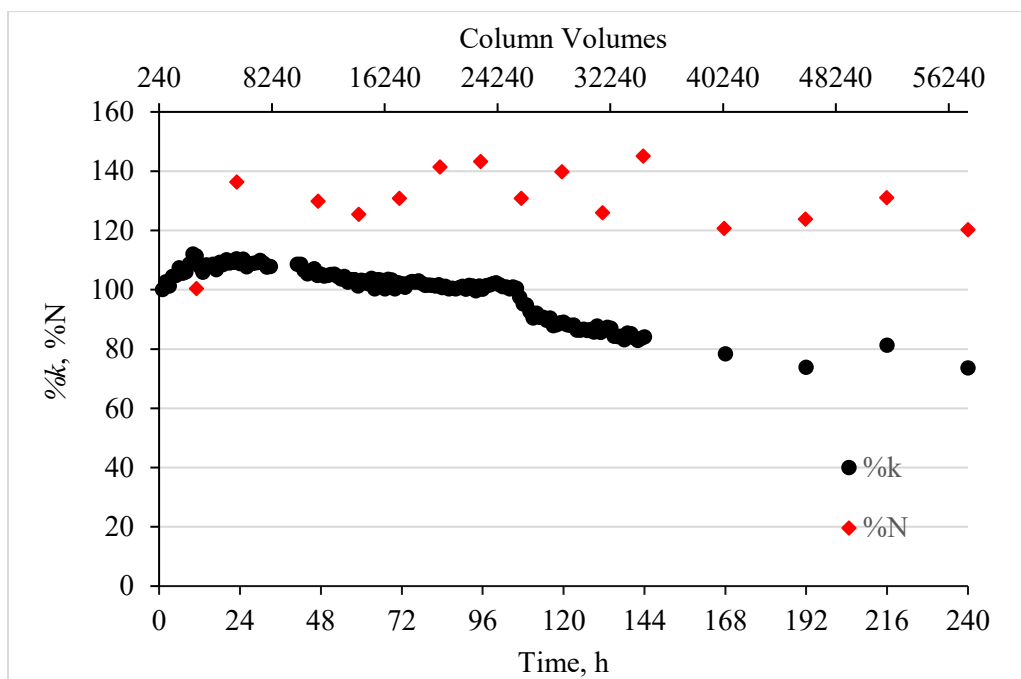
Figure A.2: Degradation study of the CTY phase at pH 0.56, 50:50 5% TFA:acetonitrile, 4 μL/min, 70 ºC, 148 nL injection of 62.5 μM uracil, heptanophenone, and octanophenone. The plot of the % k' of otanophenone vs. the time/column volumes of pH 0.56 exposure.

A.2 Intermediate pH stability test

The pH 9.0 aqueous portion of the mobile phase was made by making a 5 mM ammonium acetate solution with ammonium hydroxide and acetic acid. The mobile phase was 80:20 5mM ammonium acetate:methanol with a flow rate of 4 µL/min. The temperature was 60 ºC, and UV detector was set at 254 nm. 148 nL of a 62.5 µM methyl, ethyl, and propylparaben sample with uracil was injected on the crosslinked and SB-C18 columns for 144 h. Propylparaben's retention factor was used to monitor the column degradation.

A.3 Stability at pH 9.0

The crosslinked stationary phase was tested for its stability at a higher intermediate pH and elevated temperature. Using an aqueous ammonium acetate buffer at pH 9.03 at 60 ºC, the SB-C18 phase and the CTY phase were tested by tracking the retention factor of propylparaben over the course of six days, 144 h. The percent of the original k' versus the time exposed to the pH 9.03 mobile phase is shown in Figure A.3A. The chromatograms from the CTY phase during the hour one and hour 144 are overlayed in Figure A.3B. The two chromatograms are very similar. The first hour still has a sloping baseline indicating the column may not have been equilibrated yet, and the baseline leveled shortly thereafter. During the first day the crosslinked stationary phase experienced a decreasing k', but then it leveled out for the remainder of the study. By the sixth day the CTY phase's k' for propylparaben only decreased 12.8%. The SB-C18 phase showed steady decline over the first four days and by the sixth day the k' had decreased 56.1%.
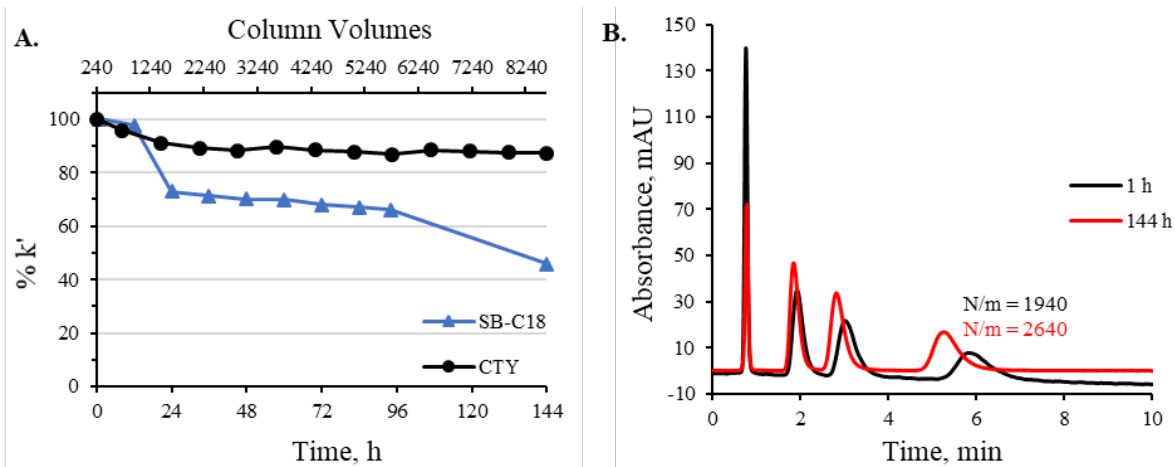
Figure A.3: Intermediate pH degradation study. Conditions were 80:20, pH 9.03 5 μM ammonium acetate:methanol, 60 °C, 4 μL/min. A. Percent of original retention factor, k', for propylparaben versus hours exposed to the pH 9.03 mobile phase. B. Chromatograms at 1 h, black, and 144 h, red, of uracil, methyl, ethyl, and propylparaben. Concentrations were 125 μM for all samples.

Appendix B Supplemental Information for Chapter 3
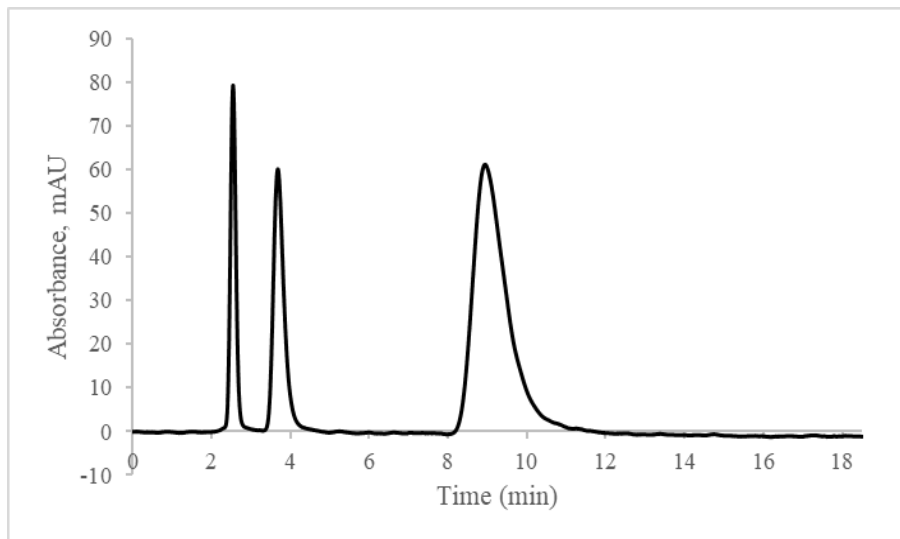
Figure B.1: Chromatogram of 62.5 μM uracil, 31 μM *o*-terphenyl and triphenylene on the CTY stationary phase at 40 ºC. The average Foley-Dorsey N_{sys} on the 10 cm column were 1322, 589, and 284, respectively. Conditions are explained in Section 3.2.6.

Table B.1: Elemental analysis data

Sample	% C	% S	% H	μmol S/m^2	Coverage (μmol/m^2)
Zorbax	0.25	0.00	0.29	-	-
Thiol	2.21	0.94	0.50	1.7	1.7
HD-Thiol	4.04	2.88	0.75	5.4	5.4
DEB	6.71	0.91	0.81	1.7	2.3[a]
HD-DEB	9.97	2.66	1.00	5.3	3.2[a]
Crosslinked	12.49	5.01	1.41	8.7	2.4[b]

The absolute error from Atlantic Microlabs is 0.30 %.

a- The DEB coverage.
b- The 1,6-hexanedithiol coverage.

Table B.2: Slope, intercept, and error data from van't Hoff plots for the crosslinked, DEB, and SB-C18 stationary phases

Phase	Solute	Slope (K)	Slope Standard Error (K)	Slope Lower 95% (K)	Slope Upper 95% (K)	Y-Intercept	Intercept Standard Error	Intercept Lower 95%	Intercept Upper 95%
Crosslinked	o-terphenyl	2923.658	89.24376	2730.858	3116.457	-8.2179	0.277094	-8.81653	-7.61928
	triphenylene	3434.423	68.34359	3286.775	3582.07	-8.26502	0.212201	-8.72345	-7.80659
SB-C18	o-terphenyl	2359.176	38.01275	2275.51	2442.841	-6.6931	0.122157	-6.96196	-6.42423
	triphenylene	2603.552	40.82027	2513.708	2693.397	-7.2611	0.131179	-7.54982	-6.97237
DEB	o-terphenyl	2590.161	20.53517	2547.68	2632.641	-8.99521	0.06376	-9.12711	-8.86331
	triphenylene	2799.823	17.87198	2762.852	2836.794	-8.48762	0.055491	-8.60241	-8.37283
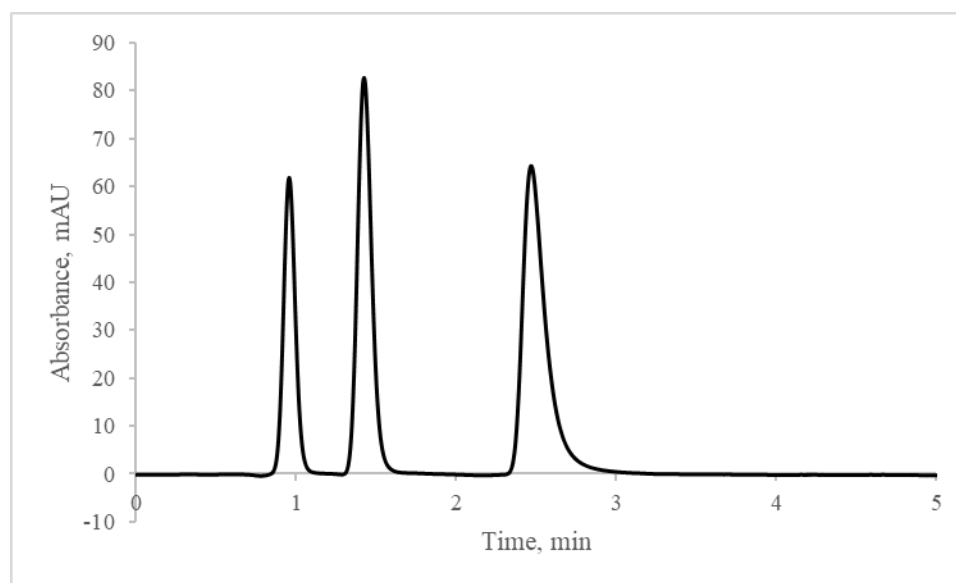
Figure B.2: Chromatogram of 62.5 μM uracil, 31 μM *o*-terphenyl and triphenylene on the DEB stationary phase at 40 ºC. The average Foley-Dorsey N_{sys} on the 10 cm column were 707, 1043, and 755, respectively. Conditions are explained in Section 3.2.6.
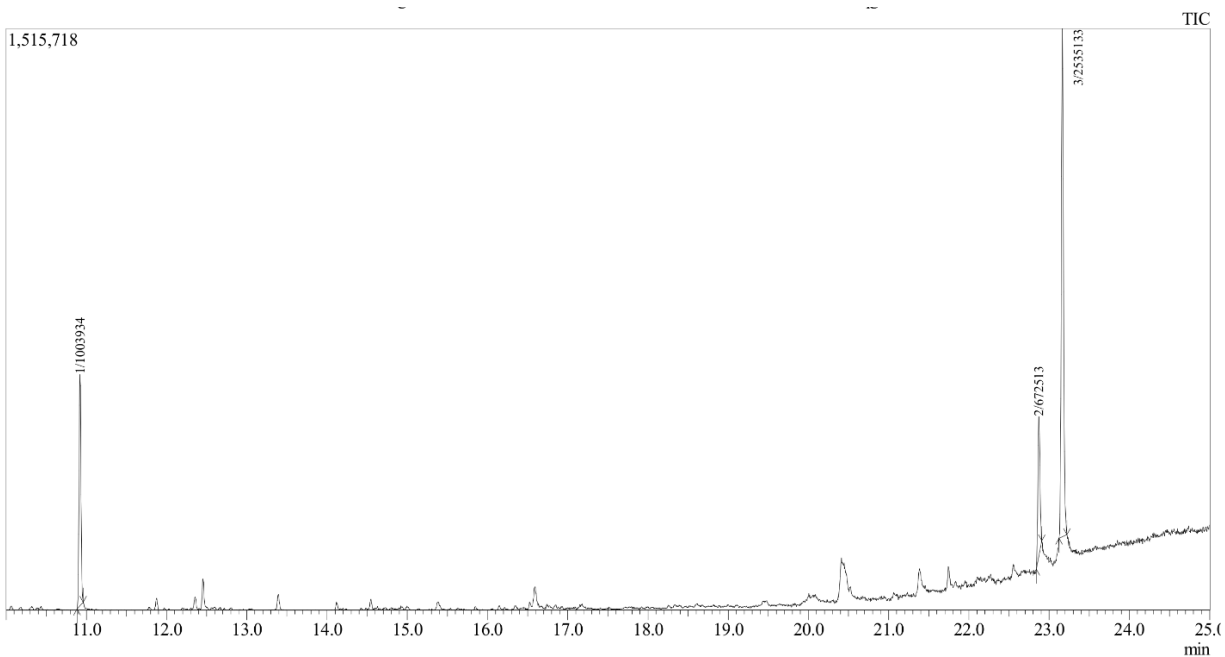
Figure B.3: GC/MS chromatogram of the silylated product of DEB and 2-mercaptoethanol. The peaks at 22.9 and 23.2 min are the isomers of the silylated disubstituted DEB molecule. The peak at 10.9 min is the silylated mercaptoethanol. The other peaks are siloxanes and THF stabilizers. Conditions are listed in section 3.2.3.
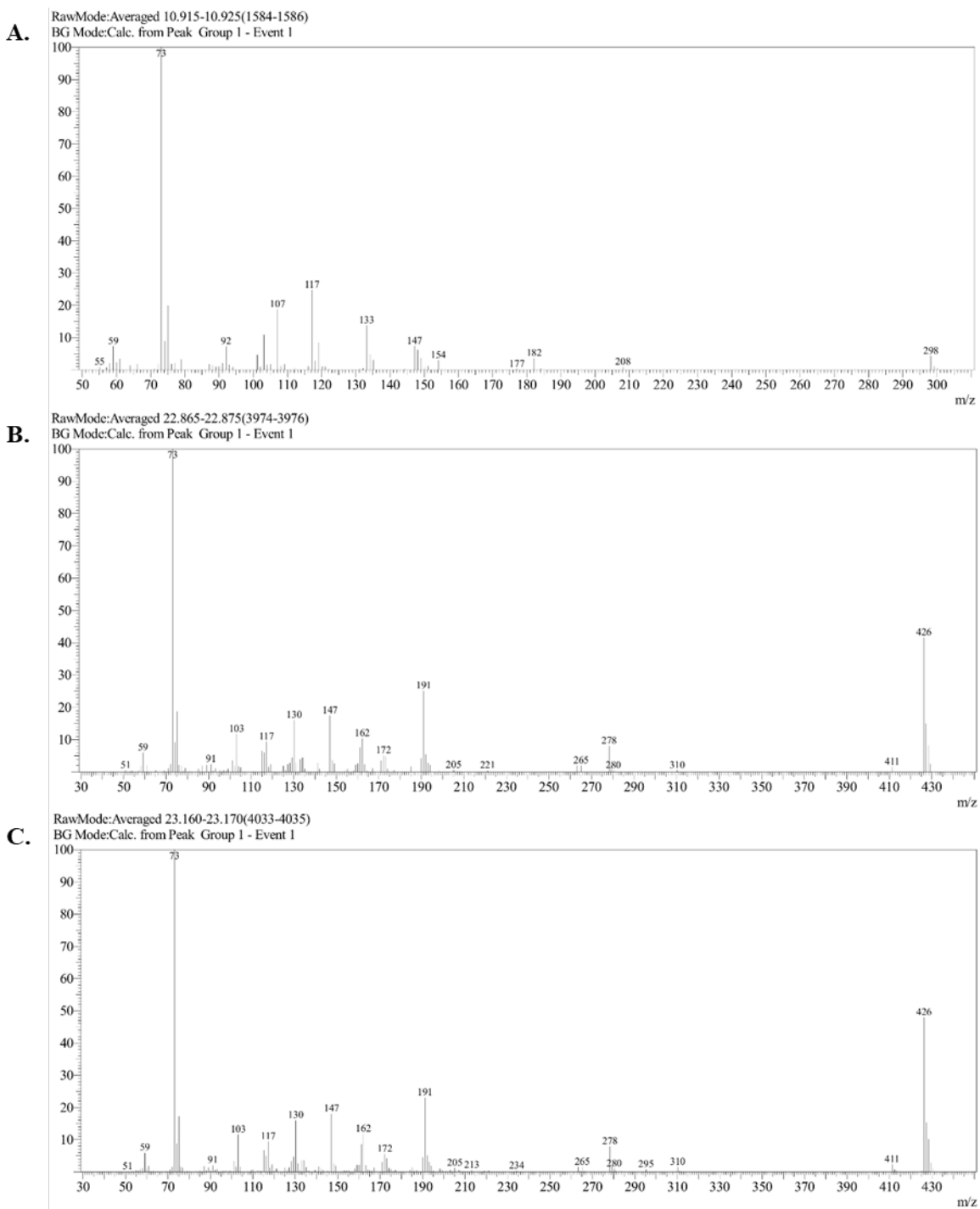
Figure B.4: Mass spectra for Figure S4. The spectra are for the peaks at 10.9 min (A), 22.9 min (B), and 23.2 min (C). The peak at 10.9 min corresponds to the silylated 2-hydroxyethyl disulfide, with the molecular ion at 298 m/z. The later peaks both have the molecular ion at 426 m/z, indicating DEB reacted with two mercaptoethanols and the alcohols were silylated. High order additions of mercaptoethanols with DEB were not seen with GC/MS.

Figure B.5: Mass spectrum and peak table for the 282 m/z region of the DEB and 2-mercaptopropanol reaction product. The molecular weight of 282 corresponds to the addition of two mercaptoethanols, with a formula of $C_{14}H_{18}O_2S_2$. The 281.067 m/z peak is the $[M-H]^+$ molecular ion, and is the most abundant peak in the mass spectrum by over two orders of magnitude.
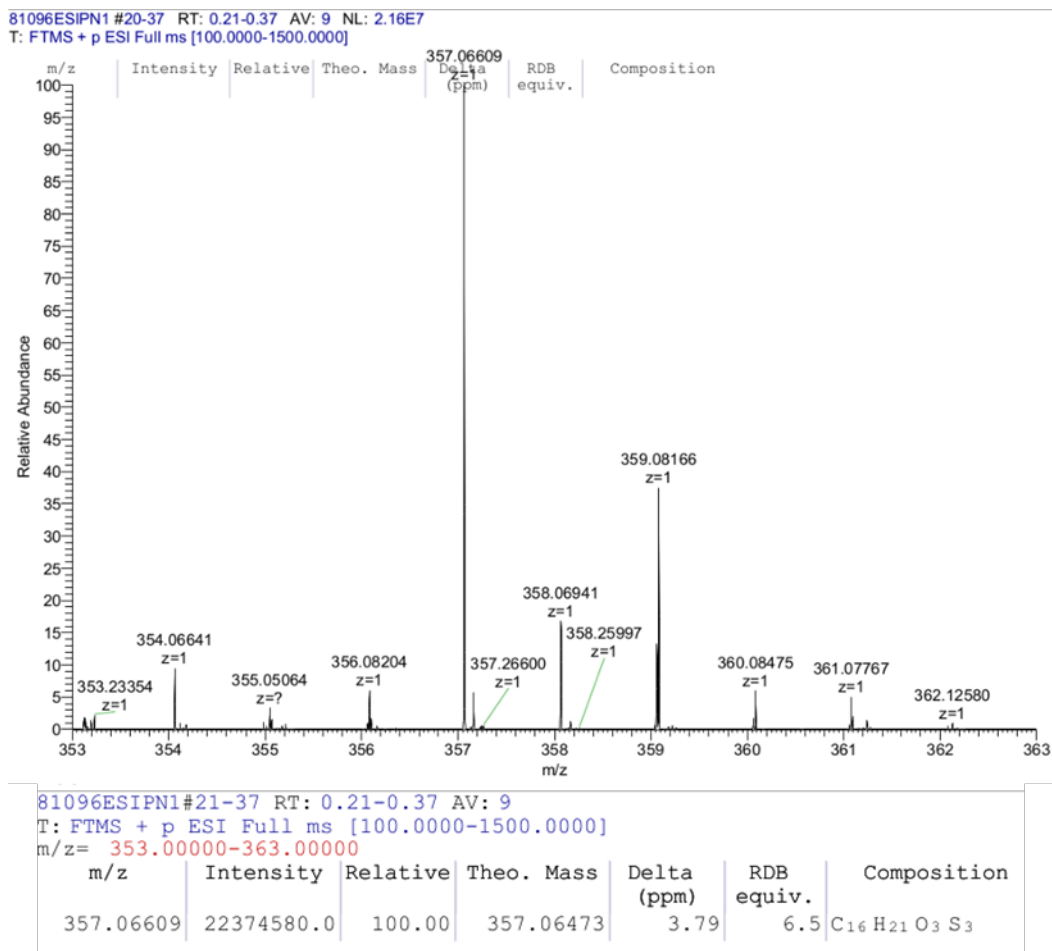
Figure B.6: Mass spectrum and data table showing the region around 358 m/z corresponding to DEB reacting with three 2-mercaptoethanols, $C_{16}H_{22}O_3S_3$. The most abundant peak in the region corresponds the [M-H]$^+$ ion.
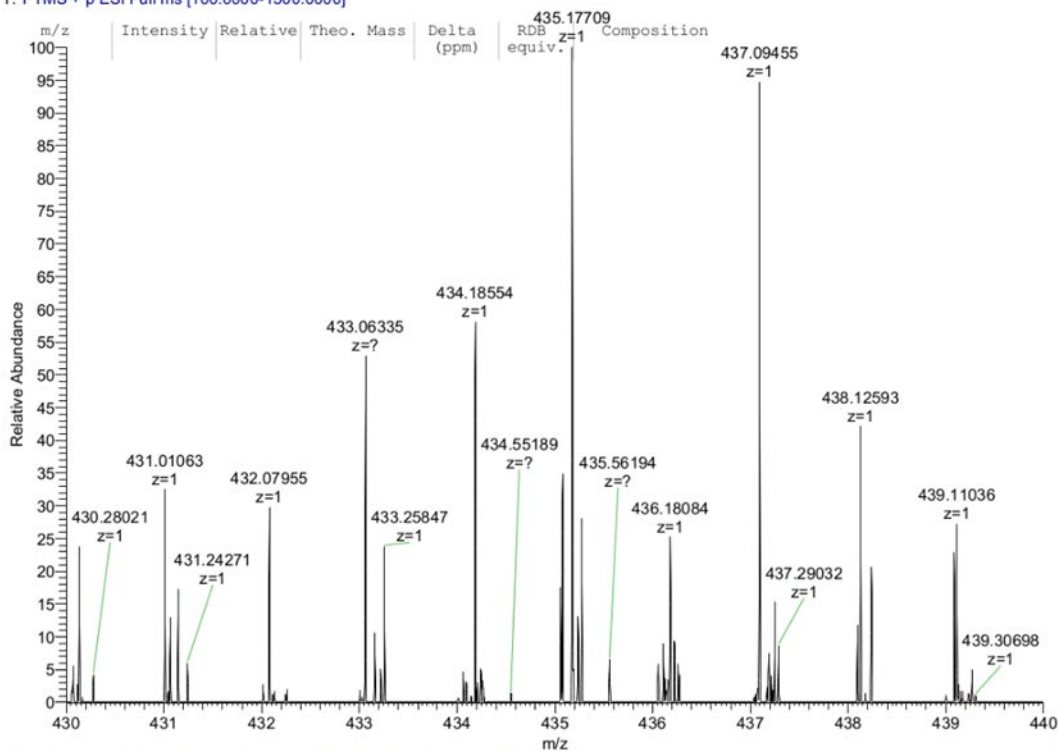
m/z	Intensity	Relative	Theo. Mass	Delta (ppm)	RDB equiv.	Composition
435.17709	1360821.6	100.00	435.07867	226.17	5.5	$C_{18} H_{27} O_4 S_4$
437.09455	1275014.1	93.69	437.09432	0.54	4.5	$C_{18} H_{29} O_4 S_4$
435.07925	475292.7	34.93	435.07867	1.34	5.5	$C_{18} H_{27} O_4 S_4$
435.27434	388089.0	28.52	435.07867	449.53	5.5	$C_{18} H_{27} O_4 S_4$
436.18084	345911.1	25.42	436.08649	216.30	5.0	$C_{18} H_{28} O_4 S_4$
435.06038	235734.7	17.32	435.07867	-42.03	5.5	$C_{18} H_{27} O_4 S_4$
437.25257	206056.2	15.14	437.09432	361.93	4.5	$C_{18} H_{29} O_4 S_4$
435.23629	178934.9	13.15	435.07867	362.16	5.5	$C_{18} H_{27} O_4 S_4$
436.22329	127825.7	9.39	436.08649	313.58	5.0	$C_{18} H_{28} O_4 S_4$
436.10952	123146.9	9.05	436.08649	52.80	5.0	$C_{18} H_{28} O_4 S_4$
437.29032	119336.1	8.77	437.09432	448.22	4.5	$C_{18} H_{29} O_4 S_4$
437.19384	102206.1	7.51	437.09432	227.63	4.5	$C_{18} H_{29} O_4 S_4$

Figure B.7: Mass spectrum and data table showing the region around 438 m/z corresponding to DEB reacting with four 2-mercaptoethanols, $C_{18}H_{30}O_4S_4$. The peaks at 435.17709 m/z and 437.09455 m/z correspond to a strange [M-3H]$^+$ and the usual [M-H]$^+$ molecular ion peaks, respectively.
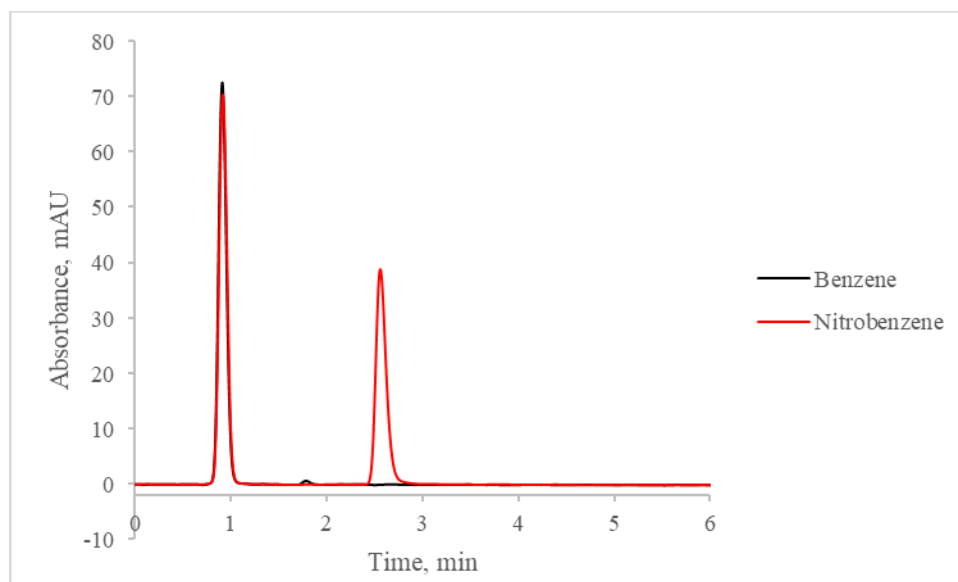
Figure B.8: Overlay of chromatograms of 62.5 µM uracil and benzene (black) and 62.5 µM uracil and nitrobenzene (red). The conditions are explained in section 3.2.6. The benzene peak is had low absorbance at 254 nm compared to the nitrobenzene, but the peak is still easily quantifiable.

Appendix C Supplemental Information for Chapter 4

Table C.1: HSM solute parameters [123]

Solute	η'	σ'	β'	α'	κ'
amitriptyline	-1.094	0.163	-0.041	0.3	0.817
n-butylbenzoic acid	-0.266	-0.223	0.013	0.838	0.045
N, N-diethylacetamide	-1.39	0.214	0.369	-0.215	0.047
5-phenylpentanol	-0.495	0.136	0.03	0.61	0.013
ethylbenzene	0	0	0	0	0
N, N-dimethylacetamide	-1.903	0.001	0.994	-0.012	0.001
5,5-diphenylhydantoin	-0.94	0.026	0.003	0.568	0.007
toluene	-0.205	-0.095	0.011	-0.214	0.005
nortriptyline	-1.163	-0.018	-0.024	0.289	0.845
acetophenone	-0.744	0.133	0.059	-0.152	-0.009
mefenamic acid	0.049	0.333	-0.049	1.123	-0.008
4-nitrophenol	-0.968	0.04	0.009	0.098	-0.021
anisole	-0.467	0.062	0.006	-0.156	-0.009
benzonitrile	-0.703	0.317	0.003	0.08	-0.03
cis-chalcone	-0.048	0.821	-0.03	0.466	-0.045
trans-chalcone	0.029	0.918	-0.021	-0.292	-0.017

Table C.2: Experimental results used for the HSM regression

Solute	k'	± 95%	$\alpha_{x/eb}$	log α
Amitriptyline	2.337	± 0.004	6.667	0.824
n-butylbenzioc acid	0.310	± 0.004	0.884	-0.054
N,N-diethylacetamide	0.105	± 0.004	0.299	-0.524
5-phenylpentanol	0.263	± 0.008	0.752	-0.124
ethylbenzene	0.350	± 0.009	1.000	0.000
N,N-dimethylacetamide	0.064	± 0.003	0.098	-1.011
5,5-diphenylhydantoin	0.189	± 0.004	0.287	-0.542
toluene	0.286	± 0.001	0.434	-0.362
nortriptyline	1.981	± 0.011	3.011	0.479
acetophenone	0.189	± 0.005	0.287	-0.542
mefenamic acid	0.585	± 0.008	0.889	-0.051
4-nitrophenol	0.145	± 0.003	0.221	-0.656
anisole	0.232	± 0.002	0.353	-0.452
benzonitrile	0.191	± 0.009	0.290	-0.538
cis-chalcone	0.505	± 0.013	0.768	-0.115
trans-chalcone	0.635	± 0.013	0.965	-0.015
berberine	2.696	± 0.028		
berberine (ph7)	7.242	± 0.081		

Table C.3: COTY phase's HSM regression results

Coefficient	Value	± 95%
H	0.501	± 0.248
S	0.140	± 0.266
A	0.137	± 0.487
B	0.105	± 0.190
C(2.8)	1.584	± 0.344
C(7.0)	2.013	± 0.344
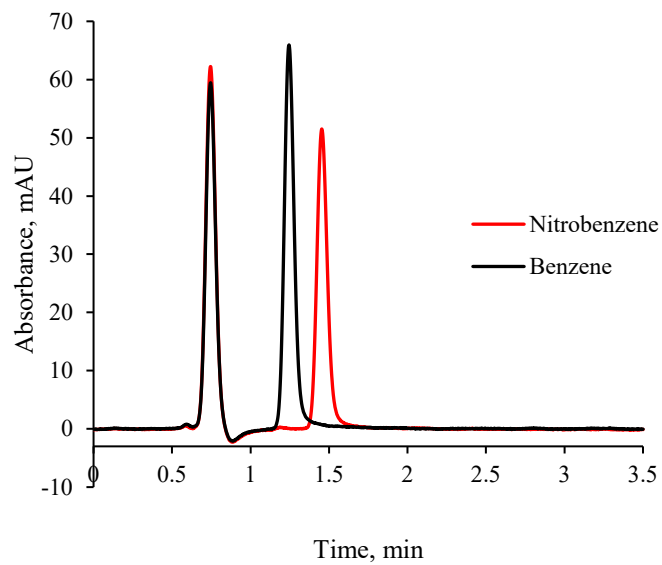
Figure C.1: Overlayed chromatograms for benzene (black) and nitrobenzene (red) with uracil as the void marker. The 100 μM sample was run with a 70:30 water:methanol mobile phase at 4.0 μL/min and 50 ºC with a 148 nL injection and the UV detector set at 205 nm.
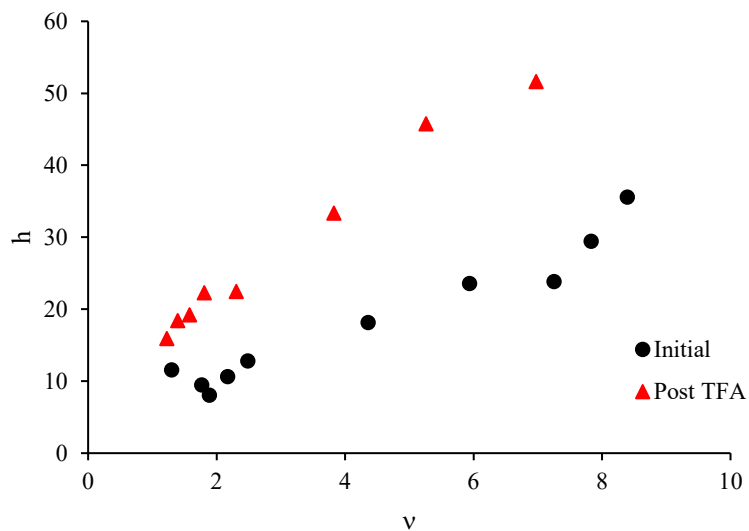
Figure C.2: The van Deemter curve, reduced plate height versus the reduced interstitial velocity, for triphenylene on the COTY column before (●) and after (▲) the TFA degradation study. The values shown are for the column, with the extra column dispersion subtracted. The particle diameter was 1.8 μm and the diffusion coefficient used was 7.0 x 10^{-6} cm^2/s for a small molecule in water at 20 ºC [177]. The diffusion coefficient was adjusted to 80:20 methanol:water and 50 ºC by accounting for the temperatures and viscosities at the given temperatures, as in [178].

Appendix D Stationary Phase Synthesis Procedures

D.1 Synthesis of thiol silica

High coverage "polymeric" phase: About 16 mL of extra dry toluene, stored over molecular sieves, were added to 2.002 g of 1.8 μm Zorbax RX-Sil silica particles that had been dried overnight in a 100 °C vacuum oven. **Note: Dry particles, glassware, syringe, and needle. Keep the solvent at about 8-10 mL per gram of particles. Use a size of round-bottom flask so that the flask is close to half full (too big of a flask, and it will evaporate, too full and it becomes dangerous).** Triethylamine (400 μL) was added and the solution was stirred for five minutes, sonicated for one minute, and stirred for three more minutes before adding 1.61 mL of MPTMS. **Note: a 3-neck flask is convenient to add the reactants with a syringe without adding much air, make sure it is tightly sealed using rubber septa.** The mixture was stirred and refluxed under nitrogen dried by passage through calcium sulfate for about 44 h. The solution was vacuum filtered using a Millipore 0.45 nm nylon membrane (Burlington, MA). **Caution: Always check the solvent/membrane compatibility, not just here but anytime filtering is required, adjust the membrane or the solvents as needed.** The flask was rinsed with 15 mL of toluene and poured over the particles on the membrane. The particles were rinsed two times with 15 mL of each of the following solvents in order: benzene, hexanes, ACN, water, and one more ACN rinse. **Note: Rinse well, at least with toluene, methanol, and then acetone or ACN.** The thiol-functionalized silica was dried at 95 °C in a vacuum oven overnight.

Low coverage phase: **Note: This is the same as above, but with the less reactive silane**

and less time. To increase the surface coverage using a particular silane, increased time reaction seems beneficial. The Zorbax RX-sil and glassware was dried in a 100 to 110 °C vacuum oven overnight. To 4.00 g Zorbax silica 25 mL of extra dry toluene stored over molecular sieves was added and the mixture was sonicated for 1 minute and stirred for 1 minute. To the slurry, 836 μL triethylamine was added and the mixture sonicated for 1 minute and stirred for 10 minutes before adding 3.00 mL MPTES. **Note: As above, a three neck flask with septa and a syringe are helpful to avoid exposure to the air.** The suspension was stirred for 10 minutes and brought to a boil. The solution was refluxed for 32 h and allowed to cool to room temperature. The suspension was vacuum filtered and rinsed two times each with 20 mL toluene, 25 mL hexanes, and 25 mL tetrahydrofuran and dried overnight in a 100 °C vacuum oven.

D.2 Synthesis of DEB silica

Around 10 mL of extra dry toluene was added to 1.120 g of the thiol silica, 32.8 mg AIBN, and 252 mg of DEB **(excess amount)** in a round bottom flask. The mixture was sonicated for one minute and stirred for two minutes before refluxing for 28 h. **Note: 28 h is not needed, the AIBN was probably all reacted before this, overnight should be sufficient.** The suspension was transferred to centrifuge tubes, the flask was rinsed and the rinse solution was added to the centrifuge tubes. These were centrifuged and the liquid decanted. **Note: The particles should now be dark brown when wet with the toluene or aromatic solvent.** The particles were rinsed one time using 15 mL of toluene, resuspended in 15 mL of toluene, and vacuum filtered using a Millipore 0.45 μm nylon membrane. The particles were rinsed two times with 15 mL of each of the following solvents: hexanes, ACN, water, and acetone **(Note: the excess DEB needs to be rinsed, the solvents should be able to dissolve DEB at**

least) and then were dried overnight in a 100 ºC vacuum oven.

D.3 Synthesis of the crosslinked CTY stationary phase

About 5 mL of extra dry toluene was added to 298 mg of DEB silica and 19.9 mg AIBN, and stirred for three min. 1,6-hexanedithiol, 100 μL, **(Caution: Thiols smell terrible, ALWAYS keep the bottle and syringe or pipette in the hood during transfer. Use bleach water to neutralize the odor on everything that the thiol touches, including gloves, before moving anything out of the hood.)** was added to the suspension and refluxing was begun for 24 h. **Note: With the small volumes a small single neck flask can help ensure the solvent does not evaporate. The thiol-yne reaction can proceed in air.** 2 mL of toluene was added to the suspension, and the mixture was refluxed 22 h. **Note: This extra reaction time is not needed, see above.** The suspension plus 10 mL of toluene rinse was centrifuged and the liquid decanted. The particles were rinsed twice with toluene, ACN, 20 mM phosphoric acid (pH 2.08), water, and one time with acetone by adding in each case 10 mL of the liquid, suspending the particles, centrifuging, and decanting the liquid. **Note: The unreacted monomers need to be removed. Rinsing with the vacuum filter is good too, and easier. It is recommended to rinse in an HPLC column as well, this is described below for the crosslinked phase below.** The particles were transferred to a glass Petri dish with 5 mL of acetone to dry in a 100 ºC oven until the acetone had evaporated. The particles were dried overnight in a 100 ºC vacuum oven.

D.4 Octadiyne silica synthesis

To 300.20 mg of the thiol silica **(this was the low coverage thiol silica)** and 3.28 mg AIBN, 4 mL of chloroform was added and the mixture was sonicated 1 minute and stirred 1 minute. **Note: Using chloroform or toluene gives a product with the same characteristics, the solubility of the reagents and the quality of the suspension are the main concerns. The higher the boiling point the shorter the reaction time needs to be (toluene refluxing overnight will use up most of the AIBN)**. While stirring 200 μL of 1,7-octadiyne was added and allowed to stir 10 minutes **(Note: Used 10+ times the amount of alkynes as thiol)**. The suspension was refluxed for 30 h and cooled. The modified silica was rinsed two times each with 20 mL chloroform, 20 mL pentane, 20 mL methanol, and one time with 20 mL chloroform on a vacuum filter. The particles were dried overnight in a 100 °C vacuum oven.

D.5 Crosslinked octadiyne silica synthesis

The octadiyne was crosslinked by adding 251.00 mg octadiyne silica, 10.42 mg AIBN, 4.00 mL chloroform, and 103.5 μL 1,6-hexandithiol **(excess)** to a flask and sonicating for 1 min and stirring for 5 minutes to suspend the particles. The suspension was refluxed for 25 h and poured into a vacuum filter to rinse 3 times each with 10 mL chloroform, 15 mL hot ethanol, and two times with 10 mL hexanes. The particles were dried in a vacuum oven at 100 °C overnight. The particles were further rinsed by suspending them in 10 mL chloroform and pouring onto a vacuum filter. The particles were rinsed with 10 mL chloroform, two times with 20 mL ethyl acetate, and 10 mL of chloroform. The particles were dried for 3 h in a 100 °C vacuum oven. **Note: Skip a**

second rinse and move onto the HPLC column rinse. A 2.1 mm ID X 5 cm stainless steel blank column was dry packed with the particles (**Note: The tip was cut off of a 200 μL pipette tip to make a funnel to tap the particles into the column. After flushing remove the head of the column and reverse the flow to push the particles out into a Petri dish to dry.**) and flushed with methanol at 0.1 mL/minute for 25 h (**Note: The excess thiol can be smelled in the eluent. This was flushed past the point where it was hard to smell. The chromatographic performance was much more stable after rinsing in this manner.**) on an Isco Model 100DM Syringe Pump (Lincoln, NE). The particles were dried overnight in a 100 ºC vacuum oven.

Bibliography

[1] L.R. Snyder, J.W. Dolan, P.W. Carr, The hydrophobic-subtraction model of reversed-phase column selectivity, Journal of Chromatography A, 1060 (2004) 77-116.

[2] J.J. Kirkland, Development of some stationary phases for reversed-phase HPLC, Journal of Chromatography A, 1060 (2004) 9-21.

[3] V.F. Samanidou, Basic LC Method Development and Optimization, in: A.B. Jared L. Anderson, Verónica Pino Estévez, and Apryll M. Stalcup (Ed.) Analytical Separation Science, Wiley-VCH Verlag GmbH & Co., 2015, pp. 25-42.

[4] J.J. Kirkland, Practical Method Development Strategy for Reversed Phase HPLC of Ionizable Compounds, LC-GC, 14 (1996) 486.

[5] S. Heinisch, J.-L. Rocca, Sense and nonsense of high-temperature liquid chromatography, Journal of Chromatography A, 1216 (2009) 642-658.

[6] P.W. Carr, J.W. Dolan, U.D. Neue, L.R. Snyder, Contributions to reversed-phase column selectivity. I. Steric interaction, Journal of chromatography. A, 1218 (2011) 1724-1742.

[7] S.R. Groskreutz, S.G. Weber, Temperature-assisted on-column solute focusing: A general method to reduce pre-column dispersion in capillary high performance liquid chromatography, Journal of Chromatography A, 1354 (2014) 65-74.

[8] E.N.D.C. Andrade, The Viscosity of Liquids, Nature, 125 (1930) 309-310.

[9] L.C. Sander, S.A. Wise, The influence of column temperature on selectivity in reversed-phase liquid chromatography for shape-constrained solutes, J. Sep. Sci., 24 (2001) 910-920.

[10] H. Kanazawa, K. Yamamoto, Y. Matsushima, N. Takai, A. Kikuchi, Y. Sakurai, T. Okano, Temperature-Responsive Chromatography Using Poly(N-isopropylacrylamide)-Modified Silica, Anal Chem, 68 (1996) 100-105.

[11] D.J. Anderson, High-performance liquid chromatography (advances in packing materials), Anal Chem, 67 (1995) 475-486.

[12] P. Gzil, N. Vervoort, G.V. Baron, G. Desmet, Advantages of Perfectly Ordered 2-D Porous Pillar Arrays over Packed Bed Columns for LC Separations: A Theoretical Analysis, Anal Chem, 75 (2003) 6244-6250.

[13] J. Nawrocki, The silanol group and its role in liquid chromatography, Journal of Chromatography A, 779 (1997) 29-71.

[14] A. Berthod, Silica: backbone material of liquid chromatographic column packings, Journal of Chromatography A, 549 (1991) 1-28.

[15] J.J. Kirkland, F.A. Truszkowski, R.D. Ricker, Atypical silica-based column packings for high-performance liquid chromatography, Journal of Chromatography A, 965 (2002) 25-34.

[16] J.J. Kirkland, J.L. Glajch, R.D. Farlee, Synthesis and characterization of highly stable bonded phases for high-performance liquid chromatography column packings, Anal Chem, 61 (1989) 2-11.

[17] V. Lenher, H.B. Merrill, THE SOLUBILITY OF SILICA, Journal of the American Chemical Society, 39 (1917) 2630-2638.

[18] K.K. Unger, N. Becker, P. Roumeliotis, Recent developments in the evaluation of chemically bonded silica packings for liquid chromatography, Journal of Chromatography A, 125 (1976) 115-127.

[19] M. Hanson, K.K. Unger, G. Schomburg, Non-porous polybutadiene-coated silicas as stationary phases in reversed-phase chromatography, Journal of Chromatography A, 517 (1990) 269-284.

[20] J.J. Kirkland, Stability of silica-based, monofunctional C18 bonded-phase column packing for HPLC at high pH, J. Chromatogr. Sci., 34 (1996) 309-313.

[21] J.J. Kirkland, J.B. Adams, M.A. van Straten, H.A. Claessens, Bidentate Silane Stationary Phases for Reversed-Phase High-Performance Liquid Chromatography, Anal Chem, 70 (1998) 4344-4352.

[22] J.J. Kirkland, J.W. Henderson, J.J. DeStefano, M.A. van Straten, H.A. Claessens, Stability of silica-based, endcapped columns with pH 7 and 11 mobile phases for reversed-phase high-performance liquid chromatography, Journal of Chromatography A, 762 (1997) 97-112.

[23] J.J. Kirkland, M.A. van Straten, H.A. Claessens, High pH mobile phase effects on silica-based reversed-phase high-performance liquid chromatographic columns, J. Chromatogr. A, 691 (1995) 3-19.

[24] J.J. Kirkland, M.A. van Straten, H.A. Claessens, Reversed-phase high-performance liquid chromatography of basic compounds at pH 11 with silica-based column packings, Journal of Chromatography A, 797 (1998) 111-120.

[25] B.C. Trammell, L. Ma, H. Luo, M.A. Hillmyer, P.W. Carr, An ultra acid stable reversed stationary phase, J Am Chem Soc, 125 (2003) 10504-10505.

[26] P.W. Carr, M.O. Rigney, E.F. Funkenbusch, P.L. Coleman, D.A. Hanggi, High-stability porous zirconium oxide spherules for use as chromatographic column support, in, University of Minnesota, USA . 1989, pp. 19 pp.

[27] J. Zhao, P.W. Carr, Synthesis and evaluation of an aromatic polymer-coated zirconia for reversed-phase liquid chromatography, Anal. Chem., 71 (1999) 5217-5224.

[28] M. Hanson, A. Kurganov, K.K. Unger, V.A. Davankov, Polymer-coated reversed-phase packings in high-performance liquid chromatography, Journal of Chromatography A, 656 (1993) 369-380.

[29] G. Schomburg, Polymer coating of surfaces in column liquid chromatography and capillary electrophoresis, TrAC Trends in Analytical Chemistry, 10 (1991) 163-169.

[30] C.G. Horvath, S.R. Lipsky, Use of Liquid Ion Exchange Chromatography for the Separation of Organic Compounds, Nature, 211 (1966) 748-749.

[31] S.S. Airapetyan, A.G. Khachatryan, Chromatographic Properties of Silica Gel Packing Materials as Influenced by Polymeric Coating, Russian Journal of Applied Chemistry, 76 (2003) 1864-1866.

[32] M. Hanson, B. Eray, K. Unger, A.V. Neimark, J. Schmid, K. Albert, E. Bayer, A model for polybutadiene coatings on porous silica, Chromatographia, 35 (1993) 403-409.

[33] G. Fischer, U. Skogsberg, S. Bachmann, H. Yüksel, S. Steinbrecher, E. Plies, K. Albert, Synthesis, Characterization, and Evaluation of Divinylbenzene-Coated Spherical Nonporous Silica†, Chemistry of Materials, 15 (2003) 4394-4400.

[34] M. Hanson, K.K. Unger, C.T. Mant, R.S. Hodges, Polymer-coated reversed-phase packings with controlled hydrophobic properties: I. Effect on the selectivity of protein separations, Journal of Chromatography A, 599 (1992) 65-75.

[35] S.S. Hayrapetyan, H.G. Khachatryan, U.D. Neue, A detailed discussion of the influence of the amount of deposited polymer on the retention properties of polymer-coated silicas, Journal of separation science, 29 (2006) 801-809.

[36] B.B. Wheals, Chemically bonded phases for liquid chromatography modification of silica with vinyl monomers, Journal of Chromatography A, 107 (1975) 402-406.

[37] A.A. Kurganov, A.B. Tevlin, V.A. Davankov, High-performance ligand-exchange chromatography of enantiomers: Studies on polystrene-type chiral phases bonded to microparticulate silicas, Journal of Chromatography A, 261 (1983) 223-233.

[38] M.R. Buchmeiser, New synthetic ways for the preparation of high-performance liquid chromatography supports, Journal of Chromatography A, 918 (2001) 233-266.

[39] T. Takeuchi, W. Hu, H. Haraguchi, D. Ishii, Evaluation of the stability of polymer-coated silica-based packing materials for high-performance liquid chromatography, Journal of Chromatography A, 517 (1990) 257-262.

[40] B.C. Trammell, L. Ma, H. Luo, M.A. Hillmyer, P.W. Carr, Synthesis and characterization of hypercrosslinked, surface-confined, ultra-stable silica-based stationary phases, Journal of Chromatography A, 1060 (2004) 61-76.

[41] B.C. Trammell, L. Ma, H. Luo, D. Jin, M.A. Hillmyer, P.W. Carr, Highly Cross-Linked Self-Assembled Monolayer Stationary Phases: An Approach to Greatly Enhancing the Low pH Stability of Silica-Based Stationary Phases, Anal Chem, 74 (2002) 4634-4639.

[42] Y. Zhang, P.W. Carr, Novel ultra stable silica-based stationary phases for reversed phase liquid chromatography--study of a hydrophobically assisted weak acid cation exchange phase, Journal of chromatography. A, 1218 (2011) 763-777.

[43] M. Petro, D. Berek, Polymers immobilized on silica gels as stationary phases for liquid chromatography, Chromatographia, 37 (1993) 549-561.

[44] H. Ihara, M. Fukui, T. Mimaki, A. Shundo, W. Dong, M. Derakhshan, T. Sakurai, M. Takafuji, S. Nagaoka, Poly(4-vinylpyridine) as a reagent with silanol-masking effect for silica and its specific selectivity for PAHs and dinitropyrenes in a reversed phase, Analytica Chimica Acta, 548 (2005) 51-57.

[45] U.G. Gautam, T. Sawada, M.P. Gautam, M. Takafuji, H. Ihara, Poly(2-N-carbazolylethyl acrylate)-modified silica as a new polymeric stationary phase for reversed-phase high-performance liquid chromatography, Journal of Chromatography A, 1216 (2009) 7422-7426.

[46] R. Ohmacht, M. Kele, Z. Matus, Polymer coated stationary phases for liquid chromatography, Chromatographia, 28 (1989) 19-23.

[47] M.J.J. Hetem, J.W. De Haan, H.A. Claessens, C.A. Cramers, A. Deege, G. Schomburg, Characterization and stability of silanized and polymer-coated octadecyl reversed phases, J. Chromatogr., 540 (1991) 53-76.

[48] C.A. Rimmer, L.C. Sander, S.A. Wise, J.G. Dorsey, Synthesis and characterization of C13 to C18 stationary phases by monomeric, solution polymerized, and surface polymerized approaches, J. Chromatogr. A, 1007 (2003) 11-20.

[49] W. Stöber, A. Fink, E. Bohn, Controlled growth of monodisperse silica spheres in the micron size range, Journal of colloid and interface science, 26 (1968) 62-69.

[50] K. Unger, J. Schick-Kalb, K.-F. Krebs, Preparation of porous silica spheres for column liquid, Journal of Chromatography A, 83 (1973) 5-9.

[51] H.W. Kohlschütter, U. Mihm, Das kugelförmige und poröse Korn von Silicagel als Reaktionsprodukt, Kolloid-Zeitschrift und Zeitschrift für Polymere, 243 (1971) 148-152.

[52] K.K. Unger, J.N. Kinkel, B. Anspach, H. Giesche, Evaluation of advanced silica packings for the separation of biopolymers by high-performance liquid chromatography: I. Design and properties of parent silicas, Journal of Chromatography A, 296 (1984) 3-14.

[53] J.J. Kirkland, J.J. DeStefano, Controlled Surface Porosity Supports with Chemically-Bonded Organic Stationary Phases for Gas and Liquid Chromatography, Journal of Chromatographic Science, 8 (1970) 309-314.

[54] J.J. Kirkland, Columns for modern analytical liquid chromatography, Anal Chem, 43 (1971) 36A-48a.

[55] Y.-F. Cheng, T.H. Walter, Z. Lu, P. Iraneta, B.A. Alden, C. Gendreau, U.D. Neue, J.M. Grassi, J.L. Carmody, J.E. O'Gara, R.P. Fisk, Hybrid organic-inorganic particle technology: Breaking through traditional barriers of HPLC separations, LC-GC, 18 (2000) 1162, 1164, 1166, 1168, 1170, 1172.

[56] C. Hudalla, B. Alden, T. Walter, D. Walsh, E. Bouvier, P. Iraneta, N. Lawrence, K. Wyndham, Synthesis and Applications of BEH Particles in Liquid Chromatography, Lc-Gc, 30 (2012) 20-29.

[57] J. Li, L. Xu, Z.-g. Shi, Waxberry-like hierarchically porous ethyl-bridged hybrid silica microsphere: A substrate for enzyme catalysis and high-performance liquid chromatography, Journal of Chromatography A, 1587 (2019) 79-87.

[58] X.-Y. Yue, D.-D. Jiang, L. Shu, S. Chen, Z.-R. Nie, Q. Wei, S.-P. Cui, Q.-Y. Li, Mesoporous C18-bonded ethyl-bridged organic-inorganic hybrid silica: A facile one-pot synthesis and liquid chromatographic performance, Microporous and Mesoporous Materials, 236 (2016) 277-283.

[59] M. Leonard, C. Fournier, E. Dellacherie, Polyvinyl alcohol-coated macroporous polystyrene particles as stationary phases for the chromatography of proteins, J. Chromatogr. B: Biomed. Sci. Appl., 664 (1995) 39-46.

[60] C.G. Huber, G. Kleindienst, G.K. Bonn, Application of micropellicular poly-styrene/divinylbenzene stationary phases for high-performance reversed-phase liquid chromatography electrospray-mass spectrometry of proteins and peptides, Chromatographia, 44 (1997) 438-448.

[61] P. Li, T. Wang, F. Lei, X. Peng, H. Wang, L. Qin, J. Jiang, Preparation and evaluation of paclitaxel-imprinted polymers with a rosin-based crosslinker as the stationary phase in high-performance liquid chromatography, J. Chromatogr. A, 1502 (2017) 30-37.

[62] Q. Fu, H. Sanbe, C. Kagawa, K.-K. Kunimoto, J. Haginaka, Uniformly Sized Molecularly Imprinted Polymer for (S)-Nilvadipine. Comparison of Chiral Recognition Ability with HPLC Chiral Stationary Phases Based on a Protein, Anal. Chem., 75 (2003) 191-198.

[63] L. Qin, X.-W. He, W. Zhang, W.-Y. Li, Y.-K. Zhang, Surface-modified polystyrene beads as photografting imprinted polymer matrix for chromatographic separation of proteins, Journal of Chromatography A, 1216 (2009) 807-814.

[64] K. Zhang, T. Zhou, K. Kettisen, L. Ye, L. Bulow, Chromatographic separation of hemoglobin variants using robust molecularly imprinted polymers, Talanta, 199 (2019) 27-31.

[65] N. Zheng, Q. Fu, Y.-Z. Li, W.-B. Chang, Z.-M. Wang, T.-J. Li, Chromatographic characterization of sulfonamide imprinted polymers, Microchem. J., 69 (2001) 153-158.

[66] K.-I. Kitahara, S. Okuya, I. Yoshihama, T. Hanada, K. Nagashima, S. Arai, Preparation of monodispersed vinylpyridine–divinylbenzene porous copolymer resins and their application to high-performance liquid chromatographic separation of aromatic amines, Journal of Chromatography A, 1216 (2009) 7409-7414.

[67] J. Ng, D. Froom, Monodisperse 2 μm non-porous and 4 μm porous poly(divinylbenzene) microspheres: new technology in reversed-phase high performance liquid chromatography: these microspheric particles result in improved column efficiency by forming a better packed bed, Can. Chem. News, 50 (1998) 24-26.

[68] J. Nawrocki, C. Dunlap, J. Li, J. Zhao, C.V. McNeff, A. McCormick, P.W. Carr, Part II. Chromatography using ultra-stable metal oxide-based stationary phases for HPLC, J. Chromatogr. A, 1028 (2004) 31-62.

[69] J. Nawrocki, C. Dunlap, A. McCormick, P.W. Carr, Part I. Chromatography using ultra-stable metal oxide-based stationary phases for HPLC, Journal of Chromatography A, 1028 (2004) 1-30.

[70] H.J. Wirth, K.O. Eriksson, P. Holt, M. Aguilar, M.T.W. Hearn, High-performance liquid chromatography of amino acids, peptides and proteins CXXIX. Ceramic-based particles as chemically stable chromatographic supports, Journal of Chromatography A, 646 (1993) 129-141.

[71] U. Trüdinger, G. Müller, K.K. Unger, Porous zirconia and titania as packing materials for high-performance liquid chromatography, Journal of Chromatography A, 535 (1990) 111-125.

[72] K. Goraieb, C.H. Collins, Evaluation of a Doubly Zirconized Silica-Based Stationary Phase for HPLC, Chromatographia, 76 (2013) 899-908.

[73] C.R. Silva, C. Airoldi, K.E. Collins, C.H. Collins, A new generation of more pH stable reversed phases prepared by silanization of zirconized silica, Journal of Chromatography A, 1191 (2008) 90-98.

[74] A.M. Faria, C.R. Silva, C.H. Collins, I.C.S.F. Jardim, Development of a polymer-coated stationary phase with improved chemical stability in alkaline mobile phases, J. Sep. Sci., 31 (2008) 953-960.

[75] J. Li, P.W. Carr, Retention Characteristics of Polybutadiene-Coated Zirconia and Comparison to Conventional Bonded Phases, Anal Chem, 68 (1996) 2857-2868.

[76] C. McNeff, Q. Zhao, P. W. Carr, High-performance anion exchange of small anions with polyethyleneimine-coated porous zirconia, Journal of Chromatography A, 684 (1994) 201-211.

[77] Y. Hu, P.W. Carr, Synthesis and Characterization of New Zirconia-Based Polymeric Cation-Exchange Stationary Phases for High-Performance Liquid Chromatography of Proteins, Anal Chem, 70 (1998) 1934-1942.

[78] J.H. Knox, B. Kaur, G.R. Millward, Structure and performance of porous graphitic carbon in liquid chromatography, Journal of Chromatography A, 352 (1986) 3-25.

[79] C. West, C. Elfakir, M. Lafosse, Porous graphitic carbon: A versatile stationary phase for liquid chromatography, Journal of Chromatography A, 1217 (2010) 3201-3216.

[80] Z. Huang, P. Yao, Q. Zhu, L. Wang, Y. Zhu, The polystyrene-divinylbenzene stationary phase hybridized with oxidized nanodiamonds for liquid chromatography, Talanta, 185 (2018) 221-228.

[81] G. Saini, D.S. Jensen, L.A. Wiest, M.A. Vail, A. Dadson, M.L. Lee, V. Shutthanandan, M.R. Linford, Core−Shell Diamond as a Support for Solid-Phase Extraction and High-Performance Liquid Chromatography, Anal Chem, 82 (2010) 4448-4456.

[82] L.A. Wiest, D.S. Jensen, C.-H. Hung, R.E. Olsen, R.C. Davis, M.A. Vail, A.E. Dadson, P.N. Nesterenko, M.R. Linford, Pellicular Particles with Spherical Carbon Cores and Porous Nanodiamond/Polymer Shells for Reversed-Phase HPLC, Anal Chem, 83 (2011) 5488-5501.

[83] Z. Xue, J.C. Vinci, L.A. Colón, Nanodiamond-Decorated Silica Spheres as a Chromatographic Material, ACS Applied Materials & Interfaces, 8 (2016) 4149-4157.

[84] H.C. Kolb, M.G. Finn, K.B. Sharpless, Click Chemistry: Diverse Chemical Function from a Few Good Reactions, Angewandte Chemie International Edition, 40 (2001) 2004-2021.

[85] C.E. Hoyle, C.N. Bowman, Thiol-Ene Click Chemistry, Angew. Chem., Int. Ed., 49 (2010) 1540-1573.

[86] A.B. Lowe, Thiol-yne 'click'/coupling chemistry and recent applications in polymer and materials synthesis and modification, Polymer, 55 (2014) 5517-5549.

[87] E. Veigl, B. Böhs, A. Mandl, D. Krametter, W. Lindner, Evaluation of silica gel-based brush type chiral cation exchangers with (S)-N-(3,5-dinitrobenzoyl)tyrosine as chiral selector: attempt to interpret the discouraging results, Journal of Chromatography A, 694 (1995) 151-161.

[88] E. Veigl, W. Lindner, Epimeric N-substituted l-proline derivatives as chiral selectors for ligand-exchange chromatography, Journal of Chromatography A, 660 (1994) 255-268.

[89] G. Huang, J. Ou, X. Zhang, Y. Ji, X. Peng, H. Zou, Synthesis of novel perphenylcarbamated β-cyclodextrin based chiral stationary phases via thiol-ene click chemistry, Electrophoresis, 35 (2014) 2752-2758.

[90] X. Tang, X. Li, Y. Sun, Y. Xiao, Y. Wang, Thiol-ene click derived structurally well-defined per(3,5-dimethyl)phenylcarbamoylated cationic cyclodextrin separation material for achiral and chiral chromatography, J. Sep. Sci., 41 (2018) 2710-2718.

[91] X. Yao, T.T.Y. Tan, Y. Wang, Thiol-ene click chemistry derived cationic cyclodextrin chiral stationary phase and its enhanced separation performance in liquid chromatography, J. Chromatogr. A, 1326 (2014) 80-88.

[92] S. Bäurer, A. Zimmermann, U. Woiwode, O.L. Sánchez-Muñoz, M. Kramer, J. Horak, W. Lindner, W. Bicker, M. Lämmerhofer, Stable-bond polymeric reversed-phase/weak anion-exchange mixed-mode stationary phases obtained by simultaneous functionalization and crosslinking of a poly(3-mercaptopropyl)methylsiloxane-film on vinyl silica via thiol-ene double click reaction, Journal of Chromatography A, 1593 (2019) 110-118.

[93] L. Qiao, X. Shi, X. Lu, G. Xu, Preparation and evaluation of surface-bonded tricationic ionic liquid silica as stationary phases for high-performance liquid chromatography, J. Chromatogr. A, 1396 (2015) 62-71.

[94] D. Liu, T. Qiao, H. Liu, X. Wang, Z.-g. Shi, A simple approach to prepare a sulfone-embedded stationary phase for HPLC, Journal of separation science, 41 (2018) 877-885.

[95] J. Horak, W. Lindner, Investigations on the chromatographic behavior of hybrid reversed-phase materials containing electron donor–acceptor systems: I. Contribution of sulfur–aromatic interactions, Journal of Chromatography A, 1043 (2004) 177-194.

[96] J. Horak, N.M. Maier, W. Lindner, Investigations on the chromatographic behavior of hybrid reversed-phase materials containing electron donor–acceptor systems: II. Contribution of π–π aromatic interactions, Journal of Chromatography A, 1045 (2004) 43-58.

[97] M. Li, X. Lei, Y. Huang, Y. Guo, B. Zhang, F. Tang, X. Wu, Ternary thiol-ene photopolymerization for facile preparation of ionic liquid-functionalized hybrid monolithic columns based on polyhedral oligomeric silsesquioxanes, Journal of Chromatography A, 1597 (2019) 167-178.

[98] Z. Liu, J. Ou, H. Lin, Z. Liu, H. Wang, J. Dong, H. Zou, Photoinduced thiol-ene polymerization reaction for fast preparation of macroporous hybrid monoliths and their application in capillary liquid chromatography, Chem. Commun. (Cambridge, U. K.), 50 (2014) 9288-9290.

[99] G. Huang, J. Ou, H. Wang, Y. Ji, H. Wan, Z. Zhang, H. Zou, G. Huang, H. Wang, Z. Zhang, G. Huang, H. Wang, X. Peng, Synthesis of a stationary phase based on silica modified with branched octadecyl groups by Michael addition and photoinduced thiol-yne click chemistry for the separation of basic compounds, Journal of separation science, 39 (2016) 1461-1470.

[100] T.T.H. Dao, M. Guerrouache, B. Carbonnier, Thiol-yne Click Adamantane Monolithic Stationary Phase for Capillary Electrochromatography, Chin. J. Chem., 30 (2012) 2281-2284.

[101] Z. Liu, J. Ou, H. Lin, H. Wang, Z. Liu, J. Dong, H. Zou, Preparation of Monolithic Polymer Columns with Homogeneous Structure via Photoinitiated Thiol-yne Click Polymerization and Their Application in Separation of Small Molecules, Anal. Chem. (Washington, DC, U. S.), 86 (2014) 12334-12340.

[102] H. Zhang, S. Ma, Y. Yao, Y. Li, Y. Li, J. Ou, M. Ye, Y. Wei, Facile preparation of multi-functionalized hybrid monoliths via two-step photo-initiated reactions for two-dimensional liquid chromatography-mass spectrometry, J. Chromatogr. A, 1524 (2017) 135-142.

[103] S. Ma, H. Zhang, Y. Li, Y. Li, N. Zhang, J. Ou, M. Ye, Y. Wei, Fast preparation of hybrid monolithic columns via photo-initiated thiol-yne polymerization for capillary liquid chromatography, J. Chromatogr. A, 1538 (2018) 8-16.

[104] P.W. Carr, D.R. Stoll, X. Wang, Perspectives on Recent Advances in the Speed of High-Performance Liquid Chromatography, Anal Chem, 83 (2011) 1890-1900.

[105] S.M.C. Buckenmaier, D.V. McCalley, M.R. Euerby, Rationalisation of unusual changes in efficiency and retention with temperature shown for bases in reversed-phase high-performance liquid chromatography at intermediate pH, Journal of Chromatography A, 1060 (2004) 117-126.

[106] D.R. Stoll, P.W. Carr, Fast, Comprehensive Two-Dimensional HPLC Separation of Tryptic Peptides Based on High-Temperature HPLC, J. Am. Chem. Soc., 127 (2005) 5034-5035.

[107] J.D. Thompson, J.S. Brown, P.W. Carr, Dependence of Thermal Mismatch Broadening on Column Diameter in High-Speed Liquid Chromatography at Elevated Temperatures, Anal Chem, 73 (2001) 3340-3347.

[108] J.D. Thompson, P.W. Carr, High-Speed Liquid Chromatography by Simultaneous Optimization of Temperature and Eluent Composition, Anal Chem, 74 (2002) 4150-4159.

[109] B. Yan, J. Zhao, J.S. Brown, J. Blackwell, P.W. Carr, High-Temperature Ultrafast Liquid Chromatography, Anal Chem, 72 (2000) 1253-1262.

[110] A. Albrecht, R. Bruell, T. Macko, F. Malz, H. Pasch, Comparison of High-Temperature HPLC, CRYSTAF and TREF for the Analysis of the Chemical Composition Distribution of Ethylene-Vinyl Acetate Copolymers, Macromol. Chem. Phys., 210 (2009) 1319-1330.

[111] S. Cheruthazhekatt, T.F.J. Pijpers, V.B.F. Mathot, H. Pasch, Combination of TREF, high-temperature HPLC, FTIR and HPer DSC for the comprehensive analysis of complex polypropylene copolymers, Anal. Bioanal. Chem., 405 (2013) 8995-9007.

[112] J.L. Glajch, J.J. Kirkland, J. Köhler, Effect of column degradation on the reversed-phase high-performance liquid chromatographic separation of peptides and proteins, Journal of Chromatography A, 384 (1987) 81-90.

[113] A. Kobayashi, K. Takezawa, H. Takasaki, T. Kanda, H. Kutsuna, Synthesis and characterization of stable polymer-coated C8 stationary phase with high durability under extreme pH conditions for high-performance liquid chromatography, Journal of Chromatography A, 1073 (2005) 163-167.

[114] S. Kobayashi, I. Tanaka, O. Shirota, T. Kanda, Y. Ohtsu, Synthesis and characterization of a polymer-coated C18 stationary phase with high carbon content for liquid chromatography, Journal of Chromatography A, 828 (1998) 75-81.

[115] L. Ma, H. Luo, J. Dai, P.W. Carr, Development of acid stable, hyper-crosslinked, silica-based reversed-phase liquid chromatography supports for the separation of organic bases, Journal of chromatography. A, 1114 (2006) 21-28.

[116] Y. Zhang, Y. Huang, P.W. Carr, Optimization of the synthesis of a hyper-crosslinked stationary phases: a new generation of highly efficient, acid-stable hyper-crosslinked materials for HPLC, Journal of separation science, 34 (2011) 1407-1422.

[117] J.T. Wu, C.H. Huang, W.C. Liang, Y.L. Wu, J. Yu, H.Y. Chen, Reactive polymer coatings: a general route to thiol-ene and thiol-yne click reactions, Macromol Rapid Commun, 33 (2012) 922-927.

[118] B.D. Fairbanks, T.F. Scott, C.J. Kloxin, K.S. Anseth, C.N. Bowman, Thiol-Yne Photopolymerizations: Novel Mechanism, Kinetics, and Step-Growth Formation of Highly Cross-Linked Networks, Macromolecules, 42 (2009) 211-217.

[119] W. Xi, T.F. Scott, C.J. Kloxin, C.N. Bowman, Click Chemistry in Materials Science, Advanced Functional Materials, 24 (2014) 2572-2590.

[120] A. Maiolica, D. Borsotti, J. Rappsilber, Self-made frits for nanoscale columns in proteomics, Proteomics, 5 (2005) 3847-3850.

[121] K. Kimata, K. Iwaguchi, S. Onishi, K. Jinno, R. Eksteen, K. Hosoya, M. Araki, N. Tanaka, Chromatographic Characterization of Silica C18 Packing Materials. Correlation between a Preparation Method and Retention Behavior of Stationary Phase, Journal of Chromatographic Science, 27 (1989) 721-728.

[122] M.R. Euerby, P. Petersson, Chromatographic classification and comparison of commercially available reversed-phase liquid chromatographic columns using principal component analysis, Journal of Chromatography A, 994 (2003) 13-36.

[123] J.J. Gilroy, J.W. Dolan, L.R. Snyder, Column selectivity in reversed-phase liquid chromatography: IV. Type-B alkyl-silica columns, Journal of Chromatography A, 1000 (2003) 757-778.

[124] L.R. Snyder, A. Maule, A. Heebsh, R. Cuellar, S. Paulson, J. Carrano, L. Wrisley, C.C. Chan, N. Pearson, J.W. Dolan, J.J. Gilroy, A fast, convenient and rugged procedure for characterizing the selectivity of alkyl-silica columns, Journal of Chromatography A, 1057 (2004) 49-57.

[125] J.P. Foley, J.G. Dorsey, Equations for calculation of chromatographic figures of merit for ideal and skewed peaks, Anal Chem, 55 (1983) 730-737.

[126] G. Srinivasan, L.C. Sander, K. Muller, Effect of surface coverage on the conformation and mobility of C18-modified silica gels, Analytical and bioanalytical chemistry, 384 (2006) 514-524.

[127] L.C. Sander, M. Pursch, S.A. Wise, Shape selectivity for constrained solutes in reversed-phase liquid chromatography, Anal. Chem., 71 (1999) 4821-4830.

[128] T. Minami, I. Niki, T. Agawa, Reactions of Dimethylvinylsulfonium Salts with Sodium Phenoxide, Phosphorous and Sulfur and the Related Elements, 3 (1977) 55-59.

[129] M.R. Euerby, P. Petersson, Chromatographic classification and comparison of commercially available reversed-phase liquid chromatographic columns containing polar embedded groups/amino endcappings using principal component analysis, Journal of Chromatography A, 1088 (2005) 1-15.

[130] M.R. Euerby, P. Petersson, W. Campbell, W. Roe, Chromatographic classification and comparison of commercially available reversed-phase liquid chromatographic columns containing phenyl moieties using principal component analysis, Journal of Chromatography A, 1154 (2007) 138-151.

[131] E.P. Shields, S.G. Weber, A liquid chromatographic charge transfer stationary phase based on the thiol-yne reaction, Journal of Chromatography A, 1591 (2019) 1-6.

[132] D.A. Dougherty, The Cation−π Interaction, Accounts of Chemical Research, 46 (2013) 885-893.

[133] S.A. Wise, L.C. Sander, Factors affecting the reversed-phase liquid chromatographic separation of polycyclic aromatic hydrocarbon isomers, Journal of High Resolution Chromatography, 8 (1985) 248-255.

[134] K.A. Lippa, L.C. Sander, S.A. Wise, Chemometric studies of polycyclic aromatic hydrocarbon shape selectivity in reversed-phase liquid chromatography, Analytical and bioanalytical chemistry, 378 (2004) 365-377.

[135] L.C. Sander, R.M. Parris, S.A. Wise, P. Garrigues, Shape discrimination in liquid chromatography using charge-transfer phases, Anal. Chem., 63 (1991) 2589-2597.

[136] U.G. Gautam, M.P. Gautam, T. Sawada, M. Takafuji, H. Ihara, Thermodynamic investigations on shape selective separation behaviors of poly(4-vinylpyridine)-grafted silica for polycyclic aromatic hydrocarbons in both normal-phase and reversed-phase high-performance liquid chromatography, J. Chromatogr. A, 1216 (2009) 3571-3577.

[137] J.W. Dolan, A. Maule, D. Bingley, L. Wrisley, C.C. Chan, M. Angod, C. Lunte, R. Krisko, J.M. Winston, B.A. Homeier, D.V. McCalley, L.R. Snyder, Choosing an equivalent replacement column for a reversed-phase liquid chromatographic assay procedure, Journal of Chromatography A, 1057 (2004) 59-74.

[138] K. Vanderlinden, G. Desmet, D.S. Bell, K. Broeckhoven, Detailed efficiency analysis of columns with a different packing quality and confirmation via total pore blocking, Journal of Chromatography A, 1581-1582 (2018) 55-62.

[139] R.M. Arnold, D.L. Patton, V.V. Popik, J. Locklin, A dynamic duo: pairing click chemistry and postpolymerization modification to design complex surfaces, Acc Chem Res, 47 (2014) 2999-3008.

[140] O.D. McNair, D.P. Brent, B.J. Sparks, D.L. Patton, D.A. Savin, Sequential thiol click reactions: formation of ternary thiourethane/thiol-ene networks with enhanced thermal and mechanical properties, ACS Appl Mater Interfaces, 6 (2014) 6088-6097.

[141] A. Shen, Z. Guo, X. Cai, X. Xue, X. Liang, Preparation and chromatographic evaluation of a cysteine-bonded zwitterionic hydrophilic interaction liquid chromatography stationary phase, Journal of Chromatography A, 1228 (2012) 175-182.

[142] G. Huang, J. Ou, H. Wang, Y. Ji, H. Wan, Z. Zhang, X. Peng, H. Zou, Synthesis of a stationary phase based on silica modified with branched octadecyl groups by Michael addition and photoinduced thiol-yne click chemistry for the separation of basic compounds, Journal of separation science, 39 (2016) 1461-1470.

[143] P. Jiang, C.A. Lucy, Retentivity, selectivity and thermodynamic behavior of polycyclic aromatic hydrocarbons on charge-transfer and hypercrosslinked stationary phases under conditions of normal phase high performance liquid chromatography, J. Chromatogr. A, 1437 (2016) 176-182.

[144] J.G. Dorsey, K.A. Dill, The molecular mechanism of retention in reversed-phase liquid chromatography, Chem. Rev., 89 (1989) 331-346.

[145] L. Limsavarn, J.G. Dorsey, Influence of stationary phase solvation on shape selectivity and retention in reversed-phase liquid chromatography, J. Chromatogr. A, 1102 (2006) 143-153.

[146] H.A. Benesi, J.H. Hildebrand, A Spectrophotometric Investigation of the Interaction of Iodine with Aromatic Hydrocarbons, Journal of the American Chemical Society, 71 (1949) 2703-2707.

[147] C.A. Hunter, J.K.M. Sanders, The nature of .pi.-.pi. interactions, Journal of the American Chemical Society, 112 (1990) 5525-5534.

[148] K. Kimata, K. Hosoya, T. Araki, N. Tanaka, E.R. Barnhart, L.R. Alexander, S. Sirimanne, P.C. McClure, J. Grainger, D.G. Patterson, Jr., Electron-acceptor and electron-donor chromatographic stationary phases for the reversed-phase liquid chromatographic separation and isomer identification of polychlorinated dibenzo-p-dioxins, Anal. Chem., 65 (1993) 2502-2509.

[149] M.T. Matyska, J.J. Pesek, V. Grandhi, Charge-transfer-like stationary phase for HPLC prepared via hydrosilation on silica hydride, J. Sep. Sci., 25 (2002) 741-748.

[150] M.C. Jung, G. Shi, L. Borland, A.C. Michael, S.G. Weber, Simultaneous Determination of Biogenic Monoamines in Rat Brain Dialysates Using Capillary High-Performance Liquid Chromatography with Photoluminescence Following Electron Transfer, Anal. Chem., 78 (2006) 1755-1760.

[151] S. Kayillo, G.R. Dennis, R.A. Shalliker, Retention of polycyclic aromatic hydrocarbons on propyl-phenyl stationary phases in reversed-phase high performance liquid chromatography, Journal of Chromatography A, 1148 (2007) 168-176.

[152] V.A. Davankov, C.S. Sychov, M.M. Ilyin, K.O. Sochilina, Hypercrosslinked polystyrene as a novel type of high-performance liquid chromatography column packing material: Mechanisms of retention, Journal of Chromatography A, 987 (2003) 67-75.

[153] H. Chung, S. Tajiri, M. Hyoguchi, R. Koyanagi, A. Shimura, F. Takata, S. Dohgu, T. Matsui, Analysis of Catecholamine and Their Metabolites in Mice Brain by Liquid Chromatography–Mass Spectrometry Using Sulfonated Mixed-mode Copolymer Column, Analytical Sciences, 35 (2019) 433-439.

[154] Y. Hu, X. Yang, P.W. Carr, Mixed-mode reversed-phase and ion-exchange separations of cationic analytes on polybutadiene-coated zirconia, J. Chromatogr. A, 968 (2002) 17-29.

[155] M. Tsunoda, C. Aoyama, H. Nomura, T. Toyoda, N. Matsuki, T. Funatsu, Simultaneous determination of dopamine and 3,4-dihydroxyphenylacetic acid in mouse striatum using mixed-mode reversed-phase and cation-exchange high-performance liquid chromatography, Journal of Pharmaceutical and Biomedical Analysis, 51 (2010) 712-715.

[156] L. Wang, W. Wei, Z. Xia, X. Jie, Z.Z. Xia, Recent advances in materials for stationary phases of mixed-mode high-performance liquid chromatography, TrAC Trends in Analytical Chemistry, 80 (2016) 495-506.

[157] C.J. Venkatramani, Y. Zelechonok, Two-dimensional liquid chromatography with mixed mode stationary phases, Journal of Chromatography A, 1066 (2005) 47-53.

[158] H. Luo, L. Ma, Y. Zhang, P.W. Carr, Synthesis and characterization of silica-based hyper-crosslinked sulfonate-modified reversed stationary phases, Journal of Chromatography A, 1182 (2008) 41-55.

[159] R. Nogueira, M. Lämmerhofer, W. Lindner, Alternative high-performance liquid chromatographic peptide separation and purification concept using a new mixed-mode reversed-phase/weak anion-exchange type stationary phase, Journal of Chromatography A, 1089 (2005) 158-169.

[160] E.P. Shields, S.G. Weber, A pH-stable, crosslinked stationary phase based on the thiol-yne reaction, Journal of chromatography. A, 1598 (2019) 132-140.

[161] K.N.M. Daeffler, H.A. Lester, D.A. Dougherty, Functionally Important Aromatic–Aromatic and Sulfur−π Interactions in the D2 Dopamine Receptor, Journal of the American Chemical Society, 134 (2012) 14890-14896.

[162] T. Fueno, Y. Yonezawa, The role of sulfur d-orbitals in the charge-transfer complexation of carbonyl cyanide with alkyl sulfides, Tetrahedron, 32 (1976) 1345-1346.

[163] E.A. Orabi, A.M. English, Sulfur-Aromatic Interactions: Modeling Cysteine and Methionine Binding to Tyrosinate and Histidinium Ions to Assess Their Influence on Protein Electron Transfer, Israel Journal of Chemistry, 56 (2016) 872-885.

[164] M. Egli, S. Sarkhel, Lone Pair−Aromatic Interactions: To Stabilize or Not to Stabilize, Accounts of Chemical Research, 40 (2007) 197-205.

[165] Y. Valadbeigi, J.-F. Gal, On the Significance of Lone Pair/Lone Pair and Lone Pair/Bond Pair Repulsions in the Cation Affinity and Lewis Acid/Lewis Base Interactions, ACS Omega, 3 (2018) 11331-11339.

[166] N.W. Tideswell, J.D. McCullough, The Dissociation Constants of Some Dihalides of Dimethyl Sulfide and Dimethyl Selenide in Carbon Tetrachloride Solution, Journal of the American Chemical Society, 79 (1957) 1031-1033.

[167] H. Tsubomura, R.P. Lang, Molecular Complexes and Their Spectra. XIII. Complexes of Iodine with Amides, Diethyl Sulfide and Diethyl Disulfide, Journal of the American Chemical Society, 83 (1961) 2085-2092.

[168] H. Golchoubian, F. Hosseinpoor, Effective oxidation of sulfides to sulfoxides with hydrogen peroxide under transition-metal-free conditions, Molecules, 12 (2007) 304-311.

[169] C. Schoeneich, A. Aced, K.D. Asmus, Mechanism of oxidation of aliphatic thioethers to sulfoxides by hydroxyl radicals. The importance of molecular oxygen, Journal of the American Chemical Society, 115 (1993) 11376-11383.

[170] B.J. Holland, X.A. Conlan, P.S. Francis, N.W. Barnett, P.G. Stevenson, Overcoming solvent mismatch limitations in 2D-HPLC with temperature programming of isocratic mobile phases, Analytical Methods, 8 (2016) 1293-1298.

[171] L.N. Jeong, R. Sajulga, S.G. Forte, D.R. Stoll, S.C. Rutan, Simulation of elution profiles in liquid chromatography□I: Gradient elution conditions, and with mismatched injection and mobile phase solvents, Journal of Chromatography A, 1457 (2016) 41-49.

[172] B.W.J. Pirok, D.R. Stoll, P.J. Schoenmakers, Recent Developments in Two-Dimensional Liquid Chromatography: Fundamental Improvements for Practical Applications, Anal Chem, 91 (2019) 240-263.

[173] H. Gu, E.L. Varner, S.R. Groskreutz, A.C. Michael, S.G. Weber, In Vivo Monitoring of Dopamine by Microdialysis with 1 min Temporal Resolution Using Online Capillary Liquid Chromatography with Electrochemical Detection, Anal. Chem. (Washington, DC, U. S.), 87 (2015) 6088-6094.

[174] Y.-S. Liu, J. Zhang, X.-M. Xu, M.K. Zhao, A.M. Andrews, S.G. Weber, Capillary Ultrahigh Performance Liquid Chromatography with Elevated Temperature for Sub-One Minute Separations of Basal Serotonin in Submicroliter Brain Microdialysate Samples, Anal. Chem. (Washington, DC, U. S.), 82 (2010) 9611-9616.

[175] K.T. Ngo, E.L. Varner, A.C. Michael, S.G. Weber, Monitoring Dopamine Responses to Potassium Ion and Nomifensine by in Vivo Microdialysis with Online Liquid Chromatography at One-Minute Resolution, ACS Chem. Neurosci., 8 (2017) 329-338.

[176] J. Zhang, A. Jaquins-Gerstl, K.M. Nesbitt, S.C. Rutan, A.C. Michael, S.G. Weber, In Vivo Monitoring of Serotonin in the Striatum of Freely Moving Rats with One Minute Temporal Resolution by Online Microdialysis-Capillary High-Performance Liquid Chromatography at Elevated Temperature and Pressure, Anal. Chem. (Washington, DC, U. S.), 85 (2013) 9889-9897.

[177] H. Xu, S.G. Weber, Effect of an open tube in series with a packed capillary column on liquid chromatographic performance. The influence of particle diameter, temperature, and system pressure, Journal of chromatography. A, 1216 (2009) 1346-1352.

[178] J. Zhang, Y. Liu, A. Jaquins-Gerstl, Z. Shu, A.C. Michael, S.G. Weber, Optimization for speed and sensitivity in capillary high performance liquid chromatography. The importance of column diameter in online monitoring of serotonin by microdialysis, J. Chromatogr. A, 1251 (2012) 54-62.